UNIVERSIDADE DE SÃO PAULO

FACULDADE DE CIÊNCIAS FARMACÊUTICAS DE RIBEIRÃO PRETO

Metabolomics analysis of Brazilian and Nigerian Asteraceae species, targeting hyperglycemia-modulating metabolites

Análise metabólica de espécies de Asteraceae brasileiras e nigerianas, visando metabólitos moduladores da hiperglicemia

OLAKUNLE ADEBOYE JAIYESIMI

Ribeirão Preto
2019

UNIVERSIDADE DE SÃO PAULO

FACULDADE DE CIÊNCIAS FARMACÊUTICAS DE RIBEIRÃO PRETO

OLAKUNLE ADEBOYE JAIYESIMI

Metabolomics analysis of Brazilian and Nigerian Asteraceae species, targeting hyperglycemia-modulating metabolites

Análise metabólica de espécies de Asteraceae brasileiras e nigerianas, visando metabólitos moduladores da hiperglicemia

Doctoral thesis presented to the Graduate Program of School of Pharmaceutical Sciences of Ribeirão Preto/USP for the degree of Doctor in Sciences.

Concentration Area: Produtos Naturais e Sintéticos

Supervisor: Prof. Dr. Leonardo Gobbo Neto

Co-supervisor: Profa. Dra. Carem Gledes Vargas Rechia

The corrected version of the Doctoral Thesis
was presented to the Graduate Program in Pharmaceutical Sciences
on 06/09/2019. The original version is available at the School of
Pharmaceutical Sciences of Ribeirão Preto/USP

Ribeirão Preto
2019

LOMBADA

JAIYESIMI, O.A.

Metabolomic analysis of Brazilian and Nigerian Asteraceae species, targeting hyperglycemia-modulating metabolites

Espaço de **2,5 cm** reservado para etiqueta de localização da biblioteca

DOUTORADO
FCFRPUSP
2019

I AUTHORIZE THE REPRODUCTION AND TOTAL OR PARTIAL DISCLOSURE OF THIS WORK, BY ANY CONVENTIONAL OR ELECTRONIC MEANS

Jaiyesimi, Olakunle Adeboye
Metabolomic analysis of Brazilian and Nigerian Asteraceae species, targeting hyperglycemia-modulating metabolites. Ribeirão Preto, 2019.
153 p.; 30 cm.

Doctoral thesis presented to the Graduate Program of School of Pharmaceutical Sciences of Ribeirão Preto/USP for the degree of Doctor in Sciences. Concentration Area: Produtos Naturais e Sintéticos
Supervisor: Prof. Dr. Gobbo Neto, Leonardo
Co-supervisor: Profa. Dra. Vargas Rechia, Carem Gledes

1. Asteraceae. 2. Hiperglicemia pósprandia.
3. Metabolômica não segmentada. 4. Espectrometria de massas.
5. Pré-diabetes

APPROVAL PAGE

Olakunle Adeboye Jaiyesimi

Metabolomics analysis of Brazilian and Nigerian Asteraceae species, targeting hyperglycemia-modulating metabolites.

Doctoral thesis presented to the Graduate Program of School of Pharmaceutical Sciences of Ribeirão Preto/USP for the degree of Doctor in Sciences.

Concentration Area: Produtos Naturais e Sintéticos.

Supervisor: Prof. Dr. Gobbo Neto, Leonardo
Co-supervisor: Profa. Dra. Vargas Rechia, Carem Gledes

Aprovado on:

Examiners

Prof.Dr._____
Instituição:_____Assinatura:_____

Prof.Dr._____
Instituição:_____Assinatura:_____

Prof.Dr._____
Instituição:_____Assinatura:_____

Prof.Dr._____
Instituição:_____Assinatura:_____

DEDICATION

To everyone struggling to maintain a good health

To everyone going to bed at night with an empty stomach

To family

Acknowledgement

To the mystery of nature that knows no bound, which we all are, in our academic adventures, perpetually probing to unravel its intricacies and benefits to herself and humanity. I can only say “yield!” for I have marveled at your brutal beauty and delicate potency, which sit at the roadside awaiting sampling, searching and savouring.

To Prof. Dr. Leonardo Gobbo Neto for accepting to supervise my research, for introducing me to metabolomics and for his time at making this phase of my academic journey a smooth one. I am particularly grateful for the experience and knowledge shared with me over the course of my study. I am eternally grateful to Profa. Dra. Carem Gledes Vargas Rechia for her co-supervision and for all the lessons I got towards improving the outcome of my research.

I will like to also thank Prof. Noberto Lopes Peperoni, who beyond welcoming me the Fifikane way and seamlessly integrating me into the Brazilian culture also assured a conducive working environment. To Prof. João Luis Callegari Lopes, Prof. Paulo Cezar Vieira, Prof. Jairo Kenupp Bastos, Profa. Dra. Niege Araçari Jacometti Cardoso Furtado and Profa. Dra. Luciane Carla Alberici, for the priceless tutelage I have had from you. It is unquantifiable.

My stay in Brazil would not have had flavor without the warmth of all FCFRP members. Every exchange we had was edifying and I will cherish the experience for a very long time. Such never ends! My appreciation goes to, amongst others, Jose Carlos Tomaz, Jacqueline Mendonça, Camila Godinho Capel, Marilia Elias Gallon, Eduardo Afonso Silva Junior, Eduarda Antunes Moreira, Matheus Coutinho Gazolla, Tamy Stringer, Daniel Demarque, Juliano Amaral, Dani, Alan Pilon, Artur Vaz, Arian Manzoni Bocamino, Aneliz Bauermeister, Ricardo da Silva and Gibson. You all are splendid, making my stay in Brazil a memorable one. I must expressly appreciate the efforts, support and dedication of the wonderfulpeople at the FCFRP posdtgraduate office, including Rosana Florêncio, Eleni Angeli Passos, Henrique Theodoro and Rosemary Ioshimine Gerolineto; without forgetting to mention Rafael Braga Poggi.

I cannot but thank the members of the laboratories of Profa. Dra. Carem and Profa. Dra Luciane, especially Ana Elisa Caleiro Seixas Azzolini, Luciana Angulo Faria Rocha,

Carlos Antônio Couto Lima and Ígor Hayaxibara Sampaio for their support throughout the period I conducted the bioassay experimental aspects of my research.

I am particularly grateful to Prof. Dr. Fernando B. da Costa for recommending me to Prof. Dr. Gobbo and for availing me the access to his laboratory. To members of his laboratory, including Gari Vidal Ccana Ccapatinta, Jolindo Freitas, Luiz Fernando da Silva and Mario Ogasawara, I say a big thank you for your support. To Giba and all members of the technical unit of FCFRP, thank you. You were so supportive that I could not imagine what doing a PhD elsewhere would have been.

My profound gratitude goes to André Barillari and his beautiful family, who provided me and my family with warmth and almost everything we needed to make our lives in Brazil worth the while. Thank you!

I appreciate my Nigerian friends in Brazil, Abayomi Ogunjimi, Oloruntoba Bankole and Michael Osunguna for all the good things we shared. May Olodumare continue to be our fortress.

And to my family, especially my parents and siblings, Olufunke, Olanrewaju and Ayobami, I say a big thank you for the support you always gave me. To Adeleke Omooba, Adieu!

To Bukola, my loving wife and kids, Iteoluwakiisi and Pipennuoluwakiiba, you were the support I held on to while I buried my head in the sand of nature. May Olodumare keep and continue to watch over us. I will choose you over again, if I have a choice.

I acknowledge my University, Obafemi Awolowo University, Ile-Ife, Nigeria for granting my study leave to undertake this PhD programme.

O presente trabalho foi realizado com apoio da Coordenação de Aperfeiçoamento de Pessoal de Nível Superior – Brazil (CAPES) – Código de Financiamento 001 and Brazilian National Council for Scientific and Technological Development (CNPq) with process number: 142006/2016-5.

RESUMO

JAIYESIMI, O. A. **Análise metabólica de espécies brasileiras e nigerianas de Asteraceae, visando metabolitos moduladores da hiperglicemia**. 2019. 153 f. Tese (Doutorado). Faculdade de Ciências Farmacêuticas de Ribeirão Preto - Universidade de São Paulo, Ribeirão Preto, 2019.

A hiperglicemia crônica no estágio pré-diabético acarreta toxicidade à glicose e dano às células β-ilhotas pancreáticas devido ao estresse oxidativo, predispondo os indivíduos ao desenvolvimento de diabetes tipo 2. Como um desafio significativo para a saúde global, a busca contínua de fitoconstituintes com potencial para prevenir, reduzir ou retardar a hiperglicemia e sua progressão final para o diabetes tipo 2, entre outros benefícios, é justificada. Este estudo avaliou 68 espécies de Asteraceae por sua capacidade in vitro de melhorar a captação de glicose, inibir as α-amilases pancreáticas de suínos (de *Aspergillus oryzae*) e porcinos, retardar a difusão da glicose e eliminar os radicais livres de DPPH. Das plantas investigadas, 11 retardaram a difusão da glicose, com *Senecio biafrae*, *Eremanthus veadeiroensis* e *Vernonia brasiliana* sendo as mais ativas; 37 inibiram a α-amilase fúngica, incluindo *Silybum marianum*, *Acanthospermum hispidum* e *Tithonia diversifolia* (nigeriana); 12 inibiram a α-amilase pancreática porcina sendo os mais ativos *S. marianum*, *Baccharis gaudichaudiana* e *E. veadeiroensis*; 36 melhoraram a captação de glicose mediada por insulina significativamente melhor que a metformina, incluindo *Micania micrantha*, *Crassocephalum crepidioides* e *E. veadeiroensis*; e 6 exibiram significativamente > 90,0% de atividade antioxidante incluindo *Arnica montana*, *Baccharis genistelloides*, *B. gaudichaudiana*, *Erigeron floribundus*, *Solidago microglossa* e *Achillea millefolium*. As matrizes Mzmine™ geradas pré-processadas das impressões digitais metabólicas de extratos vegetais obtidos com UHPLC -UV(DAD)-MS (Orbitrap) foram analisadas no SIMCA utilizando-se análise não supervisionada (Análise de Agrupamento Hieráquico e Análise de Componentes Principais) e supervisionadas análise estatística multivariada. A metabolômica não-alvo, correlacionando as impressões digitais metabólicas com as bioatividades observadas nas plantas, produziu metabólitos discriminantes significativos para cada ensaio. Os flavonóides e seus glicosídeos foram revelados como importantes variáveis responsáveis pelas atividades antidiabéticas e antioxidantes, indicando potencial adicional para a prevenção do diabetes. Tal inclui a apigenina 6-*C*-arabinoside-8-*C*-glicosídeo, kaempferol-6-metoxi-3-*O*-glicosídeo, 5-hidroxi-3,6,7,4'-tetrametoxiflavona, 5,6,7,4'-tetrametoxiflavona e 3,4',6-trimetoxiquercetagetina. Este estudo fornece mais evidências para o uso de metabolômica não direcionada para a rápida determinação de metabólitos especializados em plantas com potenciais bioativos, neste caso a redução ou a prevenção da hiperglicemia.

Palavras-chave: Asteraceae, hiperglicemia pósprandia, metabolômica não segmentada, espectrometria de massas, pré-diabetes

ABSTRACT

JAIYESIMI, O. A. **Metabolomic analysis of Brazilian and Nigerian Asteraceae species, targeting hyperglycemia-modulating metabolites**. 2019. 153 p. Thesis (Doctoral). Faculdade de Ciências Farmacêuticas de Ribeirão Preto - Universidade de São Paulo, Ribeirão Preto, 2019.

Chronic hyperglycemia in the prediabetic stage leads to glucose toxicity and pancreatic β-islet cells damage due to oxidative stress, predisposing subjects to the developement of type 2 diabetes. As a significant global health challenge, the continued search for phytoconstituents with potential to prevent, reduce or delay hyperglycemia and its ultimate progression to type 2 diabetes, amongst other benefits including reduced or absence of side effects, is warranted. This study evaluated 68 Asteraceae species for their *in vitro* ability to improve glucose-uptake, inhibit both fungal (from *Aspergillus oryzae*) and porcine pancreatic α-amylases, retard glucose diffusion and scavenge DPPH free radicals. Of the plants investigated, 11 retarded glucose diffusion with *Senecio biafrae, Eremanthus veadeiroensis* and *Vernonia brasiliana* being the most active; 37 inhibited fungal α-amylase including *Silybum marianum, Acanthospermum hispidum* and Nigerian *Tithonia diversifolia*; 12 inhibited porcine pancreatic α-amylase with the most active being *S. marianum*, *Baccharis gaudichaudiana* and *Eremanthus veadeiroensis*; 36 improved insulin-mediated glucose uptake significantly better than metformin including *Micania micrantha*, *Crassocephalum crepidioides* and *E. veadeiroensis*; and 6 significantly exhibited > 90.0% antioxidant activity including *Arnica montana*, *Baccharis genistelloides*, *B. gaudichaudiana*, *Erigeron floribundus*, *Solidago microglossa* and *Achillea millefolium*. All the extracts were analysed by LC-UV-MS for further metabolomics analyses. The LC-MS chromatograms were processed and the generated marices were analyzed by unsupervised (Hierachical Cluster Analysis and Principal Component Analysis) and supervised (Partial least square-discriminant analysis) multivariate statistical analysis. Untargeted metabolomics, correlating the metabolic fingerprints with the plants' observed bioactivities, yielded significant discriminant metabolites for each assay. Flavonoids and their glycosides were revealed as important variables responsible for the antidiabetic as well as antioxidant activities, indicating additional potential for the prevention of diabetes. Such includes apigenin 6-*C*-arabinoside-8-*C*-glucoside, 6-methoxykaempferol-3-*O*-glucoside, 5-hydroxy-3,6,7,4'-tetramethoxyflavone, 5,6,7,4'-tetramethoxyflavone and 3,4',6-trimethoxyquercetagetin. This study provides further evidence for the use of untargeted metabolomics for the rapid determination of plant specialized metabolites with bioactive potentials, in this case the reduction or prevention of hyperglycaemia.

Keywords: Asteraceae, postprandia hyperglycemia, untargeted metabolomics, mass spectrometry, prediabetes

LIST OF FIGURES

LIST OF TABLES

LIST OF ABBREVIATIONS AND CODES

AIF	All ion fragmentation
STL	Sesquiterpene lactone
PCA	Principal Components Analysis
HCA	Hierachical Cluster Analysis
PLS-DA	Partial least squares discriminant analysis
LC-MS	Liquid chromatography coupled to mass spectrometry
UHPLC-UV-MS	High performance liquid chromatography hyphenated with ultrabiolet detector and coupled to mass spectrometry
VIP	Variable importance in projection
SbiafraeNig	*Senecio biafrae* from Nigeria
GparvifBra	*Galinsoga parviflora* from Brazil
EveaiBra	*Eremanthus veadeiroensis* from Brazil
VcondenBra	*Vernonia condensata* from Brazil
BgaudichCC	Commercial *Baccharis gaudichaudiana*
VferrugBra	*Vernonanthura ferruginea* from Brazil
VbrasilBra	*Vernonia brasiliana* from Brazil
AmillefoCC	Commercial *Achillea millefolium*
TdivRtCMuR	roots of Nigerian *T. diversifolia* treated with roots of *M. koenigii*
TdivRpCMuR	roots of Nigerian *T. diversifolia* planted with roots of *M. koenigii*
TdiversiCC	Commercial *Tithonia diversifolia*
TdiversNig	*Tithonia diversifolia* from Nigeria
SrebaudiCC	Commercial *Stevia rebaudiana*
AsatureCC	Commercial *Achyrocline satureioides*
CbenedicCC	Commercial *Carduus benedictus*
AlappaCC	Commercial *Arctium lappa*
EfloriNigA	*Erigeron floribundus* from Nigeria (aerial parts)
EfloriNigL	*Erigeron floribundus* from Nigeria (leaves)
MrecutitCC	Commercial *Matricaria recutita*
CrecutiBra	*Chamomilla recutita* from Brazil
AhispidNig	*Acanthospermum hispidum* from Nigeria
BgenisteCC	Commercial *Baccharis genistelloides*
AabsinthCC	Commercial *Artemisia absinthium*
LtaraxaNig	*Launea taraxacifolia* from Nigeria
CjaponBra	*Crepis japonica* from Brazil
SmarianuCC	Commercial *Silybum marianum*
EpraeteNig	*Emilia praetermissa* from Nigeria
EfosberBra	*Emilia fosbergii* from Brazil
GrobustBra	*Grindelia robusta* from Brazil
BpilosaBra	*Bidens pilosa* from Brazil
BpilosaNig	*Bidens pilosa* from Nigeria
BpilosaCC	Commercial *Bidens pilosa*

TdivLpCMuL	leaves of Nigerian *T. diversifolia* planted with leaves of *M. koenigii*
TdivLtCMuL	leaves of Nigerian *T. diversifolia* treated with leaves of *M. koenigii*
VpolyanVPN	*Vernonanthura phosporica* from Brazil
VpolBrVPFL	*Vernonanthura phosporica* from Brazil
EmollisBra	*Elephantopus mollis* from Brazil
CcrepidiNig	*Crassocephalum crepidioides* from Nigeria
TofficinCC	Commercial *Taraxacum officinale*
CofficiBra	Commercial *Calendula officinalis*
EglomerBra	*Eremanthus glomerulatus* from Brazil
VamygdalNig	*Vernonia amygdalina* from Nigeria
IheleniuCC	Commercial *Inula helenium*
TprocumbNi	*Tridax procumbens* from Nigeria
TprocuBraM	*Tridax procumbens* from Brazil
TprocuBraN	*Tridax procumbens* from Brazil
SfilicauNig	*Spilanthes filicaulis* from Nigeria
EalbaNig	*Eclipta alba* from Nigeria
MmicrantCC	Commercial *Mikania micrantha*
MglomeraCC	Commercial *Mikania glomerata*
CscolymBra	*Cynara scolymus* from Brazil
AafricaNig	*Aspilia africana* from Nigeria
EodoratuNig	*Eupatorium odoratum* from Nigeria
AconyCC	Commercial *Ageratum conyzoides*
AconyzoNig	*Ageratum conyzoides* from Nigeria
MhirsutiCC	Commercial *Mikania hirsutissima*
SsparganNig	*Struchium sparganophora* from Nigeria
VcinereNig	*Vernonia cinerea* from Nigeria
MscandenNig	*Melanthera scandens* from Nigeria
VpolyantCC	Commercial *Vernonanthura phosphorica*
AmontanaCC	Commercial *Arnica montana*
AvulgareCC	Commercial *Artemisia vulgaris*
TdivNigCtL	leaves of Nigerian *T. diversifolia* control leaves
TvulgareCC	Commercial *Tanacetum vulgare*
SnodiflNig	Nigerian *Synedrella nodiflora*
CscolymCC	Commercial *Cynara scolymus*
SoleraceBra	*Sonchus oleraceus* from Brazil
TdivNigCtR	roots of Nigerian *T. diversifolia* control leaves

LIST OF SYMBOLS

α	Alpha
β	Beta
TM	Trademark
©	Copyright

TABLE OF CONTENTS

1. INTRODUCTION

Persistent hyperglycemia characterizes the prediabetic state, often progressing to diabetes mellitus (DM) within a few years. As a chronic endocrine disorder, DM constitutes a significant global health challenge. About 415 million people were estimated to be affected by DM in 2015 globally, with 5.0 million deaths attributed to it and it is expected to increase to 642 million by 2040 (OGURTSOVA et al., 2017)[1]. Insulin resistance, the main characteristic of type 2 diabetes (T2D), the most common class of DM, and reduction in insulin secretion lead to hyperglycemia, glucose toxicity and consequently, β-cell damage through oxidative stress (Figures 1 and 2). To prevent or delay progression of prediabetes to diabetes, and the associated glucose toxicity, with the attendant reduction of neutrophils, it is essential to reduce or prevent hyperglycemia hyperglycemia

1.1 Hyperglycemia

Chronic hyperglycemia is characteristic of diabetes and its complications, usually observed years after its onset (REUSCH, 2003). Glucose toxicity results due to various upsetting effects of chronic hyperglycemia on various cell types. The pancreatic β-cells' insulin secretory function is initially reduced by hyperglycemia and this reduction, in turn, causes an increase in insulin resistance further aggravating hyperglycemia (LEROITH, 2002; DUBOIS et al., 2007; GIRI et al., 2018). Additionally, even in the acute phase, hyperglycemia causes a decline in neutrophils (STEGANGA et al., 2008), which is the cause of wounds that refuse to heal in diabetics, posing postoperative challenges to such subjects. The pancreas, amongst other tissues and organs, is more susceptible to oxidative stress because the β-islet cells have low manifestation of antioxidative enzymes (TIEDGE et al., 1997; ROBERTSON, 2006). As a consequence, oxidative stress has been associated with the molecular mechanism responsible for the reduced biosynthesis and secretion of insulin, being the principal cause of glucose toxicity; and invariably, diabetic complications (BAYNES; THORPE, 1999; BRUNNER et al., 2009).

[1] Throughout this text, the ASSOCIAÇÃO BRASILEIRA DE NORMAS TÉCNICAS (ABNT) format was used as obtained in the USP Dissertation and Thesis Submission Guidelines, revised version 2016

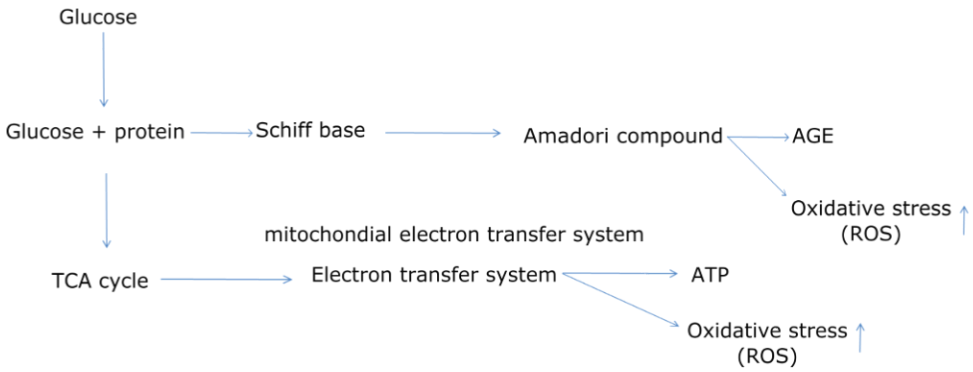

Figure 1: Development of oxidative stress by glucose.
Key: The diabetic state leads to increase in the acceleration of glycation response and intramitochondrial electron transfer system causing oxidative stress. Arrows indicate pathways; arrows facing up indicate increase. AGE: Advanced glycosylation end products; ROS: Reactive oxygen species; TCA: tricarboxylic acid; ATP: Adenosine tri-phosphate (Kawahito et al., 2009).

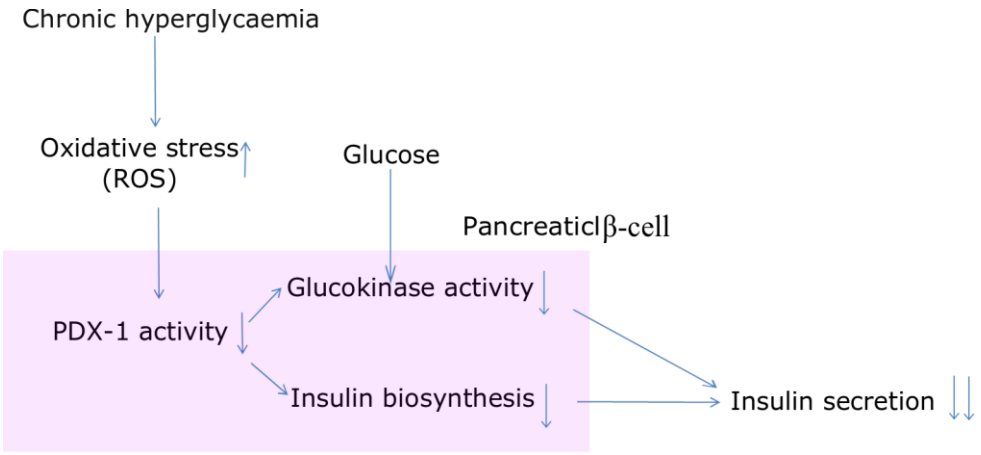

Figure 2: Reduction of insulin secretion by gglucose toxicity
Key: Hyperglycaemia causes oxidative stress which leads to reduction of DNA binding capacity of PDX-1, insulin biosynthesis and secretion. Arrows indicate pathways; arrows facing up indicate increase; arrows facing down indicate decrease. PDX-1: Pancreatic duodenal homeobox (Kawahito et al., 2009).

Additionally, glucose toxicity is involved in the development of insulin resistance. Chronic hyperglycemia has been reported to induce insulin resistance via the generation of oxidative stress (ERIKSSON, 2007). Exposing primary adipocyte cells to chronic hyperglycemia may cause oxidative stress (LU et al., 2001). The insulin-mediated glucose transport into skeletal muscles through the translocation of Glut 4 was shown to be inhibited by oxidative stress, thereby causing hyperglycemia. This, in turn, was shown to induce

insulin resistance in 3T3-L1 adipocyte cell line (RUDICH et al., 1998). Hyperglycemia therefore produces ROS and causes DNA damage; playing an important role in inflammatory responses. It has been reported to stimulate polyol and hexosamine pathways. Others may include advanced glycation end products (AGEs) formation and protein kinase C (PKC) activation (GIRI et al., 2018). It has also been demonstrated that hyperglycemia-induced insulin resistance is not readily reversible (SUN et al., 2014).

Oxidative stress constitutes an imbalance between the oxidizing system and an antioxidant system that has been compromised. Under physiological conditions, cellular metabolism generates free radicals, which are removed by the antioxidant system. There are various reports with this causal effect of hyperglycaemia (RAINS; JAIN, 2010; TIWARI et al., 2013). The oxidation of excess glucose by glycolysis and Krebs cycle leads to excess production of electron donors including NADH and FADH2. This increases ATP/ADP ratio and modifies the mitochondrial membrane potential. As proton gradient increases, more electrochemical potential difference is created, thereby reducing the electron transport machinery in complex III (GIRI et al., 2018). This results in the buildup of electrons in coenzyme Q, leading to free radical superoxide generation, and can be converted to other forms of ROS such as peroxynitrite ($ONOO^-$), hydroxyl ($^{\cdot}OH$) and hydrogen peroxide (H_2O_2) (GIRI et al., 2018). Apart from cellular mitochondria, another source for the generation of ROS is the peroxisome. It has been proposed that the generation of ROS play a critical role in mitochondrial dysfunction and mitochondrial stress, having a significant role in development of diabetes.

1.1.1. Glucose desensitization and toxicity

Glucose desensitization involves transient, physiological and reversible state of cellular dysfunction caused by successive exposure to elevated glucose concentrations similar to how receptor down-regulation occurs; whereas, glucose toxicity is significantly more serious, being a state of non-physiological, irreversible cellular dysfunction due to chronic exposure to elevated glucose concentrations (ROBERTSON et al., 1994). In relation to etiology as it affects pancreatic β-cells, expression of glucose desensitization was suggested to be at the level of insulin exocytotic apparatus or insulin stores within β-cells, while glucose toxicity was suggested to be at the level of insulin gene transcription. It has

therefore been reported that chronic hyperglycemia may aggravate β-cell dysfunction through glucose toxicity (SHARMA et al., 1995; HARMON et al., 1999).

1.1.2. Complications of diabetes

As a result of impaired glucose tolerance (IGT), reports have shown a high cardiovascular risk even before the development of T2DM. Therefore, in a Paris Prospective Study as in other studies involving European, Asian and Japanese populations, the incidence of CVD mortality was significantly higher in IGT patients than in normoglycemic subjects (FADINI et al., 2007).

Chronic hyperglycemia is important in the development of both micro- and macrovascular complications including microangiopathy, cardiovascular, cerebrovascular and metabolic syndrome diseases. Sedentary lifestyle and widespread consumption of high-carbohydrate and high-fat diets have led to the increasing prevalence of T2D (ADISAKWATTANA; CHANATHONG, 2011). Chronic hyperglycemia is one of the major causes of organ damage. Hyperglycemia-induced oxidative stress is also involved in the development of both macrovascular and microvascular diabetic complications (Table 1).

Table 1: Diabetic complications

Chronic complications	**Microvascular diseases**	retinopathy, neuropathy, nephropathy
	Macrovascular diseases	aortic sclerosis, stroke, myocardial infarction, angina pectoris, obstructive peripheral vascular disease, etc
	Others	cataract, dermatopathy, hypertension, osteopenia, osteomalacia, arthropathy, soft tissue fibromatosis, etc
Acute complications	**Diabetic coma**	ketoacidotic coma, non-ketotic hyperosmolar coma, lactic acidosis
	Acute infection	bacterial, mycotic, viral, etc

Chronic hyperglycemia can induce microvascular complications such as retinopathy, neuropathy or nephropathy (YAMAGISHI; IMAIZUMI, 2005). Chronic hyperglycemia can also induce macrovascular complications. It has been evidenced that diabetic and prediabetic chronic hyperglycemia are linked to a higher risk for developing cardiovascular disorders, the most predominant cause of death in diabetic patients (GROBBEE, 2003).

Protracted exposure of macrovessels to elevated glucose concentration increased the likelihood of cardiovascular, cerebrovascular and peripheral arterial diseases (THOMPSON, 2008). Some perioperative problems such as cardiac, neurologic and infectious complications may be aggravated by hyperglycemia, whose reduction improves the conditions (CLEMENT et al., 2004). Additionally, “hyperglycemic memory” refers to the development of retinopathy during post-hyperglycemic normoglycemia, further emphasizing the need to prevent hyperglycaemia.

1.1.3. Diabetes, prediabetes and hyperglycemia: The link

Type 2 Diabetes Mellitus develops due to a mix of primary, secondary and tertiary etiological factors (VAAG, 1999). Adverse intrauterine environment and genetics constitute primary factors that predispose subjects to the development of diabetes; whereas, obesity, low physical activity and age constitute secondary factors. The tertiary factors are constituted by glucose and lipid toxicities (VAAG; LUND et al., 2007).

The United Kingdom Prospective Diabetes Study (UKPDS) reported that before the development of overt hyperglycemia, progressive impairment of insulin secretion leads to T2DM; an impairment whose progress cannot be halted using any of the currently available hypoglycaemic agents, such as metformin, insulin secretagogues or insulin (HOLMAN, 2006; U.K. PROSPECTIVE DIABETES STUDY GROUP, 1995).

Physiologic glycaemia has beneficial regulatory effects on insulin gene transcription, translation, mRNA stabilization, insulin storage, and insulin exocytosis. Chronic hyperglycemia, however, was proposed to negatively influence these beneficial regulatory effects via glucose desensitization and glucose toxicity (ROBERTSON et al., 1994). Prolonged insulin secretion and exhaustion of the islet cells due to exposure to elevated glucose concentration has been attributed to decreased β-cell responsiveness (KAISER et al., 1991).

Prediabetes, which includes IGT and impaired fasting glucose, is a hyperglycemic state with blood glucose level higher than normal but not sufficiently high for the diagnosis of T2D (IDF, 2019). IGT, diagnosed by plasma glucose levels (7.8–11.0 mmol/L) measured 2 hours after a 75-g glucose load and fasting plasma glucose (FPG) level (> 6.1 mmol/L), are key risk factors for T2DM (UNWIN et al., 2002). IGT has long posed a significantly high

risk for the development of diabetes and cardiovascular disease. Without appropriate interventions, about 90% of IGT incidents progress to T2DM within 20 years, and at least a myocardial infarction or stroke event has been reported in half of such incidents. It was therefore suggested that preventing the progression of IGT to T2DM constitutes an important strategy in managing T2DM. In addition, in subjects with undiagnosed chronic hyperglycaemia, development of complications has been reported (JOSHI, 2007; IDF, 2019).

1.1.4. Prevention of hyperglycemia

For the reasons that chronic hyperglycemia causes glucose toxicity and leads to the development of diabetes, amongst other effects such as reduction of neutrophils and proliferative effect on cancer cells (RYU et al., 2014), it is essential to prevent its development rather than attempting to reduce it after it has been established or after diabetes has developed. It has been shown that prevention of hyperglycemia in *in vivo* model of T2D preserves insulin and PDX-1 gene expression (HARMON et al., 1999).

Postprandial hyperglycaemia is controlled by maintaining a balance between glucose absorption from the gut, tissue utilization of glucose and endogenous glucose production (MEYER, 2002). Additionally, patients usually relapse with mild to moderate hyperglycemia after an initial response to oral hypoglycemic agents; and this is in spite of the fact that sometimes with insulin therapy added to or substituted for oral agents, mild to moderate hyperglycemia is frequently reported in the so-treated diabetics, for many years (ROBERTSON et al., 1994). This relapse is usually referred to as secondary drug failure or a result of hyperglycaemic memory.

The experiments of Robertson et al. (1994) showed that exposing β-islet cells chronically to high glucose may ultimately lead to glucose toxicity, without the exclusion of the proposition that acute exposure to hyperglycemia can desensitize the islet; thereby exacerbate clinical hyperglycemia. Corroborating this, it has been reported that restoration of acute normo-glycaemia reestablishes “first-phase glucose-induced insulin secretion” (TURNER et al*.,* 1976; VAGUE; MOULIN, 1982), which is referred to as “resensitizing the islet cells to glucose.” Defective β-cell function in T2D subjects results due to glucose toxicity, glucose desensitization or both; and this situation calls for a review of how glycaemia is viewed and managed. This is in view of the fact that in prediabetic subjects, acute and

chronic hyperglycemia are frequently observed and this may predispose the subjects to the consequences of acute and chronic exposure of the β-islet cells to high glucose as previously enunciated.

It has also been demonstrated by clinical studies that lifestyle modifications are effective to prevent progression of IGT to diabetes. Data suggests that insulin sensitizers, α-glucosidase inhibitors and metformin can relatively delay the development of diabetes (LIAN et al., 2014) but their associated side effects, especially considering that they may need to be used for a long period of time discourages their use for this purpose (TEDONG et al., 2010).

Additionally, it has been reported that T2DM can be delayed and even prevented by ylifestyle modifications including increasing physical activity and low-carbohydrate diet. With the high likelihood of low compliance to this approach, alternative strategies are required for the prevention of T2DM. Delayed onset of T2DM can also be achieved with antidiabetic drugs (VAAG; LUND, 2007). The UKPDS trial demonstrated that glucose-reduction related to reducing the incidence and mortality from CVD in obese patients with T2DM was uniquely achieved with metformin (UK PROSPECTIVE DIABETES STUDY GROUP, 1998).

Although, it is not clear which is more important, of insulin resistance and impaired *β*-cell function evident in IGT, for the progression of pre-diabetes to diabetes (ERIKSSON et al., 1989; WARRAM et al., 1990; LILLIOJA et al., 1993), each one has important considerations towards preventing progression. Diet regulation and tolbutamide have together been suggested, in a 12-year trial, as a way to “prevent or postpone” progression of IGT to diabetes (SARTOR et al., 1980). Appropriate management of postprandial hyperglycemia in the prediabetic state may consequently improve overall outcome. Insulin resistance, on another hand, and as an advanced stage of the effects of hyperglycaemia, requires intervention with drugs that improve insulin sensitivity such as metformin and glitazones (THE DIABETES PREVENTION PROGRAM RESEARCH GROUP, 1999; ERIKSSON et al., 2006). The DPP study reported that metformin lowered the risk of progression to diabetes by 31% (THE DIABETES PREVENTION PROGRAM RESEARCH GROUP, 1999).

1.2. Approaches to prevent hyperglycemia

Ethnomedicinally, herbal medicines from plants and vegetables have been used for the management of hyperglycemia; many of these herbal medicines therefore offer the opportunity for developing, from natural sources, newer drugs to prevent hyperglycemia (ADISAKWATTANA; CHANATHONG, 2011) which may, in addition to their activity elicit lesser toxicity than the currently available hypoglycaemic drugs.

To evaluate the potential of plants and their specialized metabolites for the ability to prevent or reduce hyperglycaemia for the prevention of development of diabetes, glucose diffusion retardation, glucose uptake enhancement, antioxidant, as well as α-amylase inhibitory assays are essential approaches used to screen for bioactivity.

1.2.1. Inhibitory activity against α-amylase

The α-amylase inhibitory assay has been employed for the investigation of plants with potential antidiabetic properties (GALLAGHER et al., 2003; KIM et al., 2004; ADISAKWATTANA; CHANATHONG, 2011; KUMAR et al., 2011; YILMAZER-MUSA et al., 2012; NAJAFIAN, 2015) using acarbose (Figure 3) as positive control. The molecular interaction of acarbose with α-amylase is presented (Figure 4).

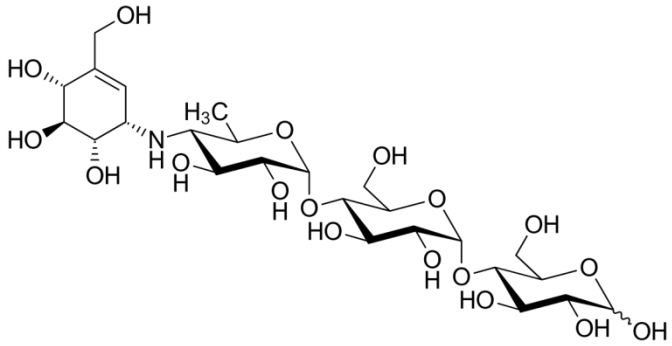

Figure 3: The chemical structure of acarbose
Saoud, Akowuah and Fatokun (2017)

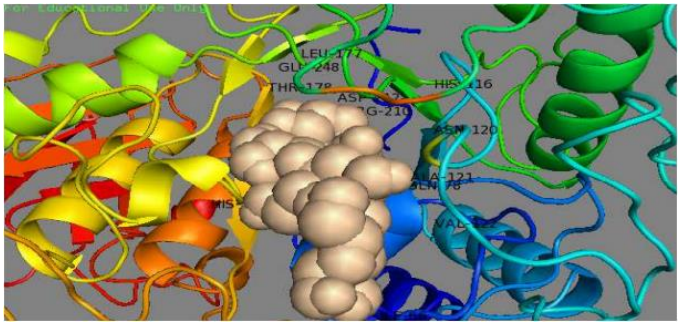

Figure 4: Molecular interaction of acarbose with α-amylase
METIBEMU et al. (2016)

The inhibition of α-amylase, aimed at reducing glucose absorption through the gut, has been reported to be significant in the prevention of postprandial hyperglycemia (SHIM et al., 2003). In 2010, it was reported that the methanolic extract of *Amaranthus spinosa* Linn. (Amaranthaceae), used ethnomedicinally for the treatment of diabetes, significantly inhibited α-amylase at concentrations 10.0, 50.0 and 100.0 µg/mL by 38.0 ± 0.1%, 55.9 ± 0.1% and 63.1 ± 0.1% respectively, with an IC_{50} of 46.0 µg/mL While it has been demonstrated that drugs, which inhibit carbohydrate hydrolyzing enzymes, decrease postprandial hyperglycemia and improve impaired glucose metabolism without inducing insulin secretion in T2DM, the study concluded that *A. spinosus* may have active component(s) with potent anti-diabetic properties (KUMAR et al*.,* 2011). Procyanidins, found in grape seed extract, strongly inhibited α-amylase activity (YILMAZER-MUSA et al*.,* 2012). An α-amylase inhibitory study, utilizing various extract concentrations between 0.1 and 5.0 µg/mL, reported a range of percentage α-amylase inhibitory activity for the barks and needles respectively of *Pinus densiflora* (89.6 ± 5.2%; 72.7 ± 4.9%), *Pinus thunbergii* (17.6 ± 2.3%; 82.4 ± 5.3%), *Pinus rigida* (18.6 ± 4.3%; 23.4 ± 1.6%), *Pinus koraiensis* (79.2 ± 8.9%; 8.6 ± 2.3%) and *Taxus cuspidate* (17.9 ± 2.7%; 0.6 ± 0.4%) (KIM et al*.,* 2004). Six groups of flavonoids were evaluated for porcine pancreatic α-amylase inhibitory activity and it was determined that luteolin (KIM et al*.,* 2000), myricetin and quercetin were potent against the enzyme with IC_{50} less than 500.0 µM (TADERA et al*.,* 2006). It was reported that the inhibitory activity was enhanced by 2,3-double bond, 5-OH, the linkage of the B ring at position 3 and a hydroxyl substitution on the B ring, while 3-OH reduced it (TADERA et al*.,* 2006). Although, an earlier study reported higher values of 97.5% and 93.8% for 1 µg/mL of methanol and successive water extracts respectively of bark of *Cinnamomum tamala* (KUMANAN et al*.,* 2010), another study evaluated 126 extracts obtained from 17 plants for

inhibition of porcine pancreatic α-amylase activity, and reported that 17 of them exhibited varying degrees of activity between 10 and 60.5% with 4 extracts showing low inhibition (< 10%) (SUDHA et al., 2011). Furthermore, it was reported by the study of ALI et al. (2006) that the hexane extract of *Phyllanthus amarus* contains α-amylase inhibitory compounds by virtue of its 24.3% inhibitory activity against the enzyme (ALI et al., 2006).

Plant phenolics have uniquely been ascribed with inhibitory potential against α- and β-glycosidases, because of their possession of a common structural feature, a hydroxylated aromatic ring resembling the sugar structures; hence, are able to compete with the sugar units for the enzyme active sites.

1.2.2. Glucose retardation activity

A study evaluated the effects of ten aqueous plant extracts (50.0 mg/mL) with proven antihyperglycemic properties on glucose diffusion across dialysis tube and reported that *Agrimony eupatoria* and *Persea americana* retarded glucose movement *in vitro* by more than 50.0% while the other plants exhibited lesser activities (GALLAGHER et al., 2003).

The glucose retardation activity of methanolic extracts of five ethnomedicinally used antidiabetic native medicinal plants of Mauritius, *Stillingia lineata*, *Faujasiopsis flexuosa*, *Erythroxylum laurifolium*, *Elaeodendron orientale* and *Antidesma madagascariensis* was evaluated. The plants exhibited significant ($P < 0.05$) “glucose entrapment capacities” between 8.0 and 29.0%, with *S. lineata* being the most active at 29.0% (PICOT et al., 2014). In another study, a higher percentage of glucose retardation (32.0 and 46.7%) was reported for 20.0 and 40.0 mg/mL of aqueous extracts of *Zingiber officinale* rhizomes respectively (SATTAR et al., 2012).

1.2.3. Glucose uptake enhancement activity

Another of the mechanisms for managing hyperglycaemia is via improving insulin sensitisation to enhance glucose uptake (VAN DE VENTER et al., 2008). Extract of *Vernonia amygdalina* leaves has been shown to significantly improve glucose utilization in C2C12 muscle cells (ERASTO et al., 2009), corroborating the ethnomedicinal antidiabetic use of the plant. Others include extracts of *Euclea undulata, Schkuhria pinnata* (DEUTSCHLÄNDER et

al., 2009), *Tanacetum nubigenum* (KHAN et al., 2018), *Ruta graveolens* and *Tulbaghia violacea,* among others (VAN HUYSSTEEN et al., 2011).

With regards to active plant metabolites, the presence of flavonoid and other phenolic compounds have been attributed to the antidiabetic activity of the plants containing them (BAHADORAN et al., 2013; KHAN et al., 2018). Isolates from *Artemisia dracunculus* L. (Asteraceae), 6-demethoxycapillarisin and 2',4'-dihydroxy-4-methoxydihydrochalcone have been reported to activate the PI3K, similar to insulin, and the AMP-activated protein kinase (AMPK) pathways (GOVORKO et al., 2007) respectively.

Stevioside, isolated from *Stevia rebaudiana* leaves, has been reported responsible for the plant's anti-hyperglycaemic, insulinotropic and glucagonostatic actions (JEPPESEN et al., 2002). The methanolic extract of *Smalanthus sonchifolius* H. Robinson, rich in flavonoids and chlorogenic acids, was reported to have anti-oxidant and antidiabetic properties (RUSSO et al., 2015) with its leaf extracts exhibiting anti-hyperglycaemic properties through the reduction of hepatic glucose production via gluconeogenesis and glycogenolysis (VALENTOVA; ULRICHOVA, 2003). It was reported that the potential of yacon to treat hyperglycemia and the cytoprotective activity of its leaves are predominantly related to its oligofructan and phenolic content, respectively. *Ageratum conyzoides* L., which has been reported antidiabetic, was found to contain some trace and macro elements, including Mg, Zn, Cl, Ca, V, Mn, Sr, Na and K (MAGILI et al., 2014) and active principles, including alkaloids, cardenolides, tannins, saponins and flavonoids (EGUNYOMI et al., 2011).

Another study found that oleuropein enhanced glucose uptake and insulin sensitivity in C2C12 cells through the activation of AMPK dose-dependently; the observed insulin sensitization is associated with translocation of GLUT4 cells by insulin-independent (AMPK/ACC and MAPKs) and insulin-dependent (PI3 kinase/Akt) pathways (HADRICH et al., 2016).

1.2.4. Antioxidant activity

The generation of reactive oxygen species (ROS) has been shown to increase due to chronic hyperglycemia, leading to overproduction of ROS and malfunction of endogenous antioxidant system often causing several chronic disorders, including DM, as a result of

oxidative stress; through the oxidative alteration of cellular components further damaging pancreatic β-cells and causing diabetes complications (CHOI, 2016).

To investigate the suggestion that oxidative stress may be managed by supplementing the physiological antioxidant system with safe alternatives including diet (AL-DABBAS et al., 2006), the aqueous extracts of *Hibiscus sabdariffa* Linn. was demonstrated to significantly scavenge free radicals, thereby preventing the oxidative damage of the pancreas (ADEMILUYI; OBOH, 2013). The study concluded that the metabolites from the species may have potential to prevent or manage T2D and complications arising from postprandial hyperglycemia due to oxidative stress. Isorhamnetin was shown to scavenge intracellular ROS in C2C12 myoblasts, additionally reducing H_2O_2-induced DNA damage and apoptosis, evidencing the cyto-protective potential of isorhamnetin to prevent oxidative-stress-induced cell toxicity (CHOI, 2016).

Oleuropein, a glycosylated seco-iridoid, and luteolin, a flavonoid, have been reported to decrease glycaemia *in vivo*, manage symptoms of hyperglycemic and enhance antioxidant activity, therefore with a potential to prevent diabetes (WAINSTEIN et al., 2012). A recent study on the effect of metformin on C2C12 cells demonstrated a new molecular mechanism of action for metformin, including the activation of Nuclear factor erythroid 2-related factor 2 (Nrf2) signaling and enhancement of tissue antioxidant capacity (YANG et al., 2014).

1.3. Asteraceae and the control of hyperglycemia

The Asteraceae, formerly known as Compositae and commonly called the aster, daisy, composite (BLACKWELL, 2006) or sunflower family, constitutes a large and widespread family of flowering plants (Angiospermae) (STEVENS, 2001; JEFFREY, 2007). The family comprises more than 23,000 currently accepted species, with over 1,620 genera and 12 subfamilies. It is the largest family of flowering plants, followed by the Orchidaceae (STEVENS, 2001).

Asteraceae has profound ecological and economic importance and occurs from the polar regions to the tropics, colonizing all available habitats. It is distributed worldwide, most commonly in the arid and semi-arid regions of subtropical and lower temperate latitudes (SOLBRIG, 1963).

Africa and Brazil have a rich history of flora and they constitute a hotspot of biodiversity. Member plants of the Asteraceae family basically store energy in the form of inulin. They produce iso/chlorogenic acid, sesquiterpene lactones, pentacyclic triterpene alcohols, acetylenes (cyclic, aromatic, with vinyl end groups), tannins and, in some few genera, alkaloids.

Numerous Asteraceae plants have been reported useful in the management of diabetes (VALENTOVA; ULRICHOVA, 2003; EGUNYOMI et al., 2011; PETCHI et al., 2013; MAGILI et al., 2014; RUSSO et al., 2015).

In addition, tannins, saponins, alkaloids, amino acids, steroids and terpenoids from *Anacyclus pyrethrum* L. (SELLES et al., 2012), the ethanolic root extract of *Arctium lappa* L. (CAO et al., 2012), flavonoids, saponins, terpenes and tannins from *Artemisia judaica* L. (NOFAL et al., 2009), aqueous seed extract of *Artemisia sphaerocephala* Krasch (ZHANG et al*.,* 2006), aqueous extract of *Bidens pilosa* L. var. *radiata* (HSU et al*.,* 2009), carotenoids, flavonoids, glycosides, steroids and sterols from *Calendula officinalis* L. (CHAKRABORTHY et al*.,* 2011), alkaloids, tannins, saponins and cardiac glycosides from *Vernonia amygdalina* Del. (EKEOCHA et al*.,* 2012) and aqueous leaf extract of *Vernonia colorata* (Wilid.) Drake (SY et al*.,* 2004) have all been reported to be responsible for the activity of these antidiabetic Asteraceae plants.

This suggests that Asteraceae may constitute an important source of metabolites with potential to manage hyperglycaemia and prevent diabetes.

1.4. Metabolomics

Untargeted metabolomics, one of the “omics” strategies, aims at the identification and quantification of the complete set of metabolites in a given organism. It has been proven to be a valuable tool in determining interesting bioactive plant specialized metabolites (FUJIMURA et al., 2011) from the complexity that makes up the metabolome.

The metabolome constitutes a collection of all metabolites, which are products of cellular processes in biological systems (JORDAN et al., 2009). Standard laboratory equipment such as NMR, IR and MS can aid the acquisition of metabolomic data for downstream processing (RADULOVIC et al., 2014).

The approaches deployed in metabolomics require efficient strategies to unravel relevant biological information, including experimental design, sample preparation and extraction, metabolites separation and detection, data processing and bioinformatics analysis of metabolite profiles (SAS et al., 2015). Metabolic fingerprint, which is a chemical fingerprint or signature of the plant, and subsequently the determination of a group of metabolites of interest responsible for observed bioactivities, can be obtained using these advanced and efficient tools.

Annotation of metabolites indicated as important by metabolomics strategies is usually performed by dereplication, which is the rapid determination of the structures of the metabolites already known and previously reported in databases such as SciFinder or the Dictionary of Natural Products (DNP) without the need for isolation. The annotated metabolites may then be isolated for structural characterization (GOBBO-NETO et al., 2008, HOSTETTMANN et al., 2001). For the metabolomic analysis of plants, the techniques of choice often include high performance or ultra-high performance liquid chromatography (HPLC or UHPLC) coupled to a diode-array detector (UV-DAD) and high resolution mass spectrometry (HRMS) - LC-UV-HRMS, and/or gas chromatography coupled to mass spectrometry (GC-MS) (VILLAS-BOAS et al., 2005). The versatility of LC-MS permits the separation and detection of various classes of metabolites, depending on the particular separation technique and mass analyzer deployed (SAS et al., 2015).

Hypothesis-generating untargeted metabolomics, which aims to detect as many metabolites (small molecules < 1000 Da) as possible in a particular sample simultaneously, is significantly reliant on MS technology for the measurement of various features as well as bioinformatics tools to handle the generated data. Routine detection of thousands of features in one run has been made possible by recent advances in MS technology; such that untargeted analysis is selectively being implemented by LC-electrospray ionization (ESI)-HRMS (HOLLENDER et al., 2017). Electrospray ionization (ESI) has innovated the ionization of bio-molecules and their preparation for detection by mass spectrometers, capable of transmitting ionized molecules to the gas phase directly from liquid phase. It has been applied in high throughput screening due to its fast and full compatibility with LC and also compliant with MS analysis of multicomponent polar natural product extracts (SAWAYA et al., 2004). ESI-MS in the negative ion mode afforded a distinction of the geographical origins

of propolis samples based on the variation in their composition including flavonoids, terpenoids or phenolic compounds (SAWAYA et al., 2004). Environmental pollutants were detected and characterized by untargeted analysis using high-resolution mass spectrometry (HRMS) (KRAUSS et al., 2010; CHIAIA-HERNANDEZ et al., 2014; SCHYMANSKI et al., 2015).

The metabolic fingerprinting spectral data obtained from the LC-UV-HRMS is greatly multivariate therefore requiring multivariate statistical methods in analyzing the huge variability of the large amount of data obtained through efficient and sensitive metabolomics analysis. For this to be implemented, preprocessing of the data is essential for chromatogram deconvolution, baseline normalization and correction (LILAND et al., 2011). Data preprocessing can be achieved using different programs such as MetAlign™ (RIKILT, The Netherlands), MSClust™ (Plant Research International, The Netherlands), XC-MS™ (METLIN, USA) and Mzmine™ (BMC Bioinformatics, UK).

To efficiently manage and analyze the preprocessed data, various *in silico* methods are used for data mining and multivariate statistical analyzes. Unscrambler X (CAMO Software, Norway), R and SIMCA are some of the statistical software that can be used to perform such procedures. The analysis of the data can be performed using appropriate statistical models to investigate the correlation between the variables and determine discriminant variables. Such may include Hierarchical Cluster Analysis (HCA), Partial Least Square Discriminant Analysis (PLS-DA), Orthogonal Partial Least Square Discriminant Analysis (OPLS-DA), Principal Components Analysis (PCA) and Soft Independent Modeling by Class Analogy (SIMCA) methods (YULIANA et al., 2011; WECKWERTH, 2005; LANG, 2008, KATAJAMAA; ORESIC, 2007).

The PCA is fundamental to most of the multivariate analytic methods, describing the variance that exists in a set of multivariate data on the basis of a set of orthogonal variables in an unsupervised fashion. These variables may be expressed as a linear combination of the principal components (PC), where each PC is responsible for a percentage of the total variance of the data. It is usual to find a small set of principal components capable of reducing the dimensionality of the data with plots providing a rapid visualization of similarities and/or differences in the data, thereby improving the discrimination of the samples (SAWAYA et al., 2004). Grouping of samples based on their chemical similarity can also be achieved using

HCA, another unsupervised method, and visualized as dendograms, with branch lengths indicating the distance between the groups (SUMNER et al., 2003). The HCA highlights the global differences or similarities existing in the huge metabolic data obtained for the plants, thereby providing a way to visualize such relationships.

Supervision with specific sample information such as bioactivity may permit PLS-DA to decompose the data more efficiently, based on the covariance between the X-variables (explanatory) and the Y-variables (response) (LILAND et al., 2011; TRIVEDI; ILES, 2012). Using PLS-DA, the variable importance in projection plots (VIP) can present the relationship between the X and Y variables, significant for the determination of the features responsible for differentiating the classes supervised in the analyzes. The higher the VIP score, the more significant the feature is in the separation of the classes (TRIVEDI; ILES, 2012).

The application of untargeted metabolomics to the study of bioactive natural products has recently been gaining interest globally. Without the need for bioactivity-guided fractionation and isolation, varied phytoconstituents can be identified in numerous plant extracts by Mass Spectrometry-based metabolomics and the significant differences between the extracts determined through HCA and PCA. Partial Least Square Discriminant Analysis can correlate the MS with bioassay data to determine the variables (metabolites) in the MS data responsible for the observed bioactivities. Such significant variables may then be annotated or identified, isolated and their structures confirmed, with further bioassays, including clinical trials, implemented to confirm their activities. The evaluation of different Asteraceae species from different tribes, countries and locations may afford a rigorous, strong and unbias correlation using multivariate statistical methods, whose success will prove a proof-of-principle for the use of untargeted metabolomics for the determination of plant specialized metabolites with antidiabetic potentials (SAWAYA et al., 2004).

There are several Asteraceae species, endemic to both Africa and Brazil. However, the family has yet to be studied with the aim of deploying metabolomics approaches for the determination of metabolites with the potential to prevent or reduce postprandial hyperglycaemia; hence, this study.

2. OBJECTIVES

The main objectives of this research were to obtain metabolic fingerprints of selected Brazilian and Nigerian Asteraceae species of plants, evaluate their *in-vitro* antidiabetic properties and correlate the observed activities with their metabolic fingerprints acquired by UHPLC-UV(DAD)-HRMS, in order to determine, *in silico*, the potentially active specialized metabolites.

Specifically, the objectives are to:

a) select Brazilian and Nigerian Asteraceae species of plants and evaluate their ability to prevent hyperglycemia using five *in vitro* assays, including glucose diffusion retardation, glucose uptake enhancement, antioxidant, as well as fungal and porcine pancreatic α-amylase inhibitory assays;
b) obtain the non-target metabolic fingerprints of the selected plants using UHPLC-UV(DAD) -HRMS (ESI-orbitrap);
c) determine the most active of the selected plants in the *in vitro* assays;
d) use multivariate statistical analyses to correlate the responses obtained from the *in vitro* assays with the plants' metabolic fingerprints to point out, *in silico*, the specialized metabolites responsible for the classification of the active plant extracts different from the inactive extracts;
e) annotate the chemical features of the metabolites indicated by the discriminant analysis using dereplication techniques and
f) isolate some of the compounds for further structural elucidation in order to validate the dereplication techniques;
g) evaluate some of the discriminant metabolites and their analogues for the ability to prevent hyperglycaemia using *in vitro* porcine pancreatic α-amylase assay, and attempt correlating the structural features with the observed activities of the compounds.
h) Determine the IC50 of the most active metabolites from (g.) above.

3. MATERIALS AND METHODS

3.1. Plants

In this study, 68 samples obtained from the Asteraceae family and belonging to 43 genera and 54 species, chosen mainly based on availability, use as functional food, reports of popular medicinal use as antidiabetic and other previously reported bioactivities, were analyzed. The voucher specimens and their numbers were deposited at the Herbaria of the Faculty of Pharmacy, Obafemi Awolowo University, Ile-Ife, Nigeria and Departament of Botany, Institute of Biology, UNICAMP, SP, Brazil, and recorded accordingly. Samples collected in Ile-Ife, Nigeria includes leaves of *Tithonia diversifolia* (Hemsl.) A. Gray (FPI1942), *Vernonia cinerea* (L.) Less. (FPI2128), *Struchium sparganophora* (L.) O. Kuntze (FPI2131), *Vernonia amygdalina* Del. (FPI2129), *Acanthospermum hispidum* DC. (FPI2115), *Launea taraxacifolia* (Willd) Amin Ex. C. Jeffrey (FPI2133), *Tridax procumbens* Linn. (FPI2123), *Tithonia diversifolia* (Hemsl.) A. Gray (FPI2127), *Emilia praetermissa* Milne-Redhead (Nig) (FPI2120), *Senecio biafrae* Oliver & Hiern J. Moore (FPI2124), *Melanthera scandens* (Schumach & Thonn.) Roberty (FPI2130), *Ageratum conyzoides* Linn. (FPI2116), *Synedrella nodiflora* (Linn.) Gaertn (FPI2126), *Eupatorium odoratum* Linn. (FPI2119), *Aspilia africana* (Pers.)C.D. Adams (FPI2117), *Bidens pilosa* Linn. (FPI2114), *Erigeron floribundus* (H.B. et K.) Sch. Bip. (FPI2122) leaves and aerial parts, *Eclipta alba* (L.) Hassk. (FPI2121), *Spilanthes filicaulis* (Schum. et Thonn.) CD Adams (FPI2125) and *Crassocephalum crepidioides* (Benth.) S. Moore (FPI2118). Samples collected in Brazil include aerial parts of *Eremanthus glomerulatus* Less. (LGN009), *Eremanthus veadeiroensis* H.Rob. (Loeuille 837), *Crepis japonica* (Linn.) Benth. (LGN060), *Sonchus oleraceus* Linn. (LGN058), *Emilia fosbergii* Nicolson (LGN059), *Galinsoga parviflora* Cav. (LGN040), *Tridax procumbens* Linn. (LGN047), *Bidens pilosa* Linn. (LGN062) and *Micania micrantha* HBK (LGN006); leaves of *Vernonia condensata* Baker (L.A. Chibli et al. 174), *Vernonia brasiliana* (L.) Druce (LGN035), *Vernonanthura ferruginea* (LESS.) H. Rob. (LGN042), *Vernonanthura phosphorica (Vell.) H. Rob.* (LGN026), *Vernonanthura phosphorica (Vell.) H. Rob.* (L.A. Chibli 173) and *Elephantopus mollis* Kunth. (LNG063).

The following were donated by the Chá e Cia - Ervas Medicinais, Jacareí, SP, Brazil: aerial parts of *Grindelia robusta* Nutt., *Baccharis gaudichaudiana* DC., *Baccharis*

genistelloides (Lam). Pers., *Matricaria recutita* L., *Artemisia vulgaris* Linn., *Tanacetum vulgare* Linn., *Tithonia diversifolia* (Hemsl.) A. Gray, *Ageratum conyzoides* Linn., *Mikania hirsuttissima* DC., *Bidens pilosa* Linn., *Cardus benedictus* Linn. and *Taraxacum officinale* Weber; leaves of *Vernonanthura phosphorica (Vell.) H. Rob.*, *Chamomilla recutita* (L.) Rauschert, *Arnica montana* Linn., *Achillea millefolium* Linn., *Cynara scolymus* Linn., *Stevia rebaudiana* Bertoni, *Artemisia absinthium* Linn., *Mikania glomerata* Spreng. and *Arctium lappa* Linn.; flowers of *Achyrocline satureioides* (Lam.) DC., *Cynara scolymus* L. and *Calendula officinalis* Linn.; roots of *Inula helenium* Linn.; and fruits of *Silybum marianum* (Linn.) Gaertn.

It is essential to state that *Vernonia condensata* Baker and *Vernonia amygdalina* Delile are synonyms of the same plant currently renamed *Gymnanthemum amygdalinum* (Delile) Sch. Bip. ex Walp. by Robinson (1999a) in a new classification. However, while *V. condensata* was collected in Brazil, *V*. *amygdalina* was collected in Nigeria, localities where they are currently still commonly referred to with these names.

Matricaria recutita L. and *Chamomilla recutita* (L.) Rauschert are synonyms of the same plant but donated by Chá e Cia - Ervas Medicinais with their respective names.

3.2. Materials and Equipment

Shimadzu™ weighing-machine (model: AUY220), Unique™ ultrasound bath (model: USC-1400), DMSO (Labsynth, Brazil), Milli Q water (Millipore, USA), phosphate buffered saline, trypsin, insulin (Sigma-Aldrich, Brazil), metformin (Sigma-Aldrich, Brazil), C2C12 muscular myoblasts cell lines (from *Mus* musculus; ATCC® CRL-1772, Manassas, VA, USA), Dulbecco's Modified Eagle's Medium - low glucose (1000 mg/L D-glucose; Sigma Aldrich, Brazil), Dulbecco's Modified Eagle's Medium - high glucose (DMEM-Hi, 4500 mg/L D-glucose; Sigma Aldrich, Brazil), Fetal Bovine Serum (Sigma Aldrich, Brazil), Horse Serum (Sigma Aldrich, Brazil), 24-well plates, Centrifuge (Thermo Scientific), Dialysis tube (15.0 mmX 30.5 m; Sigma Aldrich, Brazil), D-glucose (Synth, Brazil), Fanem™ centrifuge tubes, Gehaka™ vortex rotamixer (model: AV-MAGIC), 1-4, α-D-Glucan-glucanohydrolase (porcine pancreatic α-amylase; Sigma Aldrich, Brazil; 10.0 U/mg), fungal α-amylase (from *Aspergillus oryzae*; Sigma-Aldrich, Brazil; 31.1 U/mg), drugs and assay kits (Sigma-Aldrich Co.), UHPLC-Refractive Index and Orbitrap (Thermo Scientific). Commercial reagents which were

used in this study were of analytical grade. The metabolic fingerprints of the plants were obtained using Thermo Scientific™ *Accela* UHPLC equipment (USA) powered by Orbitrap™ technology. A Thermo Scientific diode array ultraviolet light detector (UV-DAD) was used to obtain the UV data, while ionization was effected with an electrospray ionization source (ESI). A Kinetex XB-C18 core shell column (150.0 X 2.1 mm, 1.7 µm, Phenomenex) coupled to a guard cartridge of similar material was employed for chromatographic separation. Data were analyzed using the Xcalibur™ software.

3.3. Sample preparation

The plants were respectively separated into their various parts, leaves, stems, flowers, aerial parts or whole plants (**section** 3.1), dried under air circulation and pulverized using a miller. Each sample was prepared using 10.0 g of dried powder and extracted with 100.0 mL of a solution of MeOH:H2O (9:1, v/v) on an ultrasonic bath for 10 min at room temperature and subsequently dried *in vacuo* with rotary evaporator at 35 ◦C. The extracts were kept at room temperature prior to the *in vitro* assays. To obtain the metabolic fingerprints, 1 mg of each extract was re-suspended with 1.0 mL of MeOH:H2O (9:1, v/v) and hydrocortisone (10.0 µg/mL) was added as internal standard to the extracts which, prior to the analysis, were filtered through a 0.20 µm PTFE membrane.

3.4. Glucose diffusion retardation activity

To evaluate the effects of the plant extracts on glucose movement *in vitro*, the method of Gallagher et al. (2003) was adopted with some modifications. Briefly, 1.0 mL of 50.0 mg/mL of each plant extract in DMSO and 1.0 mL of 0.15M sodium chloride containing 44.0 mM D-glucose (Merck, Darmstadt, Germany) were added into a dialysis tube (20.0 cm X 15.0 mm; Sigma-Aldrich). The tube was sealed at each end and placed in a 50.0 mL centrifuge tube containing 45.0 mL of 0.15M sodium chloride. The control consisted of 1 mL of DMSO replacing the extract. The tubes were placed on an orbital shaker and kept at room temperature. All experiments were done in triplicates. The movement of glucose into the external solution was monitored by withdrawing aliquots (1.0 mL) of the external solution at optimised time intervals (0, 0.5, 1.0, 2.0 and 3.0 h) and these aliquots were tested quantitatively for the presence of glucose using HPLC Refractive Index (Column, Supelcogel

C-611 – 30.0 cm x 7.8 mm; mobile phase, 0.1 mM NaOH; column temperature, 600 C; flow rate, 0.5 mL/min; run time, 20 min; detector, refractive index; mode, positive). The glucose retardation activity (GRA) was calculated using the following formula,

$$GRA = (A_{control} - A_{test}/A_{control}) * 100;$$

where $A_{control}$ = Amount of glucose (mg/mL) in external solution in the absence of plant extract and A_{test} = Amount of glucose (mg/mL) in external solution in the presence of plant extract (GALLAGHER et al., 2003; PICOT et al., 2014).

3.5. Assay of α-amylase activity

To evaluate the effects of the plant extracts on both fungal and porcine pancreatic α-amylase activity *in vitro*, the method of Sathiavelu et al., (2013) was adopted with some modifications. Briefly, solution of each plant extract (200.0 µg/mL; 500.0 µL) prepared with 0.3% DMSO in 0.02 M sodium phosphate buffer (pH 6.9 with 0.006 M sodium chloride) mixed with 500.0 µL of 0.02 M sodium phosphate buffer containing porcine pancreatic α-amylase (0.25 U/mL) was jointly incubated for 10 min at 24 °C. After pre-incubation, 500.0 µl of 0.5% potato starch solution in 0.02M sodium phosphate buffer was added to each tube at 5s intervals. This reaction mixture was then incubated for 30 min at 24 °C and 200.0 µl aliquot of this was subsequently withdrawn and added to a mixture of 200.0 µl of Milli Q deionised water and 600.0 µL of chromogenic 3,5-dinitrosalicylic acid (DNSA) reagent for reducing sugars assays. These tubes were incubated at 100 ^{0}C for 5 min and cooled to room temperature. Finally, the absorbance of 200.0 µL each of the resulting cooled mixture was measured, spectrophotometrically (Biotek Epoch/2 microplate reader), using 96 well plates at 540 nm (SATHIAVELU et al., 2013). The control consisted of replacing the plant extract solution with 500.0 µL of 0.3% DMSO in 0.02M sodium phosphate buffer. Blanks, with deionised water replacing the enzyme solution, were run in order to eliminate background absorbance introduced by each of the extracts. The above procedures were similarly conducted on fungal α-amylase (from *Aspergillus oryzae*; 0.25 U/mL).

3.6. Glucose uptake activity in C2C12 cells

The C2C12 mouse myoblast cell line obtained from the American Type Culture Collection were cultured in DMEM containing 4.5 g/L D-glucose with 10% heat-inactivated FBS at 37 °C, 5.0% CO_2 atmosphere. The cells were seeded into 24-well plates with three

wells left as blank and they were left to grow to confluence; then, cells were fully differentiated in DMEM with 2% Horse Serum for 5 days. For the tests, the medium was replaced by low glucose DMEM without serum and left for 5 hours to starve the cells of glucose (TEDONG et al., 2010; KIM et al., 2013). For the negative controls, only the starvation low glucose DMEM was administered while for the positive control and the tests, metformin (0.01 mM) or the test extracts (10.0 µg/mL) were respectively administered along with the starvation low glucose DMEM. At 5 hours after, an aliquot (50.0 µL) of the medium in each well was withdrawn for quantitative glucose determination using UHPLC-Refractive Index (Column, Supelcogel C-611 – 30 cm x 7.8 mm; mobile phase, 0.1 mM NaOH; column temperature, 600 C; flow rate, 0.5 mL/min; run time, 20 min; detector, refractive index; mode, positive). The medium was replaced with the DMEM-high containing each of the extracts (10.0 µg/mL), metformin (0.01 mM) or phosphate buffered saline in the absence or presence of insulin (30.0 mU/mL; control). At 0.5 h afterwards, an aliquot (50.0 µL) of the medium in each well was again withdrawn for quantitative glucose determination as above.

The amount of glucose uptake by muscle cells was obtained by using the following formula:

Glucose Uptake = [Glucose concentration of blank wells] - [Glucose concentration of cell-plated wells].

3.7. Antioxidant Assay

The antioxidant activity of extract was determined by the DPPH free radical scavenging assay in triplicates. Freshly prepared (0.5 mmol/L) ethanol solution of 2,2-diphenyl-1-picrylhydrazyl (DPPH) radical was stored (10 ºC) in the dark. An ethanol solution of each of the investigated plants was prepared. An aliquot of the ethanol extract (5.0 µl) solution was added to 1.0 mL of DPPH solution to make 100.0 µg/mL of each of the plants. Absorbance measurements were recorded immediately with a UV-visible spectrophotometer. The decrease in absorbance at 515 nm was determined continuously, with data being recorded at 1 min intervals until the absorbance attained stabilization (10 min). Quercetin was used as a positive control. A blank determination was done using 95% ethanol and the negative control constituted the DPPH radical solution without test agent. All the determinations were performed in triplicates. For the determination of the EC_{50} of the

most active plants and quercetin, varying concentrations of each was used to replace the initial concentration and the experiments were repeated.

The percentage antioxidant activity was determined using:

% DPPH radical-scavenging activity = [(Absorbance of control - Absorbance of test sample)/ (Absorbance of control)] x 100.

3.8. Confirmatory assay for discriminant metabolites and their analogues

Some of the specialized metabolites that were indicated as discriminants for the expression of bioactivity as observed in the *in vitro* assays in subsections **3.4 – 3.7** above were tested for inhibitory activity against porcine pancreatic α-amylase *in vitro* at 200.0 µg/mL each. The observed bioactivity was used to determine the potentially relevant structural features required for the observed bioactivity. Subsequently, the IC_{50} of the metabolites with percentage porcine pancreatic α-amylase inhibitory activity > 50% at 200.0 µg/mL was determined. These experiments were done in triplicates.

3.9. Statistics

The bioassay data was expressed as mean ± standard error of the mean. Difference between the samples and control was determined statistically by one-way analysis of variance (ANOVA) followed by student-newman-Keuls test with statistical significance considered as $P < 0.05$. Tests were performed with Graphpad Prism 5.01 (GraphPad Software, Inc., USA).

3.10. UHPLC-UV-MS Methodology

Elution from the UHPLC column was performed by a gradient of water (A) and acetonitrile (B), both with 0.1% v/v formic acid, as follows: 0 – 15 min, 1 – 40% B; 15 – 30 min, 40 – 100% B; 30 – 34 min (column washing), 100% B; 34 – 37 min, 100 – 1% B; 37 – 40 min (column equilibration), 1% B. An auto-sampler was used to deliver 2.0 µL injection volume of each sample kept at 10 °C with a flowrate of 400.0 µL/min and the oven temperature was kept at 45 ^{o}C. Ionisation was performed with ESI-MS (resolution of 70000) and ESI-AIF (resolution of 35000) in both positive and negative modes, simultaneously while UV-DAD was set to record between 200 to 600 nm. The data was acquired and processed

using Thermo Xcalibur 2.2 SP1.48. Mass range in full scan mode was set at m/z 100 – 1000 and for MS/MS monitoring, it was set at m/z 80 - 1000. The parameters used during UHPLC-UV-MS analyses included: 1.0 μscans/s; maximum injection time, 200 ms; sheath gas flow rate, 30; auxiliary gas flow rate, 10; capillary temperature, 300 °C; spray voltage (positive ionization mode), 3.6 kV; spray voltage (negative ionization mode), 3.2 kV and S-lens RF level, 55. The drying, nebulizer and fragmentation gas used was N_2.

3.11. Multivariate Statistical Analyses

Raw data files, generated from UHPLC-HRMS analysis, were separated into their respective positive and negative modes and subsequently converted to .mzXML format with *ProteoWizard-MSconvert* (Proteowizard Software Foundation, USA). The following settings were employed to preprocess the data using Mzmine™ (BMC Bioinformatics, United Kingdom): mass detection using exact mass algorithm (noise level, 1.0E6); chromatogram builder (minimum time span in min, 0.2; minimum height, 3.0E6; *m/z* tolerance, 0.001 *m/z* or 5.0 ppm); chromatogram deconvolution using baseline cut-off (minimum peak height, 3.0E6; peak duration, 0.2 to 5.0; baseline level, 1.0E6); isotopic peaks grouper (*m/z* tolerance, 0.002 *m/z* or 5 ppm; retention time tolerance in min, 0.2; maximum charge, 2; representative isotope, most intense); gap filling (intensity tolerance, 30%; m/z tolerance, 0.001 m/z or 5.0 ppm; retention time tolerance in min, 0.5) and alignment using join aligner (*m/z* tolerance, 0.001 *m/z* or 5 ppm; weight for *m/z*, 20; retention time tolerance, 5%; weight for retention time, 20). The data matrices of both positive and negative ionization modes were subsequently combined on one spreadsheet, after preprocessing individually, and prior to multivariate statistical analysis, the generated data matrix was subjected to log_{10}-transformation (VAN DEN BERG et al., 2006; BALLABIO; CONSONNI, 2013; OVENDEN et al., 2014). Unsupervised (HCA and PCA) and supervised (PLS-DA) statistical analysis, using the software SIMCA 13.0.3.0© (Umetrics, Sweden), were used to perform data mining. In addition, the models were statistically validated by the cross-validation tool, using the leave-1/7-out and raw permutation approaches to exclude model overfitting.

Heteroscedacity was observed in the generated data matrix by visualization of box and whisker plots created using SigmaXL add-in for excel (Figure 5a). The box and whisker plot of a data set presents a graphical view of the data with the center box representing 50%

of the data (3rd and 4th quartile of data) while the “whiskers” represent 25% of the data each (1st and 2nd quartile of data). Log transformation was applied to the data to reduce the heteroscedascity (Figure 5b) (VAN DEN BERG et al., 2006; BALLABIO; CONSONNI, 2013; DI GUIDA et al., 2016; LI et al., 2017; BAPTISTA et al., 2018).

a)

b)

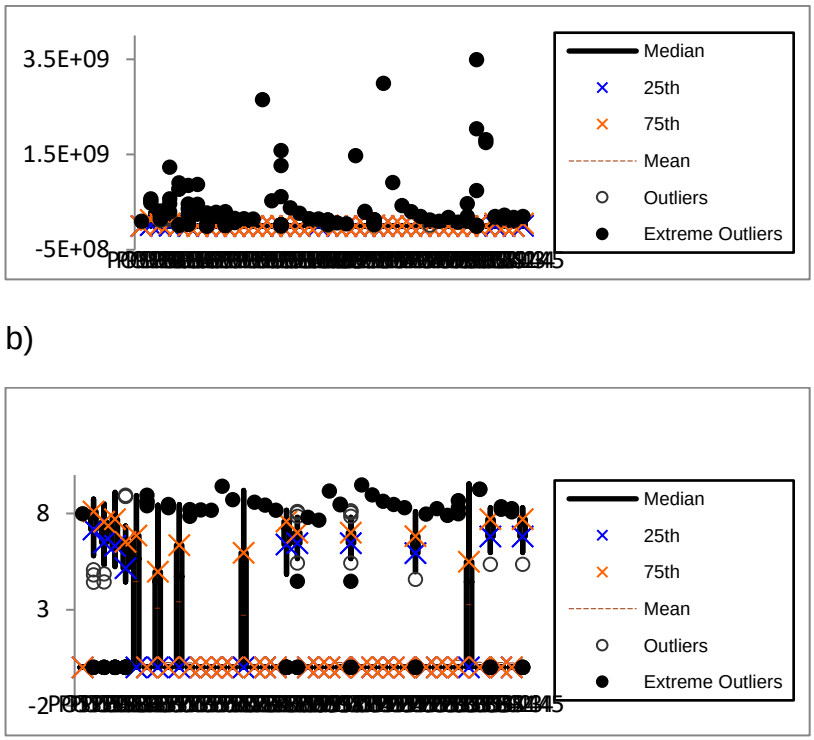

Figure 5: Box and whisker plots of the first 42 detected chemical features
Key: Raw data (a) and log-transformed data (b). The 1st and 2nd quartiles of data represent 25% of the data each constituting the top and lower whiskers, while the 3rd and 4th quartiles of the data represent 50% of the data constituting the center box.

3.12. Identification of Discriminant Variables

Discriminant variables for the active class were determined from the VIP and coefficient plots from the PLS-DA for each generated model; and the compounds annotated or identified. Dereplication was done by comparing information available in the literature with the UV and MS spectra obtained for each peak corresponding to the discriminant variables. The UV spectra were used to infer, wherever applicable, the class of the specialized metabolites. Accurate masses, obtained in the high resolution MS for precursor ions (protonated $[M+H]^+$ and or deprotonated molecules $[M-H]^-$), were used to calculate possible

molecular formulae, which were searched on databases (Scifinder, Dictionary of Natural Products and/or *in house* databases). For further characterization and to improve structural assignments, the fragmentation patterns of MS detected ions were compared with fragmentation patterns reported in the literature (GALLON et al., 2018).

4. RESULTS AND DISCUSSIONS

4.1. Hyperglycaemia prevention

Chronic hyperglycemia, which is characteristic of prediabetes, causes a reduction in insulin secretion and sensitivity as a result of glucose toxicity, thereby leading to the development of T2D. In addition, it has been associated with a reduction of neutrophils, thereby predisposing to infections as well as proliferation of cancer cells. Glucose toxicity has also been reported to cause oxidative stress, which impacts the pancreas adversely. The pancreatic β-islet cells express low antioxidant enzymes, such as superoxide dismutase, catalase and glutathione peroxidase, making the pancreas highly susceptible to oxidative stress (TIEDGE et al., 1997; ROBERTSON, 2006), underscoring the etiology of the reduced biosynthesis and secretion of insulin, being the principal cause of glucose toxicity; and invariably, diabetic complications (BAYNES; THORPE, 1999; BRUNNER *et al*., 2009).

The progression of prediabetes to diabetes can be halted with the approach of preventing hyperglycaemia by diet or its safe bioactive constituents, thereby preventing glucose toxicity and oxidative stress. However, glucose toxicity and oxidative stress, which result with chronic hyperglycaemia being unprevented (ADEMILUYI; OBOH, 2013) may be prevented with metabolites that elicit antioxidant property. Therefore, discriminant antioxidant metabolites or their analogues that are similarly discriminated to be responsible for the activity observed in the *in vitro* antidiabetic assays in this study are suggested to have additional potential for the protection of pancreatic cells from damage and prevention of diabetes (AL-DABBAS et al., 2006; ADEMILUYI; OBOH, 2013).

Pharmacological approaches for the management of diabetes vary widely depending on the associated etiology. Such may include stimulation of insulin secretion, promotion of glucose transporters, inhibition of gluconeogenesis, reduction of glucose absorption from the gut and protection of pancreatic β-cells from oxidative stress-induced damage. The control of postprandial hyperglycemia is essential to prevent the complications of chronic hyperglycemia, glucose toxicity and oxidative stress, which may further impair the structure and function of pancreatic β-cells. Variably, the investigated plants exhibited significant activity in the glucose retardation, fungal and porcine pancreatic α-amylases, glucose uptake and antioxidant assays.

4.1.1. Glucose retardation assay

The reduction or prevention of hyperglycaemia is essential in averting hyperglycaemic complications, development of diabetes and its associated complications. Postprandial hyperglycaemia, which has been associated with the development of diabetes and diabetic complications, can be managed through modulations of gut glucose absorption. Plants with high amounts of dietary fibre and complex polysaccharides have been proposed for the reduction of the incidence of postprandial hyperglycaemia in type 2 diabetes subjects (JENKINS, et al., 1976) as a result of their ability to retard the movement of glucose, thereby prolonging gastric emptying. Such plant products include guar gum, which has variously been shown to reduce postprandial hyperglycaemia (GROOP et al., 1993) through the mechanism of retarding gut glucose movement; however, its high viscousity and unpleasantness limit its dietary use in diabetes management (EDWARDS et al., 1987). Towards circumventing these limitations, the aqueous plant extracts of *Agrimony eupatoria* and *Persea americana* were reported to retard *in vitro* glucose movement; and were suggested to have potential as dietary supplements in type 2 diabetes (GALLAGHER et al., 2003).

The glucose retardation assay in this study yielded 11 extracts with significant ($P<0.05$) glucose diffusion retardation, selected based on their significant activities of ≥ 15.0% at 0.5 h and ≥ 10.0% at 1 h and/or 2 h, with variable activities at 3 h compared with the control (Figure 6). At 0.5 h, the range of activity was 15.0 - 39.0%. Plants that decrease glucose diffusion with activity between 6 and 48% have been reported to have moderate activity (WOOD et al., 2000). At 0.5 h, the extracts of *V. condensata* and *S. biafrae* significantly ($P < 0.05$) exhibited the highest but comparable activities of 39.3 ± 2.0% and 37.7 ± 1.0% respectively. At 1 h, *S. biafrae* had significantly ($P < 0.05$) the highest activity of 30.8 ± 1.5% while at 2 and 3 h, the most active extracts were *S. biafrae* (22.1 ± 1.9%, 19.5 ± 1.5%) and *V. brasiliana* (21.9 ± 0.7%, 24.1 ± 0.5%) compared with control. *V. condensata* from Brazil and *V. amygdalina* from Nigeria, representing the same plant, renamed *Gymnanthemum amygdalinum* by Robinson (1999a), exhibited a similar pattern of positive glucose retardation activity at 1, 2 and 3 h. They respectively exhibited at 1 h, 10.1 ± 0.3% and 9.6 ± 0.3% activity; at 2 h, 7.7 ± 0.2% and 13.9 ± 0.6% activity and at 3 h, 2.7 ± 0.1% and 2.3 ± 0.1% activity. However, at 0.5 h, *V. condensata* from Brazil exhibited a significantly

higher activity (39.3 ± 2.0%) than *V. amygdalina* from Nigeria (12.8 ± 1.2%). The similar pattern of activity, particularly between 1 and 3 h, may be justified based on their similarity. Similarly, commercial Brazilian *T. diversifolia* and *T. diversifolia* from Nigeria, exhibited comparable activity, respectively at 0.5 h (15.4 ± 0.8% and 16.4 ± 0.5%) and 1 h (15.0 ± 0.5% and 14.1 ± 0.5%), with variable activity at 2 h (12.5 ± 0.2% and 6.1 ± 0.3%) and 3 h (-4.2 ± 0.3% and 2.8 ± 0.1%). Furthermore, commercial *M. recutita* and *C. recutita,* which are synonyms of the same plant, exhibited a similar pattern of activity. At 0.5, 1, 2 and 3 h, *M. recutita* and *C. recutita* respectively had -4.1 ± 0.2%, -0.4 ± 0.03%, -0.6 ± 0.04% and -2.6 ± 0.1% activity; and -3.9 ± 0.1%, -7.6 ± 0.4%, 1.3 ± 0.1% and -1.3 ± 0.1% activity compared with negative control. While their glucose retardation activity was low, they both were observed not to significantly increase the movement of glucose across the dialysis tube compared with negative control. However, although commercial Brazilian *A. conyzoides* and *A. conyzoides* from Nigeria both increased glucose diffusion across the dialysis tube compared with negative control, respectively at 0.5 h (-1.4 ± 0.1% and -7.8 ± 0.3%) and 1 h (-5.3 ± 0.2% and -14.9 ± 0.6%), with the sample from Nigeria exhibiting a higher increase in glucose diffusion; at 2 and 3 h, the commercial Brazilian *A. conyzoides* retarded glucose diffusion with activity of 18.4 ± 0.3% and 11.2 ± 0.6% respectively, while *A. conyzoides* from Nigeria increased glucose diffusion across the dialysis tube at these times, respectively at -11.9 ± 0.5% and -18.3 ± 0.8%. This showed that while *A. conyzoides* from Nigeria exhibited no glucose retardation activity at all times tested, while the commercial Brazilian *A. conyzoides* significantly retarded glucose movement at later times. This *in vitro* glucose retardation activity of plant extracts (BASHA; KUMARI, 2012; PICOT et al., 2014) is relevant to reducing or delaying the gut absorption of glucose, as a product of polysaccharide metabolism especially where salivary or pancreatic hydrolytic enzymes evades inhibition, thereby retarding postprandial hyperglycaemia (TABÁK et al., 2012). Aqueous-methanolic extracts may contain phenolic constituents with this potential. Additionally, it was observed that a significant number of the extracts, at different times, either exhibited comparable activity with control or significantly increased the movement of glucose across the dialysis tube. This information may be potentially beneficial in assessing plants that diabetics or prediabetics need to evade in order to avoid the development of postprandial hyperglycaemia, which will exacerbate their conditions (TABÁK et al., 2012).

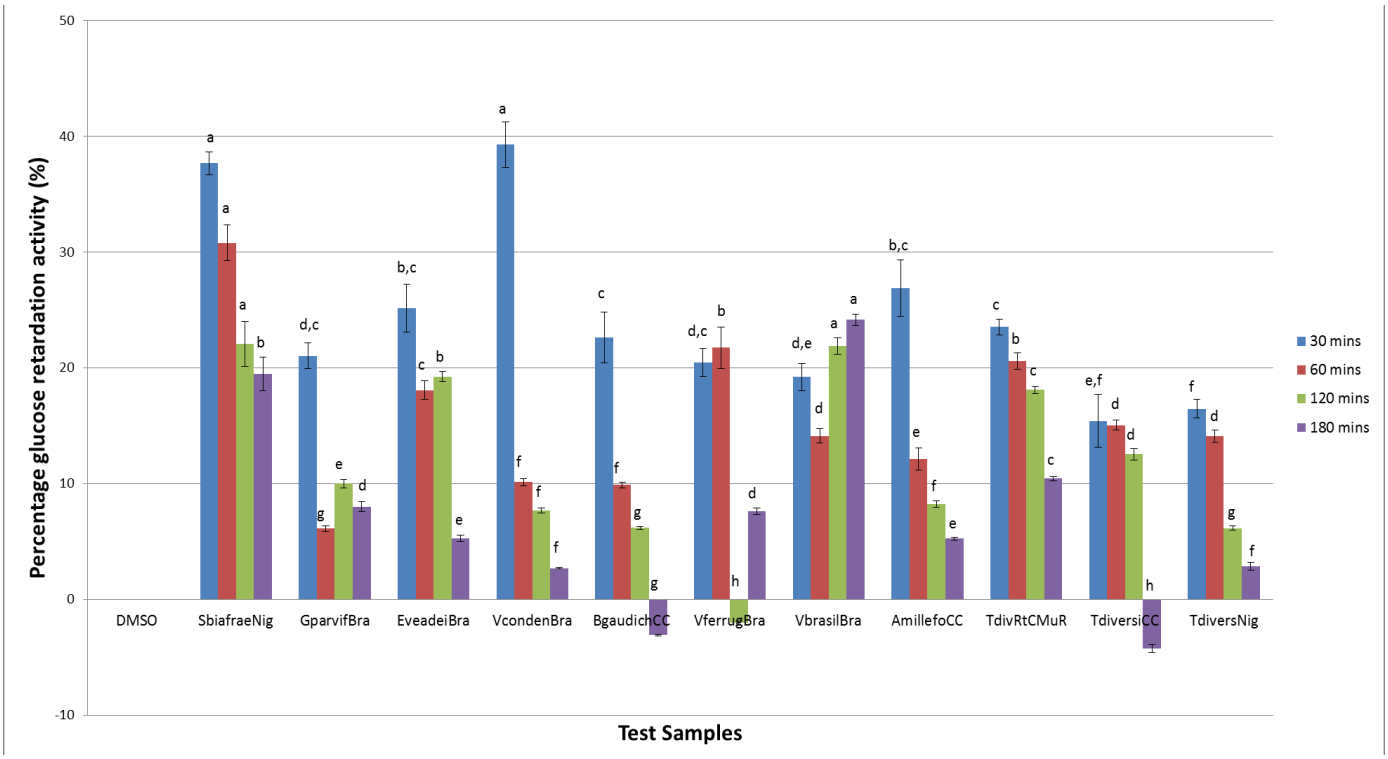

Figure 6: Percentage glucose retardation activity of the most active extracts (50 mg/ml) compared with negative control (DMSO)
Key: Alphabets indicate statistical comparison of the activity of each extract compared with negative control (DMSO) per time investigated. For each timepoint, "a" indicates statistically the highest activity; followed by subsequent alphabets, indicating decreasing activity. The codes represent the names of investigated plants (see LIST OF ABBREVIATIONS AND CODES)

4.1.2. Inhibitory activity against fungal α-amylase

Among other mechanisms elaborated for the management of diabetes, the inhibition of α-amylase is essential as this constitutes the initial step at controlling postprandial hyperglycaemia. This lowers the mono- or disaccharide products of starch metabolism, reducing their availability for gut absorption. It has been shown that even the healthy human gut is colonized by several species of fungi, with dietary or environmental sources, including a fermentation and probiotic agent, *Saccharomyces cerevisiae* and ubiquitous molds, *Aspergillus species* (HALLEN-ADAMS; SUHR, 2017). The fungi may, in addition to the human salivary and pancreatic α-amylase, also contribute to the α-amylase load in the gut, thereby increasing the products of starch metabolism available for gut absorption. While the currently used α-glucosidase inhibitor, acarbose, may have pronounced activity against human salivary and pancreatic α-amylases, it has been shown to be ineffective against α-amylase from *Aspergillus oryzae* (YOON; ROBYT, 2003). Therefore when administered to

subjects whose gut is colonized by microorganisms that produce acarbose-resistant α-amylase, such subjects are unnecessarily being exposed to the side effects of the drug without the benefits as the fungal amylase will continue to hydrolyse starch irrespective of the inhibition of the human salivary or pancreatic α-amylase by acarbose. Screening natural sources for the presence of metabolites capable of inhibiting fungal α-amylase in this study may provide insights into metabolites from natural sources with multiple mechanisms of activity, offering an advantage over acarbose.

The inhibitory activity of the investigated Asteraceae plants on fungal α-amylase was therefore investigated *in vitro*. More than half, consisting 37 extracts, variably but significantly ($P < 0.05$) inhibited α-amylase ≥ 30.0% compared with control (Figure 7); whereas acarbose clearly displayed no inhibitory activity against fungal amylase. This varied activity based on source of the enzyme has previously been reported. Fungal α-amylase from *Aspergillus oryzae* was shown to be the least inhibited of four investigated α-amylases, while porcine pancreatic α-amylase was inhibited the most by acarbose and its analogues, with acarbose inhibiting PPA 338 times better than the fungal amylase (YOON; ROBYT, 2003). Another study reported that pine extracts and acarbose elicited similarly significant inhibitory activity against mammalian α-amylase but none against *A. oryzae* α-amylase. This variability, reflecting structural differences between the enzymes from different sources, was further shown with the pine extract eliciting higher inhibitory activity against bacteria than mammalian α-amylase, with acarbose showing 10 times lesser activity (KIM et al., 2004). It must be noted, however, that a study reported that acarbose (5.0 mg/mL) elicited a significantly high inhibition (60.0%) against *A. oryzae* α-amylase (FRED-JAIYESIMI et al., 2009). Previous studies have reported that methanolic extracts of plants possess α-amylase inhibitory compounds (CHETAN et al., 2014). *S. marianum* had the highest significant ($P < 0.05$) α-amylase inhibition (70.4 ± 1.9%) in this study, followed by *A. hispidum* (60.7 ± 0.9%). Similarly, extracts of *M. recutita* and *C. recutita* exhibited comparable inhibitory activities of 49.9 ± 1.1% and 51.5 ± 0.9%, respectively in this study being similar species.

These results also showed comparable activities especially with plants related taxonomically and with similar geographical sources (Figure7), evident with their proximity in HCA (Figure 12), including *V. amygdalina* (35.9 ± 0.2%) and *V. condensata* (38.6 ± 0.5%), both of which represent the same plant; *B. pilosa* from Nigeria (35.2 ± 0.6%), *B. pilosa* from

Brazil (32.1 ± 0.6%) and commercial *B. pilosa* (36.9 ± 1.9%); *A. conyzoides* from Nigeria (40.9 ± 0.9%) and commercial *A. conyzoides* (41.6 ± 0.8%) showing, irrespective of location, an activity of about 41.0%; leaves of Nigerian *T. diversifolia* treated with *M. koenigii* leaves (59.3 ± 0.2%) and roots of *T. diversifolia* treated with *M. koenigii* roots (54.9 ± 0.1%); and extracts of Nigerian *T. diversifolia* (40.4 ± 0.3%) and commercial Brazilian *T. diversifolia* (40.8 ± 0.7%) (Figure 7). Corroborating the α-amylase inhibitory activity of the aqueous methanolic extracts of plants in this study, it has been previously shown that methanolic extracts were the active agents (TADERA et al., 2006; MAHAJAN et al., 2014; SONAWANE et al., 2014; KUMAR et al., 2016). This study provides further evidence of fungal α-amylase inhibitory activity of the aqueous-methanolic extracts of investigated plants and offers opportunity for further investigations into the mechanisms of activity of plants with antidiabetic potential. These active plants may therefore be beneficial in preventing the development of postprandial hyperglycaemia, its complications evident in diabetics and progression of prediabetes to diabetes (TABÁK et al., 2012), through the additional mechanism of inhibiting fungal α-amylase.

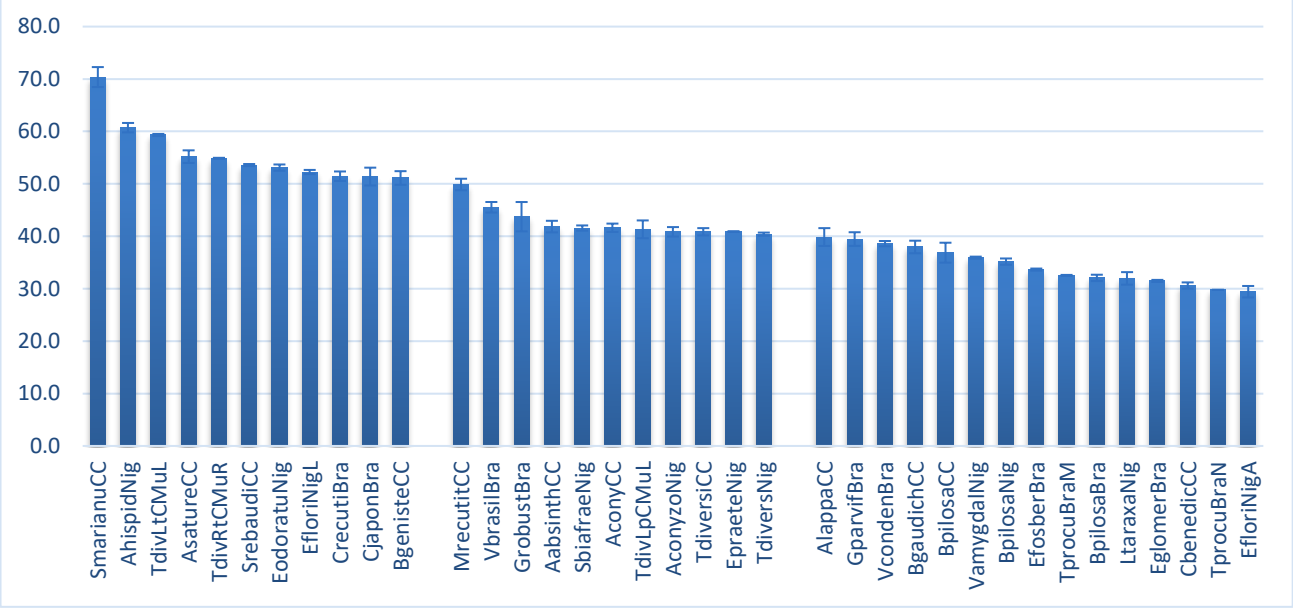

Figure 7: Percentage inhibitory activity of most active plant extracts (≥ 30.0%) in the fungal (*Aspergillus oryzae*) α-amylase inhibitory assay
Key: Data represents mean percentage inhibition ± standard error of mean; the codes represent the names of investigated plants (see LIST OF ABBREVIATIONS AND CODES)

4.1.3. Inhibitory activity against porcine pancreatic α-amylase

An approach for the management of diabetes is the reduction of postprandial hyperglycemia. Pancreatic α-amylase hydrolyses starch to maltose and oligosaccharides in the small intestine; its inhibition reduces the rate of starch digestion, thereby resulting in reduced postprandial hyperglycaemia. Such inhibitors from natural sources, while offering an affordable and accessible approach to managing or preventing the development of diabetes, especially in developing countries, may serve as safer alternatives to currently used antidiabetic drugs in more advanced countries. Additionally, inhibiting the hydrolysis of starch may have beneficial effects on insulin resistance and the control of glycemic index in diabetic subjects (GHAVAMI et al., 2001; NOTKINS, 2002).

The *in vitro* inhibitory activity of the selected plants against porcine pancreatic α-amylase was therefore studied. Of the plants screened, 12 elicited significant activity > 9.0% (Figure 8) (SUDHA et al*.,* 2011). The positive control agent, acarbose, elicited significantly higher inhibition of this enzyme (70.4 ± 0.1%) at 10 µg/mL compared to negative control. Acarbose is a pseudotetrasaccharide, (2R,3R,4R,5S,6R)-5-[(2R,3R,4R,5S,6R)-5-[(2R,3R,4S,5S,6R)-3,4- dihydroxy-6-methyl-5-[[(1S,4S,5S,6S)-4,5,6-trihydroxy-3-(hydroxymethyl)-1-cyclohex-2-enyl]amino]oxan-2-yl]oxy-3,4-dihydroxy6-(hydroxymethyl)oxan-2-yl]oxy-6-(hydroxymethyl)oxane-2,3,4-triol (Figure 3), with molecular weight and formula of 645.61 and $C_{25}H_{43}NO_{18}$ respectively. The lower activity observed with the extracts investigated compared with acarbose may constitute an advantage as in the case of a novel pseudotetrasaccharide α-glucosidase inhibitor, CKD-711, isolated from *Streptomyces* sp. which exhibited significantly lower α-amylase inhibition than acarbose, with no toxicity. As a consequence, it was suggested that CKD-711 may elicit lesser side effects than commonly observed with significantly high inhibition of α-amylase (DE MELO et al., 2006). It was observed that S. marianum, which had significantly the highest inhibitory activity (70.4 ± 1.9%) against fungal amylase (Section **4.1.2.** above) similarly exhibited the highest porcine pancreatic α-amylase inhibitory activity (24.8 ± 0.4%), comparable with that of *E. veadeiroensis* (25.3 ± 1.4%) among the studied plants but lower when compared with the former enzyme. However, *E. veadeiroensis* had a significantly lower fungal α-amylase inhibitory activity of 12.7 ± 0.7%. With *C. recutita,* it was observed that the inhibition reduced from 51.5 ± 0.9% as observed in the fungal α-amylase assay to 11.7 ± 0.2% in the PPA

assay. There was observed a reduction in the PPA compared with the fungal α-amylase *in vitro* assays respectively for commercial *B. gaudichaudiana* (21.5 ± 1.3% and 38.0 ± 1.2%); commercial *A. conyzoides* (12.9 ± 0.1% and 41.6 ± 0.8%); commercial *A. satureioides* (12.0± 0.7% and 55.2 ± 1.2%); *V. condensata* from Brazil (15.6 ± 0.1% and 38.6 ± 0.5%); commercial *T. diversifolia* (15.7 ± 0.3% and 40.8 ± 0.7%); *T. diversifolia* from Nigeria (10.0 ± 0.1% and 40.4 ± 0.3%); *Vernonanthura phosphorica* from Brazil (17.5 ± 0.3% and 23.9 ± 0.5%); and commercial *A. millefolium* (15.2 ± 0.4% and 22.5 ± 0.4%). Only the *V. phosphorica* from Brazil had a little increase (15.9 ± 0.2% and 10.8 ± 0.3%) (Figures 7 and 8). This observed reduced inhibition suggests possible lesser side effects than commonly observed with significantly high inhibition of α-amylase (DE MELO et al., 2006) offering the plants with this reduced activity to be employed as beneficial diets. Additionally, previous reports have shown that excessive inhibition of α-amylase could lead to abnormal bacterial fermentation of undigested starch in the colon and therefore low α-amylase inhibitory activity is useful (KWON et al., 2002).

Comparing the PPA inhibitory activity of taxonomically related species, irrespective of geographical source, it was observed that the commercial Brazilian *T. diversifolia* (15.7 ± 0.3%) and *T. diversifolia* from Nigeria (10.0 ± 0.1%) exhibited significantly high activity being part of the most active investigated plants, as they similarly were for the glucose retardation and fungal α-amylase inhibitory assays. It was therefore observed that the Brazilian sample exhibited a significantly higher activity than the Nigerian sample. This pattern of activity was observed similarly with the glucose retardation and fungal α-amylase inhibitory assays, which showed that the Brazilian sample had higher or slightly higher activity than the Nigerian sample. It was similarly observed with other samples related taxonomically but collected from the different countries. For example, while *V. amygdalina*, *B. pilosa*, *T. procumbens* from Nigeria exhibited no PPA inhibitory activity, *V. condensata* (15.6 ± 0.1%), *B. pilosa* (4.1 ± 0.1%), *T. procumbens* (7.8 ± 0.01%) from Brazil exhibited a significantly high inhibitory activity against PPA. Similarly, *A. conyzoides* (12.9 ± 0.1%) from Brazil exhibited significantly higher activity than *A. conyzoides* (0.9 ± 0.1%) from Nigeria.

Taken together, plants such as *T. diversifolia, S. marianum*, *B. gaudichaudiana*, *A. conyzoides*, *V. condensata, A. satureioides* and *C. recutita,* which significantly inhibited both PPA and fungal α-amylase may have potential for use as dietary supplement due to their

additional ability to inhibit the enzyme that may be produced if fungi colonize the gut (HALLEN-ADAMS; SUHR, 2017).

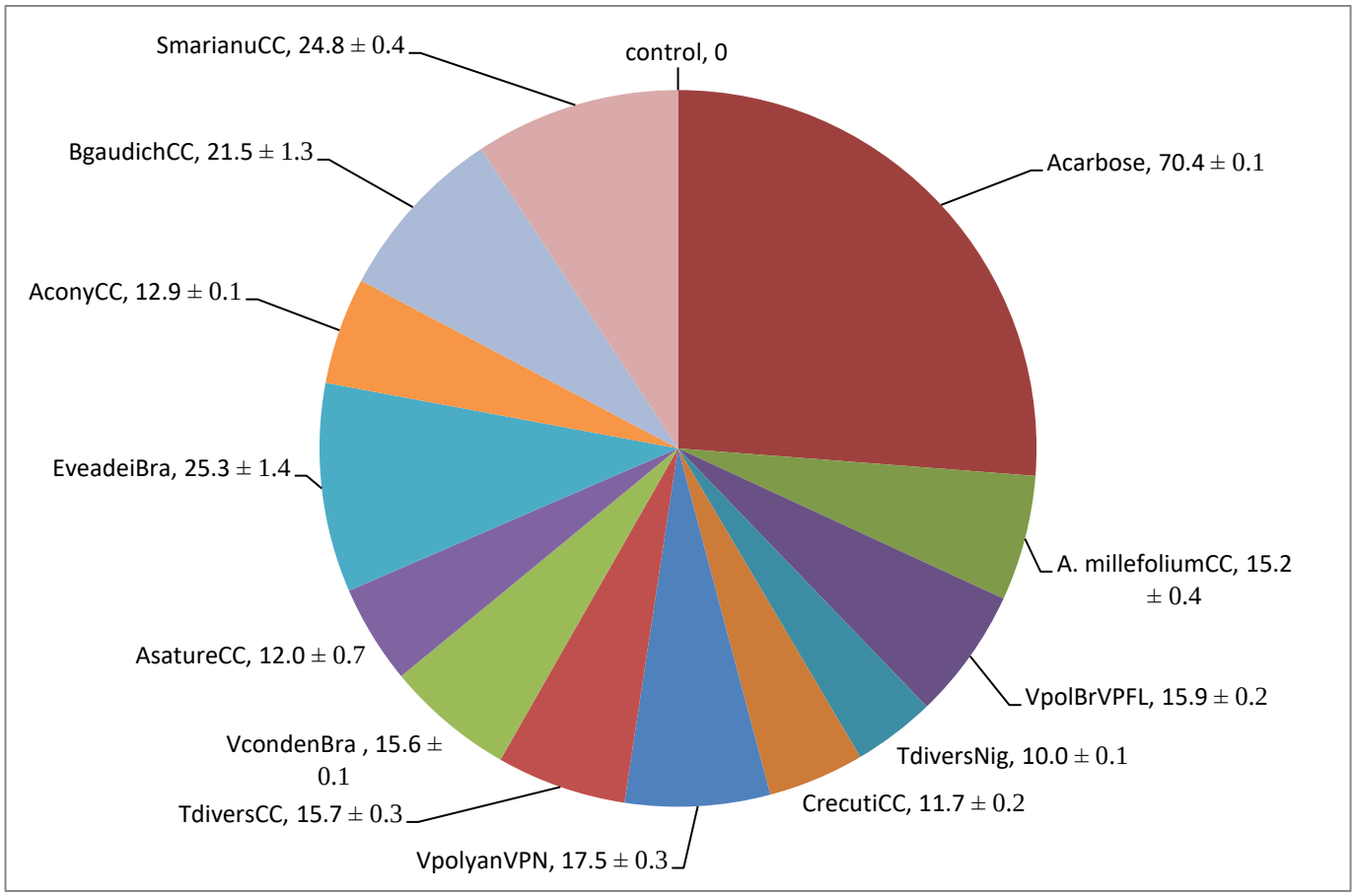

Figure 8: Percentage inhibitory activity of most active plant extracts (≥ 9.0%) in the porcine pancreatic α-amylase inhibitory assay
Key: Data represents mean percentage inhibition ± standard error of mean; the codes represent the names of investigated plants (see LIST OF ABBREVIATIONS AND CODES)

4.1.4. Glucose uptake activity in C2C12 cells

Chronic hyperglycemia may aggravate diabetes through its effect on insulin action in tissues targeted by insulin, such as the skeletal muscle (DAVIDSON et al., 1994). Glucose uptake stimulation in skeletal muscle cells is effected through GLUT4 translocation to the cell surface from intracellular storage sites. Defects in insulin action in the skeletal muscles may account for the insulin resistance observed in diabetics (KOISTINEN; ZIERATH, 2002). Therefore, metabolites from natural sources with the potential to stimulate the action of insulin may offer an advantage in ameliorating insulin-resistance, especially when mechanisms for reducing or preventing postprandial hyperglycaemia through glucose

retardation and α-amylase inhibition fail. It has been shown that in differentiated C2C12 myotubes, with basic GLUT4 translocation system, the translocation of these GLUT4 can be activated through insulin stimulation (NEDACHI; KANZAKI, 2006). Nedachi and Kanzaki (2006) also proposed the use of C2C12 in assessing the effect of GLUT4 translocation in skeletal muscle because it is highly expressed in cells that display significant insulin-stimulated glucose uptake. About 70 to 80% of insulin-stimulated glucose is associated with skeletal muscle, which constitutes a major insulin-target (NUUTILA et al., 1994).

The investigated plants (10 µg/mL) were therefore additionally screened for their ability to enhance glucose uptake in C2C12 myotubes and 36 of them were observed to have significant activity that was comparable or higher than metformin (16.6 ± 1.7%; 10.0 µg/mL) compared with negative control (Figure 9). Extract of *Vernonia amygdalina* leaves, which elicited 27.4 ± 0.7% glucose uptake activity in this study, was previously reported to significantly improve glucose utilization in C2C12 muscle cells (ERASTO et al*.,* 2009). The extracts of *S. marianum* and *V. polyanthes* from Brazil, which showed inhibitory activity against both α-amylases (Figures 7 and 8) tested in this study, also improved glucose uptake by 21.8 ± 1.3% and 24.2 ± 0.5% respectively. While *A. conyzoides* from Nigeria, which inhibited porcine pancreatic amylase, additionally improved glucose uptake (27.7 ± 1.1%) (Figures 8 and 9). Some extracts that were able to retard glucose movement across the dialysis tube also increased glucose uptake including *S. biafrae* (23.0 ± 2.9%), *E. veadeiroensis* (37.3 ± 1.9%) and *V. brasiliana* (16.3 ± 3.8%) (Figures 6 and 9). The following extracts elicited activity in the glucose retardation assay, PPA and fungal α-amylase assays and glucose uptake assay, *B. gaudichaudiana* (26.9 ± 2.3%), *V. condensata* (22.5 ± 1.9%), commercial *T. diversifolia* (31.3 ± 3.3%), commercial *A. millefolium* (21.9 ± 1.9% and *T. diversifolia* from Nigeria (17.0 ± 2.1%) (Figures 6, 7, 8 and 9). Overall, extracts with the highest insulin-mediated glucose uptake activity > 30.0% include *C. crepidioides* (41.6±2.7%), *M. micrantha* (41.2 ± 1.5%), *E. veadeiroensis* (37.3 ± 1.9%), commercial *M. recutita* (32.9 ± 2.1%) and commercial *T. diversifolia* (31.3 ± 3.3%) (Figure 9).

As with glucose retardation, PPA and fungal α-amylase inhibitory assays, in which it was observed that commercial Brazilian *T. diversifolia* exhibited significantly higher activity than *T. diversifolia* from Nigeria, it was similarly observed that the former exhibited significantly higher insulin-mediated glucose uptake enhancement activity than the latter.

However, contrary to the other assays where Brazilian samples exhibited higher activity than similar Nigerian samples, it was observed in insulin-mediated glucose uptake assay that the Nigerian samples, *V. amygdalina* (27.4 ± 0.7%), *B. pilosa* (18.8 ± 1.4%) and *A. conyzoides* (27.7 ± 1.1%) exhibited higher activity than the Brazilian samples respectively, *V. condensata* (22.5 ± 1.9%), commercial Brazilian *B. pilosa* (11.6 ± 0.4%) and *B. pilosa* (15.5 ± 0.9%); and Brazilian commercial *A. conyzoides* (20.6 ± 0.8%). This was due to differential abundances of some of the detected features across the samples.

In addition to screening the investigated plants for insulin-mediated glucose uptake enhancement activity, the insulin-like glucose uptake activity of the investigated plants was also evaluated to provide further insights to other mechanisms of action of the plants and the following, which exhibited insulin-mediated glucose uptake enhancement activity also exhibited insulin-like activity respectively, commercial *M. glomerata* (25.6 ± 4.3%, 36.0 ± 2.3%), *M. micrantha* (41.2 ± 1.5%, 32.4 ± 2.1%), *E. alba* (17.7 ± 2.1%, 39.5 ± 3.3%), *S. filicaulis* (28.5 ± 2.2%, 39.2 ± 1.6%), *B. gaudichaudiana* (26.9 ± 2.3%, 32.9 ± 2.3%), *B. genistelloides* (26.6 ± 2. 6%, 41.5 ± 2.2%), *V. amygdalina* (27.4 ± 0.7%, 41.5 ± 1.9%), *T. officinale* (28.8 ± 1.2%, 39.7 ± 6.0%), *C. crepidioides* (41.6 ± 2.7%, 33.5 ± 0.7%) (Figure 10). It was similarly observed that some of the Nigerian samples exhibited a higher insulin-like glucose uptake enhancement activity than similar Brazilian samples. For example, a comparable activity was observed with *B. pilosa* from Brazil (26.2 ± 1.2%) and *B. pilosa* from Nigeria (24.2 ± 4.5%), which were higher than the activity exhibited by commercial Brazilian *B. pilosa* (17.8 ± 0.7%). Furthermore, *V. amygdalina* (41.5 ± 1.9%) and *A. conyzoides* from Nigeria (28.1 ± 3.4%) exhibited higher activity than *V. condensata* (21.3 ± 2.7%) and Brazilian commercial *A. conyzoides* (19.2 ± 1.6%), respectively. On another hand, the commercial Brazilian *T. diversifolia* (23.7 ± 2.4%) exhibited comparable activity with the *T. diversifolia* from Nigeria (18.5 ± 3.2%) (Figure 10).

These Asteraceae plants with glucose uptake enhancement activity may have the potential to reduce post-prandial hyperglycaemia if the approaches for preventing or reducing hyperglycaemia through the retardation of glucose absorption and/or inhibition of α-amylase fail.

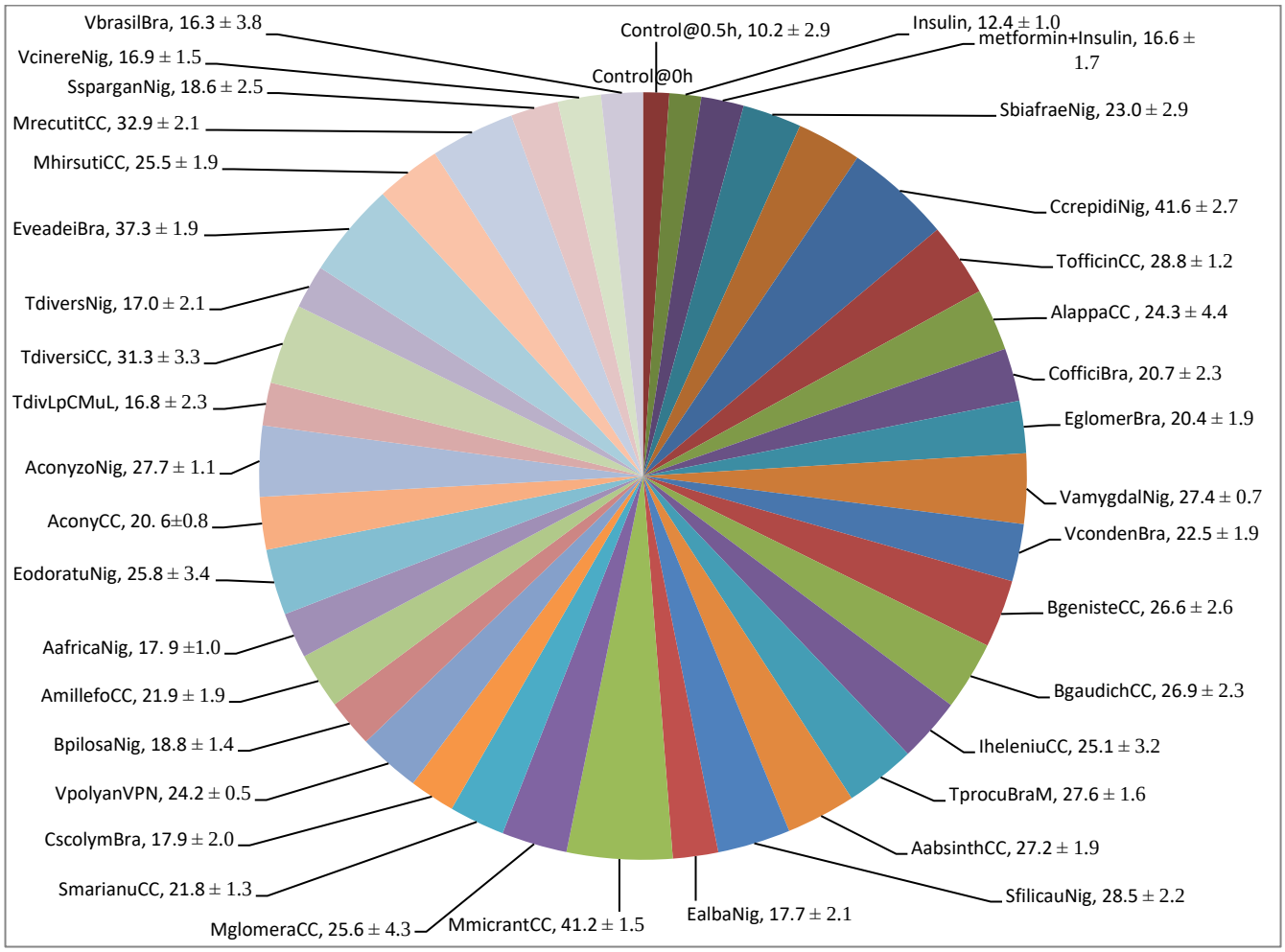

Figure 9: Percentage insulin-mediated glucose uptake enhancement activity of most active plant extracts (10 µg/mL) assessed with C2C12 cells (> 16.0%)
Key: Data represents mean percentage insulin-mediated glucose uptake enhancement activity ± standard error of mean; the codes represent the names of investigated plants (see LIST OF ABBREVIATIONS AND CODES)

4.1.5. Antioxidant Assay

Chronic hyperglycaemia causes oxidative stress, which adversely imparts pancreatic β-cells, among other effects, further exacerbating hyperglycaemia, diabetes and its complications. In many cases, where postprandial hyperglycaemia remains undetected for a protracted period or unmanaged, when detected, or where it evades management due to therapeutic failure, oxidative stress results and this may lead to irreversible damage. The investigated plants were therefore finally screened for their antioxidant property. This was

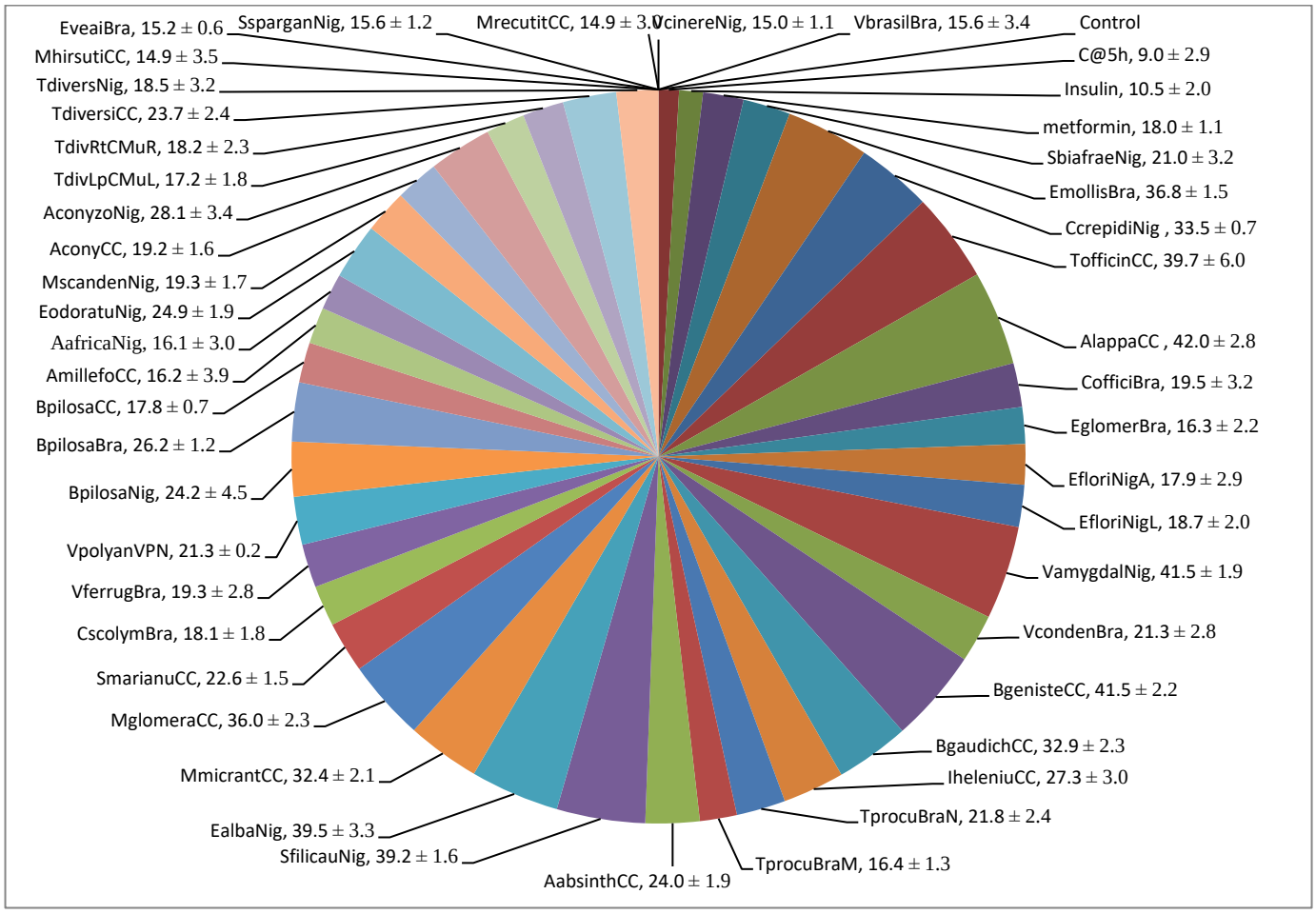

Figure 10: Percentage insulin-like glucose uptake enhancement activity of most active plant extracts (10.0 µg/mL) assessed with C2C12 cells (> 16.0%)
Key: Data represents mean percentage insulin-like glucose uptake enhancement activity ± standard error of mean; the codes represent the names of investigated plants (see LIST OF ABBREVIATIONS AND CODES)

to determine their additional ability to prevent or reduce the generation of ROS, which has the potential to prevent the development of oxidative stress and protect the pancreatic β-islet cells from oxidative stress-induced damage *in vivo*. The investigated plants were screened for antioxidant property at 100.0 µg/mL using DPPH free radical scavenging assay. The absorbance was read at 515 nm every 10 min and it was observed that, for most of the experimental points, the most significant activity was observed within the first ten minutes (Figure 11). In this study, the most significant antioxidant activity was elicited by commercial *A. millefolium*, *S. microglossa, A. montana, B. gaudichaudiana, B. genistelloides* and *E. floribundus* aerial parts from Nigeria, all having significantly better activity than the positive control drug, quercetin at 100.0 µg/mL (Fig 11) compared to the control. As a result, the EC_{50}

values were determined for these extracts and quercetin (Table 2). Here, it was observed that quercetin yielded the highest activity, fifty percent of the effect being elicited with the lowest concentration, 2.6 µg/mL. According to the EC_{50} values, the extracts, in decreasing order of activity, were *A. montana* > *B. genistelloides* > *B. gaudichaudiana* > *E. floribundus* > *S. microglossa* > *A. millefolium* (Table 2).

Table 2: EC_{50} values (µg/mL) for plants with antioxidant activity > 90%

Sample name	**EC_{50} for antioxidant activity (µg/mL)**
Quercetin	2.6
A. millefolium	82.9
S. microglossa	60.7
A. montana	14.2
B. gaudichaudiana	30.1
E. floribundus	54.4
B. genistelloides	23.0

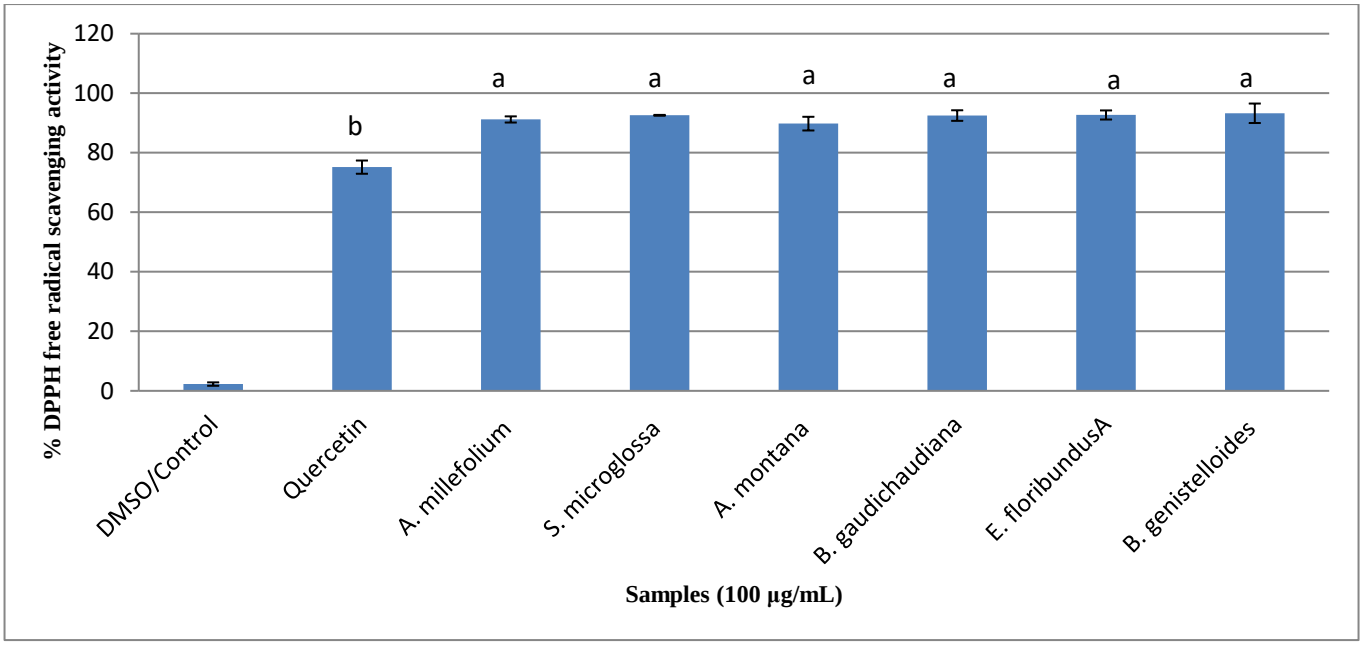

Figure 11: DPPH free radical scavenging activity of most active samples (> 90.0%) at 100.0 µg/mL

Key: DPPH, 2,2-Diphenyl-1-picrylhydrazyl; Alphabets indicate statistical comparison of the activity of each extract compared with negative control (DMSO); "a" indicates statistically the higher activity; "b" indicates lesser activity.

4.2. Multivariate Statistical Analysis

Metabolic fingerprints of the investigated plants were obtained with a UHPLC-ESI-MS (Orbitrap) in both positive and negative ionization modes simultaneously. The generated data was preprocessed using the software Mzmine*TM* (BMC Bioinformatics, United Kingdom) to perform deconvolution, alignment, centralization, filtering, gap-filling, isotope grouping and normalization; and the data from the so-treated MS chromatograms was extracted and exported as .csv tables, with data from the positive and negative ionization modes, independently and subsequently combined. The blanks were subtracted from the data across samples. Using SIMCA 13.0.3.0© (Umetrics, Sweden), the generated data matrix was used for the analyses of supervised (PCA) and unsupervised (PLS-DA) multivariate statistics while the software, R was used to generate the unsupervised HCA.

4.2.1. Hierarchical Cluster Analysis

The HCA was performed in order to observe possible groupings among the investigated samples especially for the purpose of gaining more insight into the metabolome of the investigated plants. It was observed, from the dendogram (Figure 12), a comparison of the metabolic fingerprints based on phylogeny and geographical sources of the plants. The plants were generally clustered into four groups with the first two groups belonging to all the plants obtained from Brazil and the other two groups from Nigeria, showing similarity based on geographical source. Exceptionally, *S. biafrae* and the two samples of *E. floribundus*, *M. scandens* and *S. filicaulis* obtained from Nigeria were observed in the first and second groups respectively while *V. condensata*; and *I. helenium* and *G. robuta* from Brazil were observed in the third and fourth groups respectively. This could indicate that the components of such plants are related to those of the plants together with which they were clustered. As observed (Figure 12), the second and third groups belonging to plants collected from Brazil; and Nigeria respectively were clusted together; suggesting chemical similarity between the plants in these groups irrespective of geographical source. Additionally, the clustering of some Nigeria plants with some Brazilian plants, separately from other investigated Nigerian plants reveal the chemical dissimilarity between these plants collected from similar sources. Specifically, it was observed that taxonomically related plants were clustered together. For example, in the first group, the following belonging to similar tribes

were clustered together, Cichorieae tribe, *S. oleraceus* and *C. japonica*; Coreopsideae tribe, commercial *B. pilosa* and *B. pilosa* from Brazil; Cynareae tribe, commercial *C. scolymus* and *C. scolymus* from Brazil close to *C. benedictus, S. marianum*; Eupatorieae tribe, commercial *A. conyzoides* and *M. micrantha*; Anthemideae tribe, commercial *C. recutita* and *M. recutita* and Heliantheae tribe, *G. parviflora* and *T. procumbens* from Brazil. The second group presented clusters of Astereae tribe, *B. gaudichaudiana* and *B. genistelloides* along with *A. satureioides* (Inuleae); Astereae tribe, the two *E. floribundus* from Nigeria; Heliantheae tribe, *M. scandens* and *S. filicaulis*; Anthemideae tribe, *A. millefolium*, *A. vulgare* and *T. vulgare* and Vernonieae tribe, *E. glomerulatus*, *E. veadeiroensis*, commercial and Brazilian *V. phosphorica*, *E. mollis* and *V. brasiliana*. The third group presented clusters of Eupatorieae tribe, *E. odoratum* and *A. conyzoides* from Nigeria; Heliantheae tribe, *A. Africana* and *S. nodiflora*; Senecioneae tribe, *C. crepidioides* and *E. praetermissa* from Nigeria; Vernonieae tribe, *V. condensata* and its synonym from Nigeria, *V. amygdalina, V. cinerea* and *S. sparganophora* from Nigeria along with *A. hispidum* (Heliantheae) and *L. taraxacifolia* (Lactuceae). The fourth group presented clusters of Heliantheae tribe, *T. procumbens*, control leaves of *T. diversifolia*, commercial *T. diversifolia*, and all the samples of *T. diversifolia* planted or treated with *M. koenigii* parts from Nigeria along with *G. robusta* (Astereae), *Tridax procumbens* from Nigeria (Heliantheae) and *I. helenium* (Inuleae). The diverse clusters formed suggest that the specialized metabolites detected as features in the investigated plants were capable of classifying the plants into their various tribes or genera. However, there were mixed classifications where plants belonging to different tribes were clustered such as *V. ferruginea* (Vernonieae), *A. montana* (Madieae) and *S. rebaudiana* (Eupatorieae); *T. officinale* (Cichorieae), *A. lappa* (Crepidioides), *C. officinalis* (Calenduleae) and *E. fosbergii* (Senecioneae); *C. crepidioides* (Senecioneae), *E. alba* (Heliantheae) and *C. crepidioides* (Crepidioides).

4.2.2. Principal Components Analysis

As an unsupervised multivariate statistical analysis, PCA affords the graphical visualization of the relatedness of investigated samples, based on the composition of their metabolic fingerprints. The PCA score plot of the first and seventh principal components, similar to the results obtained with HCA (Figure 12), revealed a general clustering of species

related taxonomically (Figure 13). It provided the following, R^2X (fraction of the data variation explained by each component), 0.93; and Q^2 (coefficient of prediction), 0.9 (Figure 13). The random sampling of the investigated plants, involving ethnomedicinal use, previous antidiabetic reports, use as functional food and donation may account for the numerous clusterings observed.

The visualization of clustering, trends or outliers, related to chemical similarities between the samples was achieved with PCA (Figure 13). It provides insights into the relatedness that exist between variables, in turn revealing the numerical influence of metabolites on how related or disparate the samples were, based on correlations between the observations and the variables. The observed classification of the plants into their various tribes or genera is thus based on the chemical diversity that they possess. Importantly, it was observed that *Tridax procumbens* from Nigeria (Heliantheae) and *I. helenium* (Inuleae) were observed outside the correlation cycle as outliers; they were similarly observed in a cluster in HCA, suggesting their composition of unique metabolite(s) that warrant(s) further study.

Similarly, *V. condensata* from Brazil and *V. amygdalina* and *A. hispidum* from Nigeria were observed, as in HCA, in a cluster within a quadrant in PCA, suggesting the relatedness of the components of such plants that were observed in similar clusters. Other HCA clusters that were similarly observed in PCA, further revealing the composition of related metabolites, include commercial *C. recutita* and *M. recutita*; commercial Brazilian *A. lappa*, *C. officinalis, T. officinale* and *G. parviflora*, *T. procumbens* and *E. fosbergii* from Brazil; *B. gaudichaudiana*, *B. genistelloides* and *A. satureioides*; *C. crepidioides*, *E. alba*, *A. conyzoides* and *E. praetermissa* from Nigeria; cultivated *T. diversifolia* control leaves, cultivated *T. diversifolia* roots coplanted with *M. koenigii* roots and cultivated *T. diversifolia* roots treated with *M. koenigii* roots from Nigeria; and cultivated *T. diversifolia* leaves coplanted with *M. koenigii* leaves and cultivated *T. diversifolia* leaves treated with *M. koenigii* leaves from Nigeria. Similar to HCA therefore, the diverse clusters formed in PCA also suggest that the specialized metabolites detected as features in the investigated plants were capable of classifying the plants into their various tribes or genera. More of these correlations would be detected if the PCA score plots of the different correlations of the principal components were visualized.

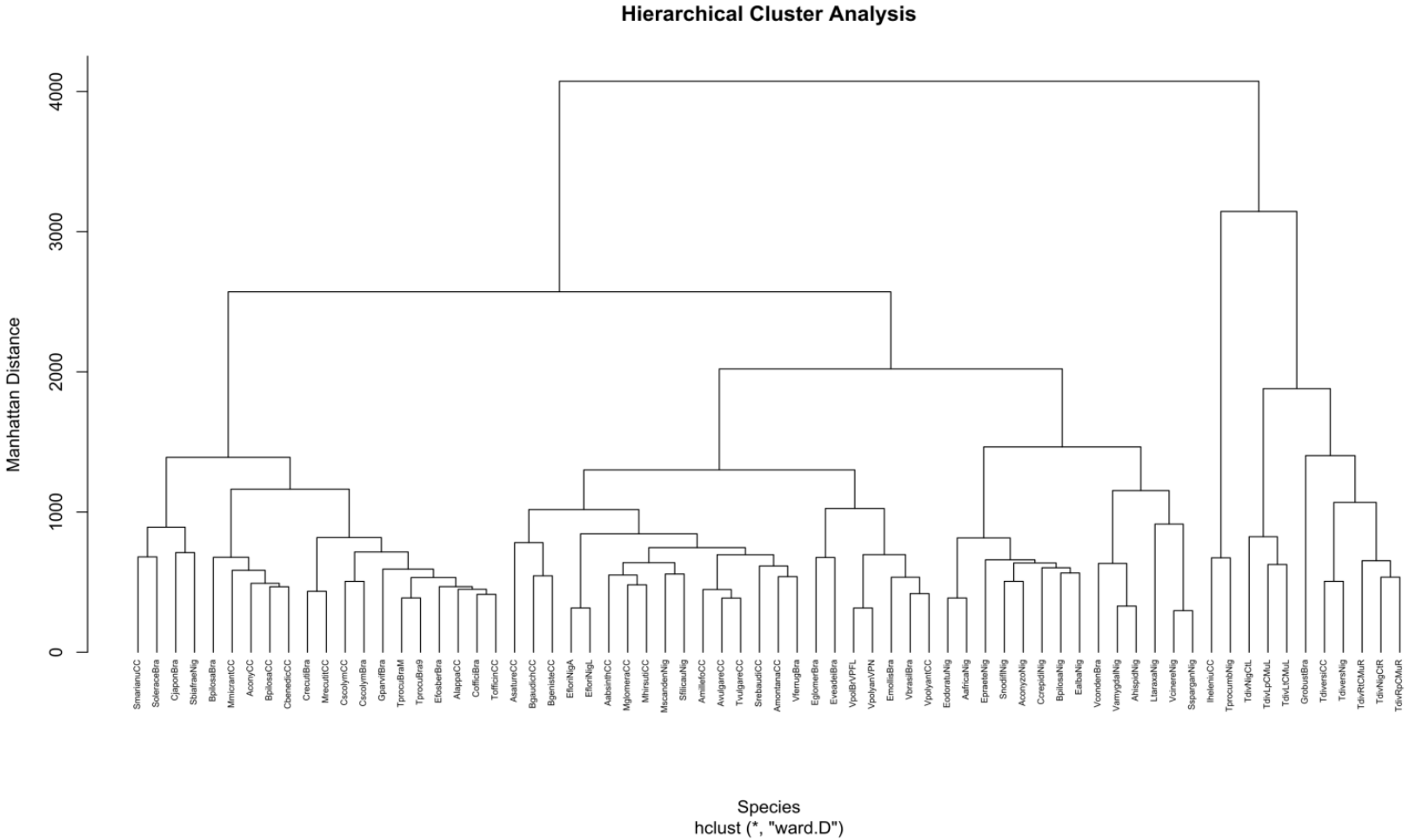

Figure 12: Hierarchical Cluster Analysis of sixty eight Brazilian and Nigerian Asteraceae species analyzed by UHPLC-HRMS, using log transformation, Manhattan distance and Ward's method with the software, R
Key: the codes represent the names of investigated plants (see LIST OF ABBREVIATIONS AND CODES)

4.2.3. Partial Least Square Discriminant Analysis

Based on the PCA (Figure13) model developed, PLS-DA models (Figures 14, 18, 22, 26 and 30) were developed for the glucose retardation, fungal and porcine pancreatic α-amylases inhibitory, glucose uptake and antioxidant activity assays respectively using the information of bioactivity obtained from each assay. The PLS-DA models developed for these assays enabled the discrimination between the classes of active and inactive plants for each assay; aiming to determine the group of variables responsible for the discrimination of the active plants. To achieve this, the variable importance in projection (VIP) plot was deployed to provide all the variables with a score, indicating their level of importance in the discrimination of the two groups, with variables having a VIP score ≥ 1.0 considered as significant in the discrimination, irrespective of class. The coefficient plot was also deployed to determine the variables particularly responsible for the classification of each class, active (positive coefficient) or inactive (negative coefficient).

4.2.3.1. Glucose retardation assay PLS-DA model

Supervised PLS-DA was deployed to determine the correlation between the UHPLC-ESI-MS metabolic fingerprints of the investigated plants and their percentage glucose retardation using dialysis tube. Two classes were therefore defined respectively as active and inactive with the 11 active plants (Figure 6) supervised into one class, while the remaining relatively inactive 57 plants were supervised into the second class. The statistical measures for the PLS-DA model developed were $R^2X(cum)$, 0.911, $R^2Y(cum)$, 0.925 and $Q^2(cum)$, 0.541 (Figure 14).

From the VIP (Figure 15) and coefficient (Figure 16) plots, the first few variables respectively with positive coefficients and VIP scores greater than 1 were selected as the significant features responsible for the observed glucose retardation in the active plants. The selected variables were subjected to dereplication techniques in order to annotate them (as stated in section 3.12; Table 3).

For example, the feature with *m/z* 301.07 $[M+H]^+$ and 299.056 $[M-H]^-$ and retention time 18.06 min and annotated as chrysoeriol, discriminated in this assay as active, occurs with high relative abundance in the plants that were observed to have a similar pattern of activity, including the commercial *B. gaudichaudiana*, Brazilian *E. veadeiroensis* and

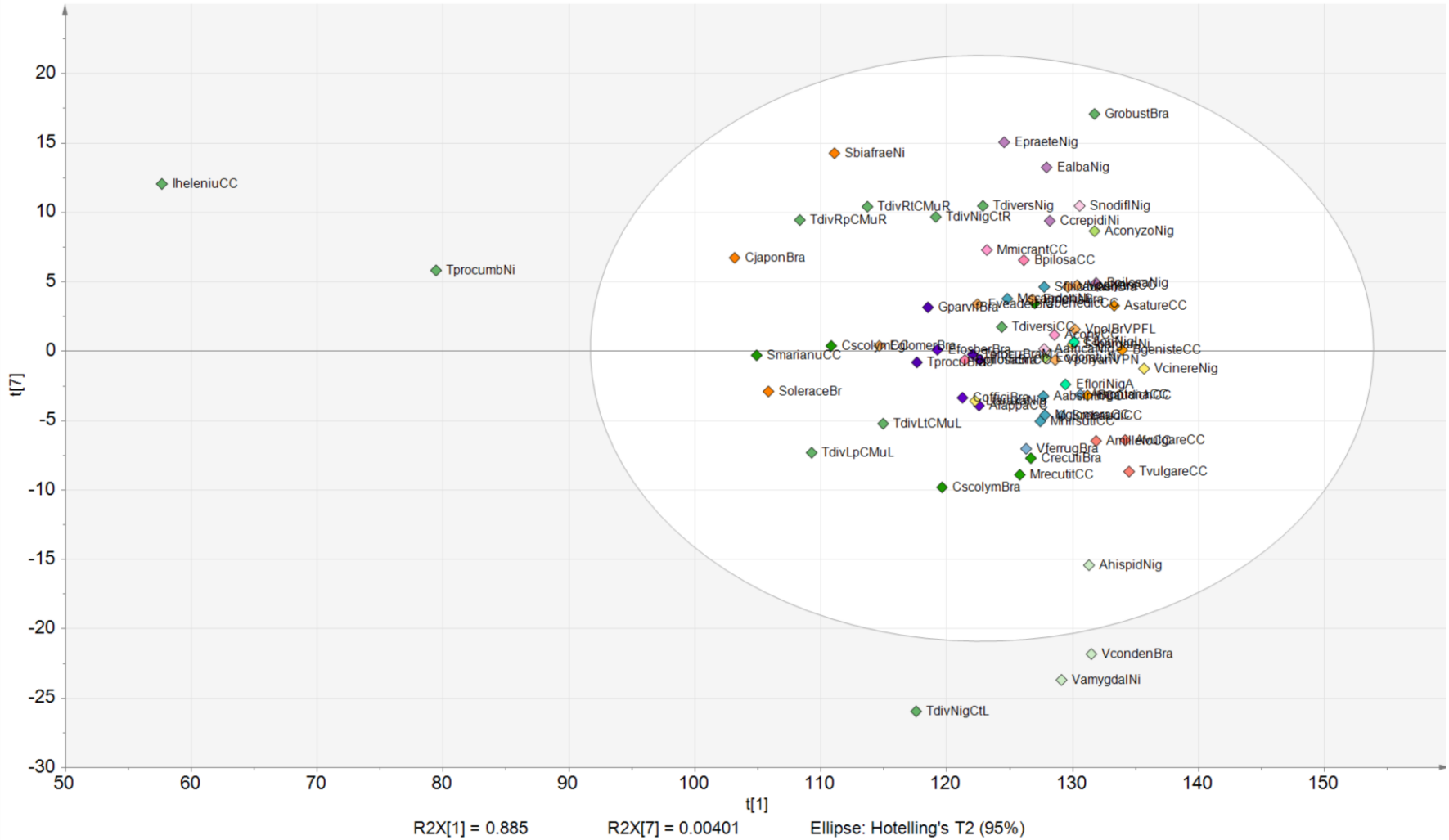

Figure 13: Principal Components Analysis score plot (PC1 vs. PC7) of the sixty eight investigated plants

Key: The first component explains 88.5% of the variation and the seventh component 0.4%, coloured according to clusters observed in Hierachichal Cluster Analysis. A, number of components, 7; $R^2X(cum)$, 0.93; Q^2 (cum), 0.90; the codes represent the names of investigated plants (see LIST OF ABBREVIATIONS AND CODES)

Nigerian *T. diversifolia*. The feature with *m/z* 565.155 $[M+H]^+$ and 563.14 $[M-H]^-$ at retention time 8.05 min corresponding to apigenin 6-*C*-arabinoside-8-*C*-glucoside, which was discriminated as active in this assay was detected to occur only in three of all the investigated plants, including commercial *B. gaudichaudiana* and commercial *A. millefolium*, belonging to a similar HCA group, both of which were observed to elicit activity > 20.0% at 30 min and at least 10.0% at 60 mins (Figure 6). apigenin 6-*C*-arabinoside-8-*C*-glucoside occurred with higher abundance in the *A. millefolium,* which correspondingly elicited the higher activity of the two plants. It was additionally detected, in the negative mode, in *B. genistelloides*, although with a significantly lower abundance, and observed activity, than in the related *B. gaudichaudiana*. The feature with *m/z* 611.16 $[M+H]^+$ and 609.145 $[M-H]^-$ at retention time 8.82 min was annotated as rutin and detected with the highest abundance in HCA clustered *V. brasiliana* and *V. ferruginea*, both of which have comparably high activity at 30 min with the latter eliciting higher activity at 60 min compared to the former, in agreement with their relative content of rutin (Figure 6). *M. micrantha*, which exhibited significantly high activity, especially at 30 min (17.3 ± 0.9%) and 5.9 ± 0.3% at 60 min also expressed a high relative abundance of rutin, although lower than that expressed by the *Vernonia* species above. It should be noted that though rutin was detected with a high relative abundance in the commercial *A. montana* than in the *M. micrantha*, the former had lower glucose retardation activity than the latter. This is suggested to be the possible presence of other metabolites in *A. montana*, which either antagonize rutin or enhance glucose movement across the dialysis tube. The sesquiterpene lactone with the feature at *m/z* 321.133 $[M+H]^+$ and retention time 18.44 min was detected with high relative abundance in some of the plants observed active in this assay, including *V. brasiliana* and *S. biafrae*, which were significantly the highest active especially at the later times, 120 and 180 mins, indicating their potential activity for a longer period of time than other active plants at retarding gut glucose absorption. Other active plants that expressed this annotated metabolite, however with a lower abundance include *A. millefolium*, *B. gaudichaudiana, G. parviflora*, *E. veadeiroensis*, commercial and Nigerian samples of *T. diversifolia*; and *V. condensate* from Brazil. The feature with *m/z* 530.129 and retention time 9.66 min, corresponding to the annotated 4-*O*-feruloyl 5-*O*-caffeoylquinic acid was detected with a high relative abundance in *V. ferruginea*¸which

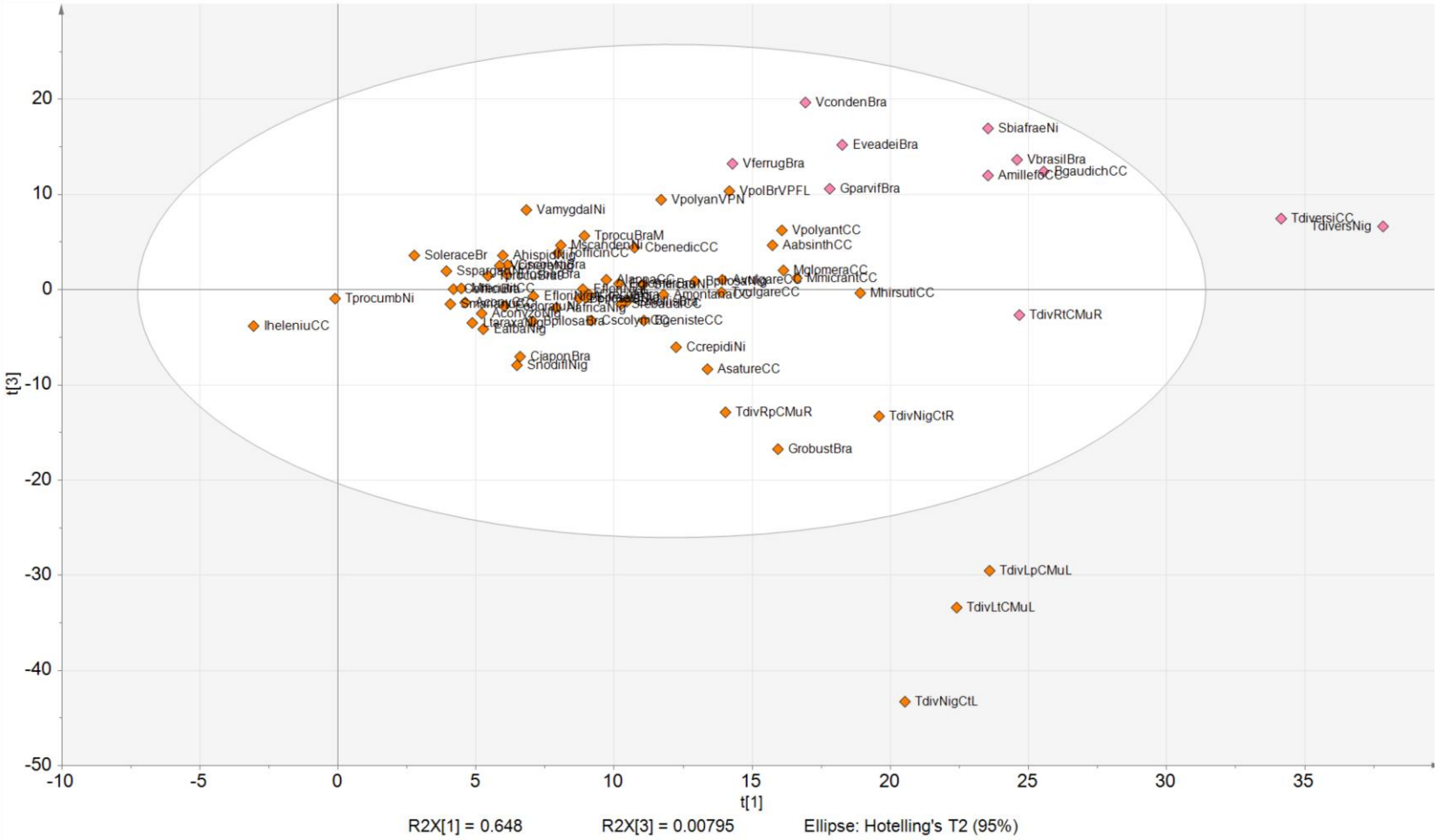

Figure 14: Partial Least Square Discriminant Analysis score plot of the first versus the third principal component in glucose retardation assay

Key: active class (pink) and inactive class (orange); -1, inactive class, +1, active class; A, number of components, 5; R^2X(cum), 0.911; R^2Y(cum), 0.925 and Q^2(cum), 0.541; the first component explains 64.8% of the variation and the third component 0.8%; the codes represent the names of the investigated plants (see LIST OF ABBREVIATIONS AND CODES)

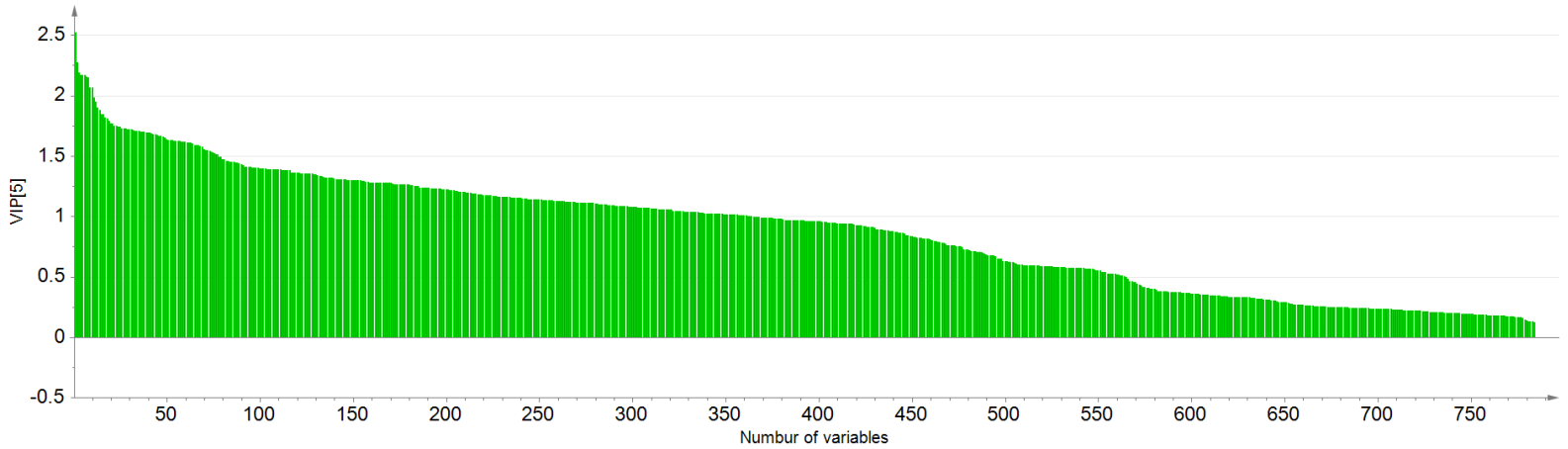

Figure 15: Variable importance in projection (VIP) plot obtained from partial least squares discriminant analysis (PLS-DA), supervised according to the active and inactive plants in the glucose retardation assay

Key: VIP, Variable importance in projection; the higher the VIP score (>1), the more the importance of the variable on the model, irrespective of activity class

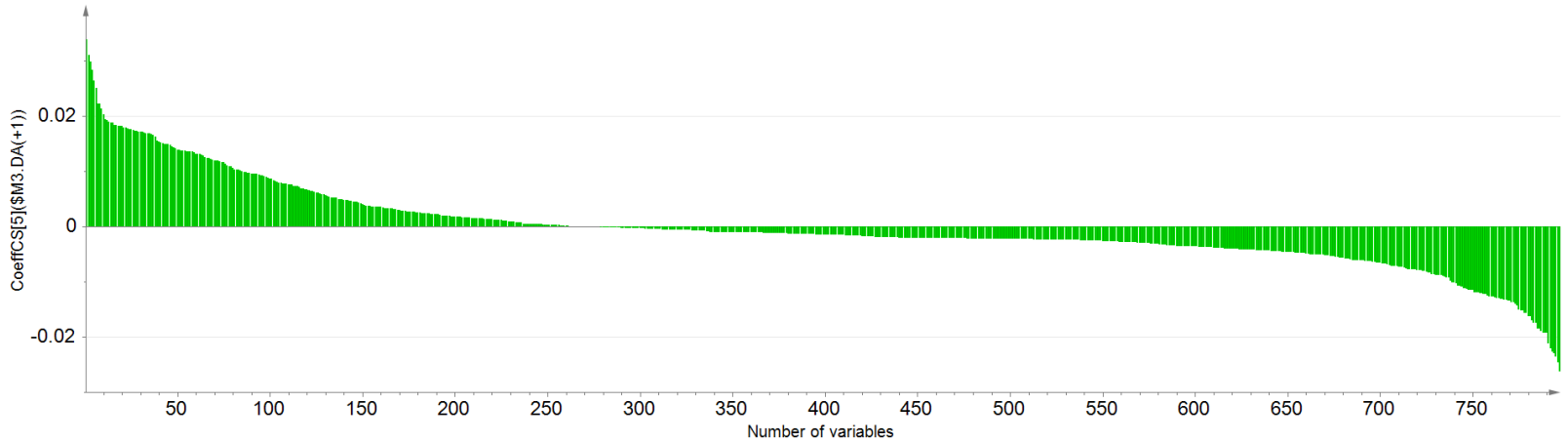

Figure 16: Coefficient plot obtained from partial least squares discriminant analysis (PLS-DA), supervised according to the active and inactive plants in the glucose retardation assay

Key: The variables, grouped to the right, with positive coefficients are important in the classification of the active group; while the variables, grouped to the left of the plot, with negative coefficients are important in the classification of the inactive group

similarly exhibited significant glucose retardation. In the positive mode, the feature with *m/z* 595.145 at retention time 12.65 min was detected only in *E. veadeiroensis* with a high relative abundance in agreement with observed activity. It was also detected with high relative abundance in the plant in the negative mode. All other active plants in this assay expressed tiliroside, as annotated, in varying abundances, as detected in the negative mode, except *B. gaudichaudiana*, the roots of cultivated *T. diversifolia* treated with *M. koenigii* roots, *G. parviflora*, commercial *T. diversifolia* and *S. biafrae.* The presence of tiliroside in the Nigerian sample of *T. diversifolia* and absence in the commercial and all the parts of the cultivated Nigerian samples of *T. diversifolia* may indicate the possibility of chemical diversity based on geographical source of similar plants. Additionally, the active plants had the presence of umbelliferone 7-*O*-glucopyranoside detected as *m/z* 325.092 at retention time 5.86 min; except *S. biafrae*, which was active but lacked the feature. Another discriminant variable in the positive mode that was annotated in this study was quercetin with *m/z* 303.05 at retention time 8.93 min. Similar to rutin, a quercetin glucoside, quercetin was detected with a high relative abundance in the commercial *A. montana* and Brazilian *V. ferruginea*, with the abundance in the former being slightly higher than in the latter while reverse is the case with the observed activity. This further agrees with the possibility of an antagonism against quercetin and its glycoside or presence of metabolites in commercial *A. montana* that enhance glucose movement across the dialysis tube. All the active plants, except *E. veadeiroensis* and the roots of cultivated *T. diversifolia* treated with *M. koenigii* roots, expressed the feature at *m/z* 417.25 and retention time 11.17 in the negative mode. The features at *m/z* 381.191 and retention time 17.53 min and *m/z* 349.164 and retention time 14.60 min, respectively annotated as tithonin and tagitinin C were detected only in both commercial and Nigerian samples of *T. diversifolia*, supporting their dereplication as STLs. Also, the feature at *m/z* 365.161 $[M-H]^-$ and retention time 13.26 min was detected with highest abundance observed in the leaves of *Tithonia* samples, irrespective of their source. Control leaves of cultivated *T. diversifolia* from Nigeria, leaves of cultivated *T. diversifolia* co-planted with the leaves of *M. koenigii*, leaves of cultivated *T. diversifolia* treated with the leaves of *M. koenigii*, leaves of commercial *T. diversifolia* and leaves of *T. diversifolia* from Nigeria all were observed to have the highest abundance of this feature with other investigated

plants having significantly lesser abundance. These samples elicited significant glucose retardation activity throughout the time tested, 30, 60, 120 and 180 min. Although, *G. robusta* expressed a relatively lower abundance than these *Tithonia* samples, the abundance was higher than in most of the other investigated samples, suggesting the rationale behind the clustering of *G. robusta* with the Tithonia *samples* (Figure 12). And with the reduction compared to the *Tithonia* samples was a corresponding reduction in the glucose retardation activity. Based on its fragmentation patterns, it was annotated as the ammonium adduct of tagitinin C $[M+NH_4]^+$. Furthermore, the feature with *m/z* 283.05 $[M-H]^-$ and retention time 17.81 min, corresponding to acacetin was detected variably in the plants. It was observed to be absent in the leaves of all the *Tithonia* samples while it was detected with low abundance in the control roots of cultivated *T. diversifolia* from Nigeria and the roots of cultivated *T. diversifolia* treated with *M. koenigii* roots.

Apigenin, corresponding to the feature with *m/z* 269.046 and retention time 13.80 min, was detected, as expected, in most of the plants with a high relative abundance observed in the active plants whereas the leaves of cultivated *T. diversifola* co-planted with *M. koenigii* leaves expressed low abundance. This is similar with the abundance of flavanokanin represented by the feature with *m/z* 287.056 at 11.82 min.

Table 3: Annotated discriminant metabolites for glucose retardation assay

RT (min)	**Compound name**	**$[M+H]^+$ (m/z)**	**AIF $[M+H]^+$**	**$[M-H]^-$ (m/z)**	**AIF $[M-H]^-$**	**UV_{max} (nm)**
5.86	umbelliferone 7-*O*-glucopyranoside	325.0917 VIP, 1.9	325 > 163, 162			
8.06	apigenin 6-*C*-arabinoside-8-*C*-glucoside	565.1551bp VIP, 1.6		563.1407 bp VIP, 1.5	563 > 503, 473, 443, 383, 353	270, 333
8.82	rutin	611.1602bp, 633 $[M+Na]^+$ VIP, 1.6	611 > 593, 465, 453, 331, 303, 273, 245, 217	609.1458 bp VIP, 1.1	609 > 591, 300, 271, 255, 151	255, 355
8.93	quercetin	303.0496 VIP, 1.1	303 > 287, 259, 153, 149			257, 284sh, 317, 335, 343, 354

9.66	4-*O*-feruloyl 5-*O*-caffeoylquinic acid	530.1291 VIP, 1.2	531 > 517, 369, 355, 337, 193, 175	529.0988 VIP, 1.1	529, 515, 367, 353, 335, 191, 173	245, 328
11.17	benzenemethanol, α-[1-[2,6-dimethoxy-4-(2-propenyl)phenoxy]ethyl]-3,4,5-trimethoxy-	417.2497 VIP, 1.7	417 > 241, 227, 222, 212, 199, 184, 177, 170			
11.82	flavanokanin			287.0561 VIP, 1.3	287 > 269, 151, 135, 123	286, 336
12.65	tiliroside	595.1449 VIP, 1.1	595 > 449, 309, 287	593.1304 VIP, 1.4	593 > 447, 307, 285	267, 315
12.91	wedelolactone	315.0494bp VIP, 1.2	315 > 297, 287, 269, 259, 161	313.0348bp VIP, 1.8	313 > 295, 285, 151	254sh, 306, 349
13.26	tagitinin C	367.1749	367 $(M+NH_4)^+$, 349, 333, 243, 279, 261	365.1606 VIP, 2.2	365, 331, 259, 241	248
13.80	apigenin			269.0456 VIP, 1.1	269 > 225, 201, 159, 151, 149, 117, 107	267, 338
14.33	8-epidesacylcynaropicrin-3-*O*-glucoside	442.1716 $[M+NH_4]^+$, 423.166 VIP, 1.6	423 > 261, 243, 162			
14.60	tagitinin C	349.1643 VIP, 1.3	367 $[M+NH_4+H]^+$, 349, 333, 279, 261, 243	393.1558 VIP, 1.0	393 > 365, 347, 331, 261, 241	248
17.52	tithonin	381.1905 VIP, 1.4	381 > 363, 349, 331, 293, 279, 261, 243, 215, 197, 169	379.1760	379 > 361, 347, 277, 260, 241, 229, 214, 205, 187, 179, 133	219

17.81	acacetin	285.0613 VIP, 1.2	285 > 287, 270, 243, 153, 133	283.0405 VIP, 1.5	283 >268, 244, 151, 136	267, 290, 325, 336, 345
18.06	chrysoeriol	301.0706	301 > 286	299.0558bp VIP, 1.4	299 > 284, 153, 151	269, 290sh, 346, 367
18.44	4-(acetyloxy)-3,3a,4,5,9a,9b-hexahydro-6-(hydroxymethyl)-3,9-dimethyl-azuleno[4,5-*b*]furan-2,7-dione	321.1328 VIP, 1.4	321 > 291, 249, 235			-

Key: ID – Compound identity; RT – retention time (min); AIF, All Ion Fragmentation; UVmax, wavelength of maximum absorption in the ultraviolet spectral region; sh, shoulder

It was observed from the dereplication results that flavonoids and their glycosides were predominant in the discrimination of the class of plants observed with glucose retardation activity. Other significant annotated metabolites include a coumestan, some sesquiterpene lactones and a quinic acid derivative (Table 3; Figure 17). It was observed that wedelolactone was detected in relatively high amount in all the plants that elicited activity in this assay. However, the metabolite additionally occurs in some of the inactive plants, including *B. genistelloides*, which elicited some activity (13.7 ± 0.6%, 5.9 ± 0.2% and 4.6 ± 0.1% at 30, 60 and 120 min) better than the control but lower than the threshold of activity chosen in this study. *S. nodiflora* and *E. alba*, which were observed in a cluster using HCA, also expressed a relatively high content of wedelolactone but have a low glucose retardation activity and it is suggested that, along with wedelolactone, they possess other specialized metabolites that may be antagonizing the activity of wedelolactone. Furthermore, the metabolites annotated in this study occurred variably in all the plants with the glucose retardation activity.

This is the first study for the application of metabolomics to determine the influence of plants specialized metabolites on glucose diffusion *in vitro*. The results showed that flavonoids, their glycosides and sesquiterpene lactones may retard gut glucose absorption, which is an important mechanism, should α-amylase inhibition fails.

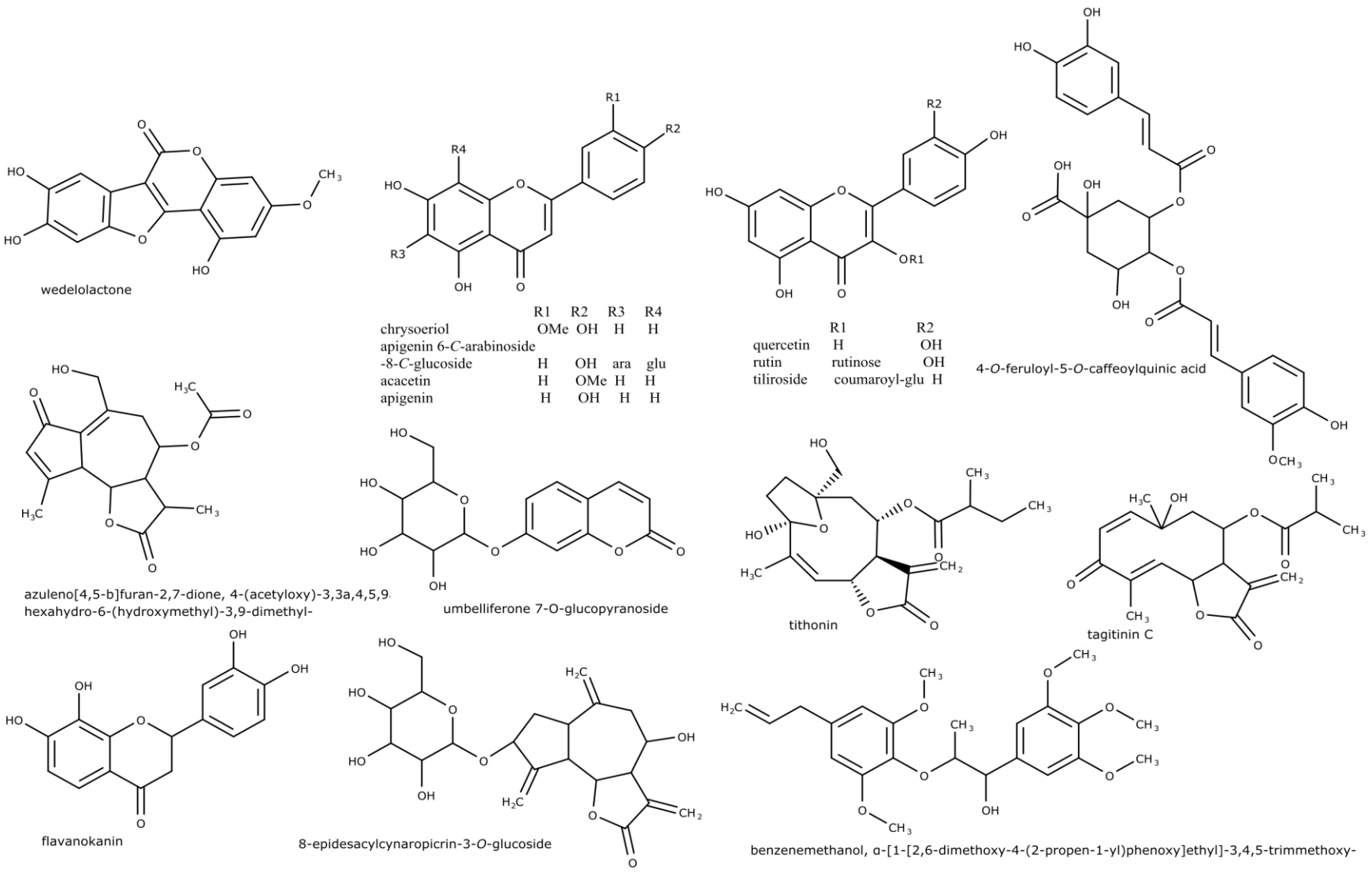

Figure 17: Structures of discriminant metabolites for glucose retardation assay

4.2.3.2. Fungal α-amylase inhibitory assay PLS-DA model

For the correlation of the metabolic fingerprints of the investigated plants with their percentage fungal α-amylase inhibition, a PLS-DA model was also developed. Two classes were defined respectively as active and inactive with the 37 extracts that significantly ($P < 0.05$) inhibited fungal α-amylase ≥ 30.0% compared with control (Figure 7) supervised into one class, while the remaining inactive 31 plants were supervised into the second class (Figure 18). The statistical measures for the PLS-DA model developed were R^2X(cum), 0.994; R^2Y(cum), 0.899 and Q^2(cum), 0.614.

From the VIP (Figure 19) and coefficient (Figure 20) plots, the first few variables respectively with positive coefficients and VIP scores greater than 1 were selected as the significant features responsible for the observed fungal α-amylase inhibition in the active plants. The selected variables were subjected to dereplication techniques in order to annotate the discriminant substances (as stated in section 3.12; Table 4).

It was observed from the dereplication results that flavonoids and a glycoside were similarly predominant in the discrimination of the class of the plants observed with fungal α-amylase inhibitory activity. Flavones with unsaturation at C2-3, and presence of -OH at C4', 5 together with a glycosylation at C3 have been reported to inhibit α-amylase activity (LIAO et al., 2018). Such variables that were discriminated in this assay include the flavones, luteolin, apigenin, 5,7,4'-trihydroxy-8- methoxyflavone and isorhamnetin which possed a C2-3 unsaturation, hydroxyl groups at positions 5 and 7 of the A ring and 4 of the B ring, justifying their indication as important, although isorhamnetin has an hydroxyl group at position 3 of the C ring, which has been shown to reduce the inhibition (TADERA et al., 2006). Flavanokanin, which is though a flavanone, has hydroxyl groups at positions 7 of the A ring and 4 of the B ring, which may justify its discrimination in this assay. Also, quercetin-3-*O*-glucuronide was indicated as important. It has been shown that monoglycosides of flavonoids better inhibit metabolic enzymes than their polyglycoside forms (KIM et al., 2000). Also, the discrimination in this assay may be due to the glucuronidation at position 3 on the C ring. Other flavonoids indicated as important include 3',4'-dimethoxyluteolin and 3,4'-dimethoxyquercetin, which may exhibit reduced activity compared with the other flavonoids with a 4'-OH. This may explain why they appeared lower on the coefficient plot with lower coefficeients. Other significant annotated

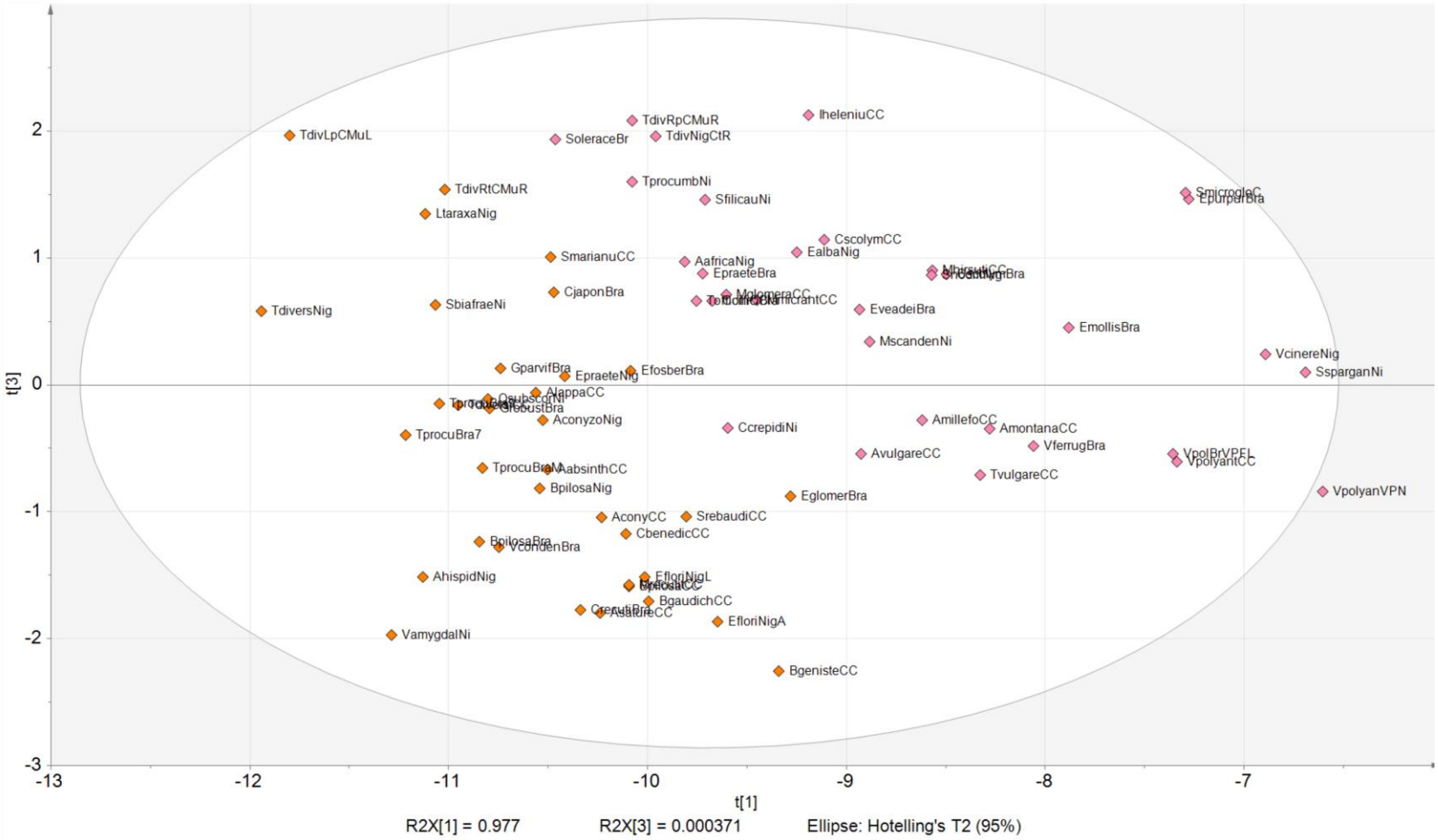

Figure 18: Partial Least Square Discriminant Analysis score plot of the first versus the third principal component in fungal α-amylase inhibitory assay

Key: Active class (pink) and inactive class (orange) -1, inactive class, +1, active class; A, number of components, 4; R^2X(cum), 0.994; R^2Y(cum), 0.899 and Q^2(cum), 0.614; the first component explains 97.8% of the variation and the third component 0.03%; the codes represent the names of the investigated plants (see LIST OF ABBREVIATIONS AND CODES)

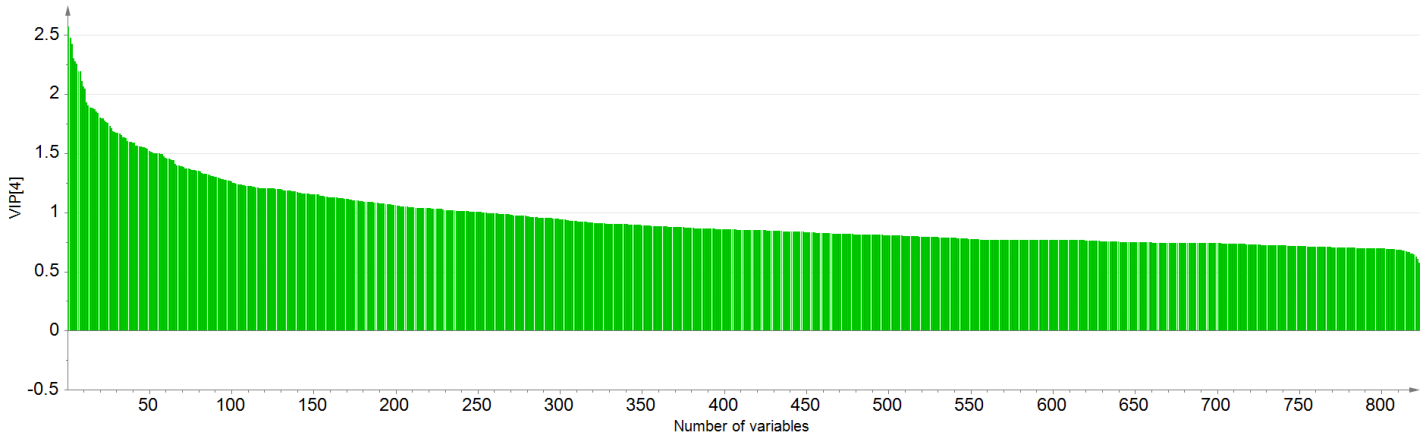

Figure 19: Variable importance in projection (VIP) plot obtained from partial least squares discriminant analysis (PLS-DA), supervised according to the active and inactive plants in fungal α-amylase inhibitory assay

Key: VIP, Variable importance in projection; the higher the VIP score (>1), the more the importance of the variable on the model, irrespective of activity class

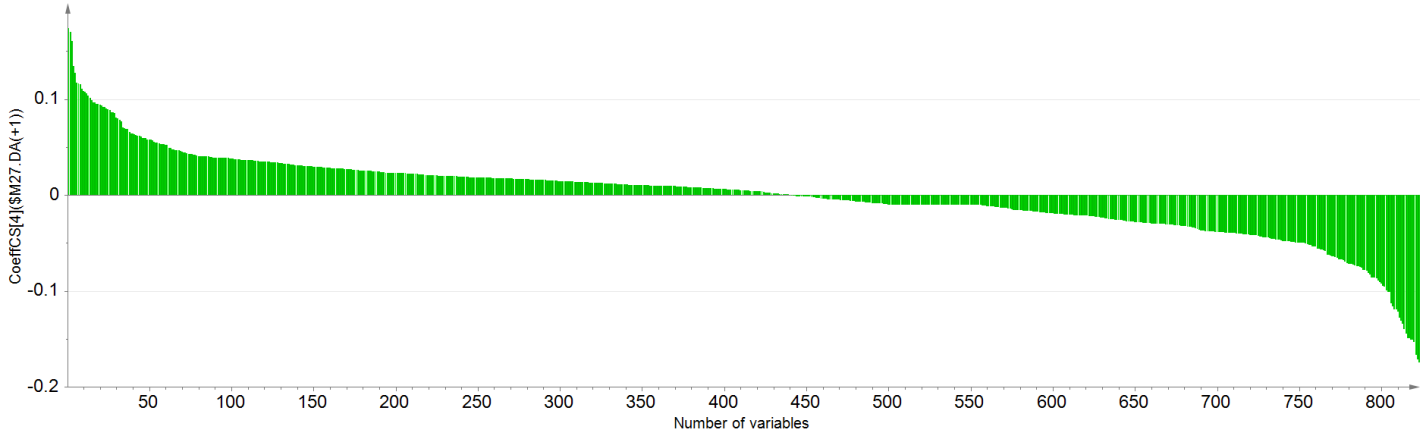

Figure 20: Coefficient plot obtained from partial least squares discriminant analysis (PLS-DA), supervised according to the active and inactive plants in fungal α-amylase inhibitory assay

Key: the variables, grouped to the right, with positive coefficients are important in the classification of the active group; while the variables, grouped to the left of the plot, with negative coefficients are important in the classification of the inactive group

Table 4: Annotated discriminant metabolites for fungal α-amylase inhibitory assay

RT (min)	Compound name	$[M+H]^+$ (m/z)	AIF $[M+H]^+$	$[M-H]^-$ (m/z)	AIF $[M-H]^-$	UV_{max} (nm)
7.78	5-*O*-feruloylquinic acid			367.1034 VIP, 1.9	367 > 193, 191, 179, 173, 134	233, 323
9.10	quercetin-3-*O*-glucuronide			477.0675 VIP, 1.8	477 > 384, 301, 175,	254, 291, 345
11.82	flavanokanin			287.0561 VIP, 2.2	287 > 269, 151, 135, 123	286, 336
12.30	luteolin			285.0405 VIP, 1.7	285 > 175, 151, 133, 107	266, 278sh, 348
12.91	isorhamnetin			315.0511 VIP, 2.4	315 > 300, 271	255, 304sh, 356
13.80	apigenin			269.0456 VIP, 2.6	269 > 225, 201, 159, 151, 149, 117, 107	267, 338
14.27	5,7,4'-trihydroxy-8- methoxyflavone			299.0562 VIP, 2.0	299 > 284, 255, 227, 211, 182, 117	272, 336
14.43	tagitinin C	367.1749 VIP, 1.6	367 $(M+NH_4+H)^+$, 349, 333, 243, 279, 261	365.1605 VIP, 1.0	365, 331, 259, 241	248
15.23	3,4'-dimethoxyquercetin			329.0668 VIP, 1.9	329 > 316, 301, 286, 180, 151, 135	253, 266sh, 296sh, 352
15.88	cynarascoloside C			425.1820, 851 $[2M-H]^-$ VIP, 1.0	425 > 263, 162	220
15.88	tithonin	381.1905	381 > 363, 349, 331, 293, 279, 261, 243, 215, 197, 169	379.1760 VIP, 1.6	379 > 361, 347, 277, 260, 241, 229, 214, 205, 187, 179, 133	219

18.35	3',4'-dimethoxyluteolin	315.0859	315 > 300bp, 272, 243	313.0716 VIP, 2.5	313 > 298, 283, 269, 255, 163	268, 304sh, 347
18.48	molephantinin	361.1641 VIP, 1.5	361 > 343, 83bp			

Key: ID – Compound identity; RT – retention time (min); AIF, All Ion Fragmentation; UVmax, wavelength of maximum absorption in the ultraviolet spectral region; sh, shoulder

metabolites include some sesquiterpene lactones and feruloylquinic acid derivative (Table 4; Figure 21). The metabolites annotated in this study occurred variably in all the plants with the fungal α-amylase inhibitory activity.

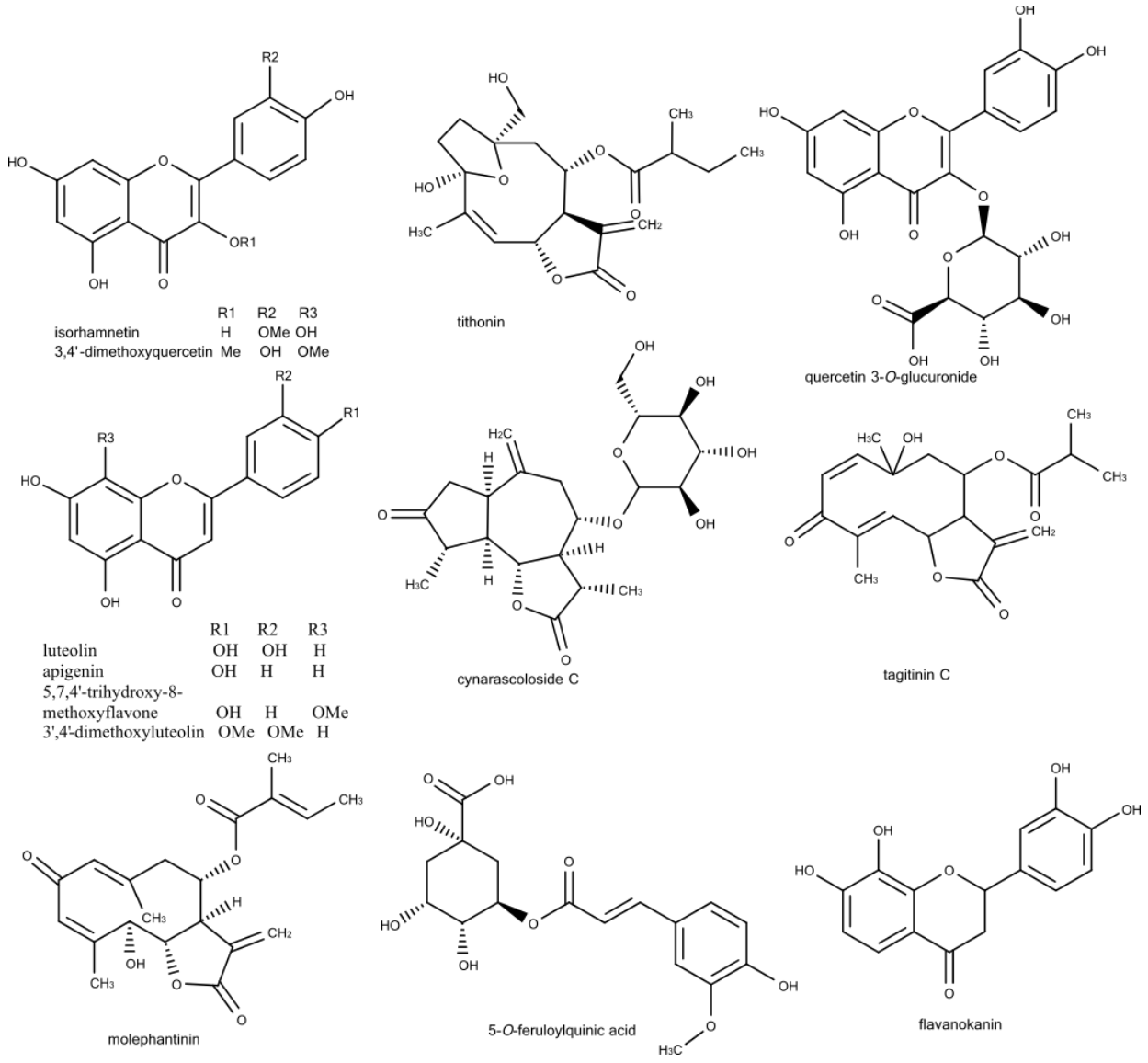

Figure 21: Structures of discriminant metabolites for fungal α-amylase inhibitory assay

4.2.3.3. Porcine pancreatic α-amylase inhibitory assay PLS-DA model

The results obtained from the porcine pancreatic α-amylase inhibitory assay were also subjected to correlation with the metabolic fingerprints of the investigated plants, and a PLS-DA model was accordingly developed. Two classes were defined respectively as active and inactive with the 12 extracts that elicited significant activity > 9.0% compared with negative control (Figure 8) supervised into one class, while the remaining inactive 56 plants were supervised into the second class (Figure 22). The statistical measures for the PLS-DA model developed were R^2X(cum), 0.917; R^2Y(cum), 0.959 and Q^2(cum), 0.614.

From the VIP (Figure 23) and coefficient (Figure 24) plots, the first few variables respectively with positive coefficients and VIP scores greater than 1 were selected as the significant features responsible for the observed porcine pancreatic α-amylase inhibition in the active plants. The selected variables were subjected to dereplication techniques in order to annotate them (as stated in section 3.12; Table 5).

It was observed from the dereplication results that flavonoids and their glycosides were similarly predominant in the discrimination of the class of the plants observed with porcine pancreatic α-amylase inhibitory activity. Other significant annotated metabolites include some sesquiterpene lactones and feruloylquinic acid derivative (Table 5; Figure 25). The metabolites annotated in this study occurred variably in all the plants with the porcine pancreatic α-amylase inhibitory activity.

Computational ligand docking-assisted structure-activity relationships of some α-amylase inhibitors have shown that flavonols and flavones inhibit amylase by hydrogen bonds between the hydroxyl groups of the polyphenol ligands and the catalytic binding site; and formation of a conjugated π-system, stabilizing the interaction with the active site. In the study, apigenin, kaempferol and isorhamnetin exhibited significant binding degrees and invariably higher α-amylase inhibition (LO PIPARO et al., 2008). The importance of this hydrogen bond in the binding between flavonoids and α-amylase has also been reported (LIAO et al., 2018). As observed with the fungal amylase assay, where quercetin-3-O-glucuronide was discriminated for the observed activity, in the case of PPA, glycosides of flavonoids were observed to be the more important discriminants with the diglycoside, apigenin 6-*C*-arabinoside-8-*C*-glucoside, detected in both positive, *m/z* 565.155 $[M+H]^+$ and negative modes, *m/z* 563.141 $[M-H]^-$ both at the retention time 8.05

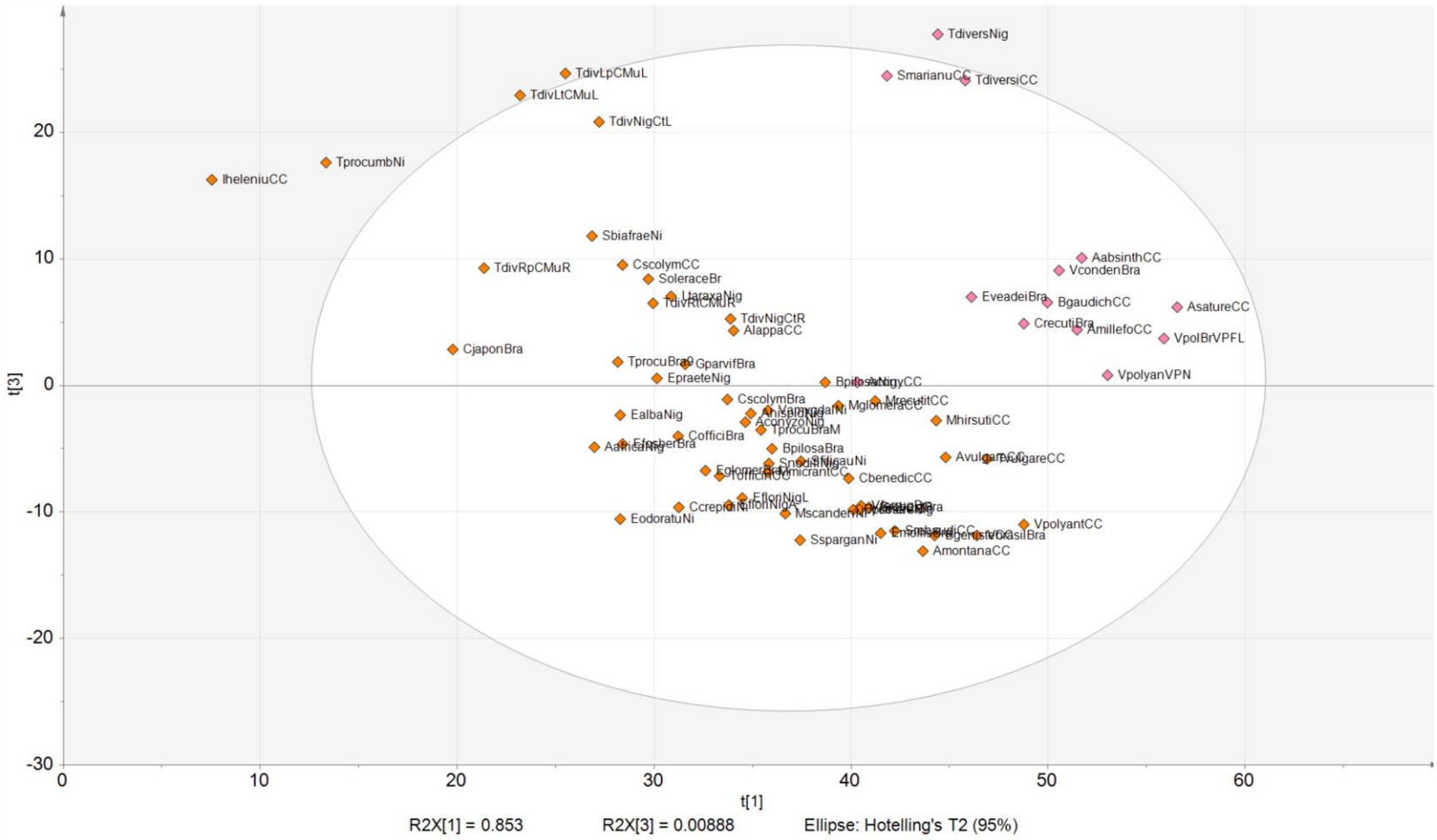

Figure 22: Partial Least Square Discriminant Analysis score plot of the first versus the third principal component in porcine pancreatic α-amylase inhibitory assay

Key: Active class (pink) and inactive class (orange) -1, inactive class, +1, active class; A, number of components, 6; R2X(cum), 0.917; R2Y(cum), 0.959 and Q2(cum), 0.614; the first component explains 85.3% of the variation and the third component 0.8%; the codes represent the names of the investigated plants (see LIST OF ABBREVIATIONS AND CODES)

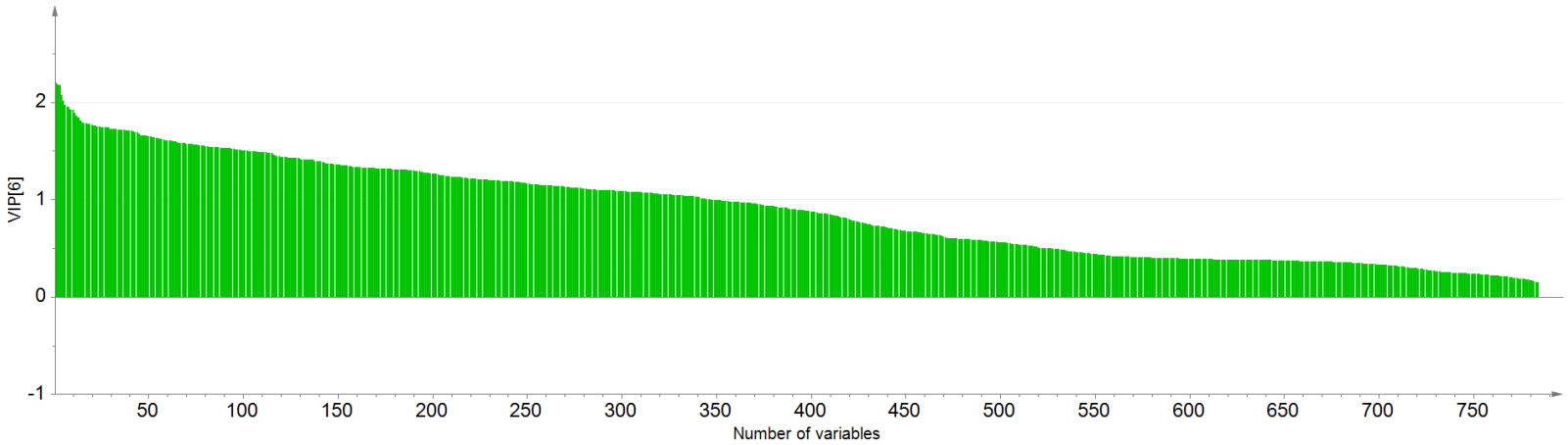

Figure 23: Variable importance in projection (VIP) plot obtained from partial least squares discriminant analysis (PLS-DA), supervised according to active and inactive plants in porcine pancreatic α-amylase inhibitory assay

Key: VIP, Variable importance in projection; Key: the higher the VIP score (>1), the more the importance of the variable on the model, irrespective of activity class

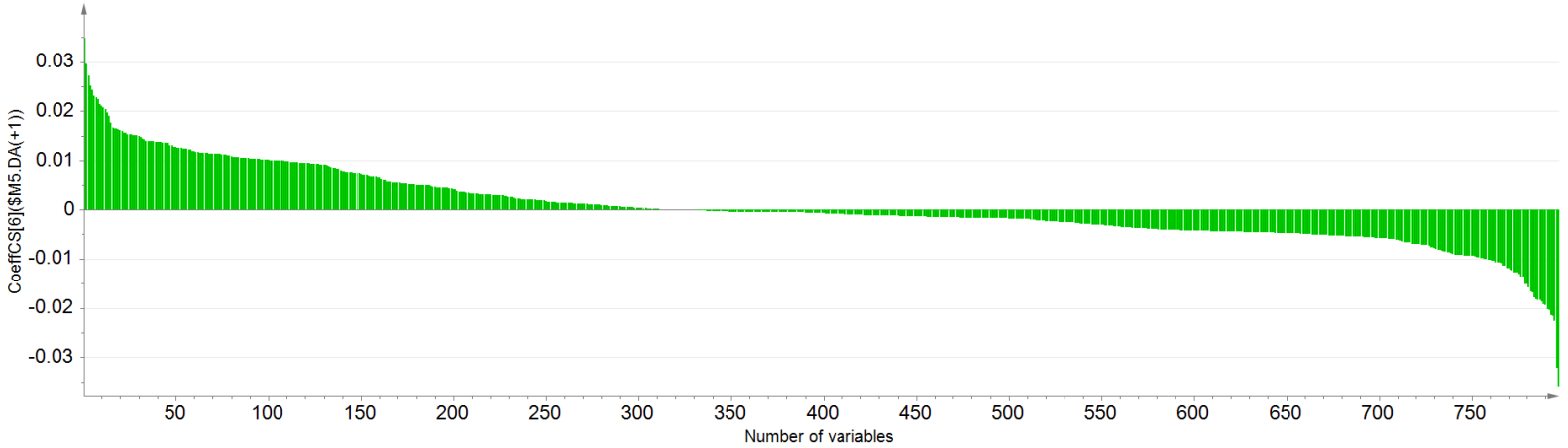

Figure 24: Coefficient plot obtained from partial least squares discriminant analysis (PLS-DA), supervised according to the active and inactive plants in porcine pancreatic α-amylase inhibitory assay

Key: the variables, grouped to the right, with positive coefficients are important in the classification of the active group; while the variables, grouped to the left of the plot, with negative coefficients are important in the classification of the inactive group

Table 5: Annotated discriminant metabolites for porcine pancreatic α-amylase inhibitory assay

RT (min)	Compound name	$[M+H]^+$ (m/z)	AIF $[M+H]^+$	$[M-H]^-$ (m/z)	AIF $[M-H]^-$	UV_{max} (nm)
8.06	apigenin 6-*C*-arabinoside-8-*C*-glucoside	565.1551bp VIP, 1.3		563.1407 bp VIP, 1.1	563 > 503, 473, 443, 383, 353	270, 333
9.20	6-methoxyquercetin-7-*O*-glucoside			493.0991 VIP, 1.1	493 > 331, 316	253sh, 336, 352
9.87	quercetin	303.0510 VIP, 1.2	303 > 287, 259, 153, 149			257, 284sh, 317, 335, 343, 354
9.94	kaempferol-6-methoxy-3-*O*-glucoside			477.1039 VIP, 1.3	477 > 315, 299, 271	253sh, 352
11.74	4-*O*-feruloyl 5-*O*-caffeoylquinic acid	530.1291	531 > 517, 369, 355, 337, 193, 175	529.1353 VIP, 1.0	529 > 515, 367, 353, 335, 191, 173	245, 328
13.26	tagitinin C	367.1749	367 $[M+NH_4]^+$, 349, 333, 243, 279, 261	365.1606 VIP, 1.8	365, 331, 259, 241	248
13.91	tithofolinolide			409.1506 VIP, 1.4	409 > 339, 295, 277, 259	
14.33	8-epidesacylcynaropicrin-3-*O*-glucoside			423.1664 VIP, 1.6	423 > 261, 243, 162	
14.43	tagitinin C	367.1749 VIP, 1.4	367 $[M+NH_4]^+$, 349, 333, 279, 261, 243	365.1605 VIP, 1.8	365, 349, 331, 259, 241	248
14.60	tagitinin C	349.1643 VIP, 1.1	367 $[M+NH_4]^+$, 349, 333, 279, 261, 243	393.1558 VIP, 1.2	393 > 365, 347, 331, 261, 241	248

15.39	3,4',6-trimethoxyquercetagetin			359.0773 VIP, 1.1	359 > 344, 329, 314, 301, 286, 258	268, 337, 345, 362, 372
15.72	4-(acetyloxy)-3,3a,4,5,9a,9b-hexahydro-6-(hydroxymethyl)-3,9-dimethyl-azuleno[4,5-*b*]furan-2,7-dione	321.1328 VIP, 1.1	321 > 291, 249, 235			
15.88	tithonin	381.1905 VIP, 1.2	381 > 363, 349, 331, 293, 279, 261, 243, 215, 197, 169	379.1760 VIP, 1.7	379 > 361, 347, 277, 260, 241, 229, 214, 205, 187, 179, 133	219
17.81	acacetin	285.0613 VIP, 1.0	285 > 287, 270, 243, 153, 133	283.0405 VIP, 1.1	283 > 285, 268, 244, 151, 136	267, 290, 325, 336, 345

Key: ID – Compound identity; RT – retention time (min); AIF, All Ion Fragmentation; UVmax, wavelength of maximum absorption in the ultraviolet spectral region; sh, shoulder

min, having the highest coefficient after 8-epidesacylcynaropicrin-3-*O*-glucoside, a sesquiterpene lactone glucoside, which was also discriminated in the glucose retardation assay. The feature at *m/z* 423.166, retention time 14.33 min, corresponding to 8-epidesacylcynaropicrin-3-*O*-glucoside was detected with moderate abundance in all the plants observed to be active in this assay. Whereas the feature with *m/z* 565.155 $[M+H]^+$ and *m/z* 563.141 $[M-H]^-$ and retention time 8.05 min corresponding to apigenin 6-*C*-arabinoside-8-*C*-glucoside was detected in commercial *B. gaudicahudiana* and *A. millefolium* with high relative abundance, suggesting this metabolite is responsible for the 21.0 ± 1.3 and 15.0 ± 0.4% activity elicited by the plants respectively. Additionally, kaempferol-6-methoxy-3-*O*-glucoside, which fulfills the 3-*O*-glycosilation of flavonoids for amylase inhibition, and 6-methoxyquercetin 7-*O*-glucoside, which fulfills the flavone requirement were also discriminated in this assay. It must be noted that the hydroxyl

group at position 7 on the A ring of 6-methoxyquercetin 7-*O*-glucoside has been replaced by *O*-glycosyl, which may reduce its activity; justifying the lower coefficient of the discriminant. It has however been shown, in support of these monoglycosides of flavonoids, that they are better inhibitors of metabolic enzymes than their polyglycoside forms (KIM et al., 2000). The report of this study also showed that two monoglycosides of flavonoids, 6-methoxyquercetin 7-*O*-glucoside and kaempferol-6-methoxy-3-*O*-glucoside, were determined for this activity with one di-glycoside, apigenin 6-*C*-arabinoside-8-*C*-glucoside (KIM et al., 2000). Acacetin, an *O*-methylated flavone and quercetin, a flavonol, were also observed as discriminants for this assay, fulfilling some of the structural requirements for inhibition of α-amylase including an unsaturation at C2-3 and the presence of hydroxyl groups at positions 5 and 7 on the A ring. The C3-OH present in quercetin, which has been shown to reduce activity, may be responsible for the lower coefficient compared with acacetin. The presence of a single -OCH_3 on the B ring, as observed with acacetin may be unimportant because it has been reported that the inhibitory potential is enhanced with a -OCH_3 beside an -OH on the B ring. Similarly, 5,7,3'-trihydroxy-3,6,4'-trimethoxyflavone was discriminated in this assay in agreement with previous report that shows that -OCH_3 beside an –OH on the B ring enhances activity and the presence of -OCH_3 at C3, which increases the electron density of the ring system, may contribute to enhancing activity. However, while some of the active plants do not have this feature with *m/z* 359.077 and retention time 15.39 min, others expressed low abundance. It was also observed that with this feature, there is a negative correlation between the abundance and the observed activity. Other metabolites discriminated in this assay include tithonin, tagitinin C and its ammonium adduct, similar with the fungal amylase assay; and tithofolinolide. Tithonin, detected at *m/z* 381.19 $[M+H]^+$, was expressed only by the leaves of commercial *T. diversifolia* and the same plant from Nigeria suggesting that it may contribute to the elicited 16.0 and 10.0% activity of these plants respectively. This is similar with the features at *m/z* 349.164 $[M+H]^+$ and 367.175 $[M+NH_4+H]^+$ and retention time 14.60 and 14.43 min corresponding to the metabolite annotated as tagitinin C and its ammonium adduct, *m/z* 367.175 $[M+NH_4+H]^+$ and retention time 13.26 min, all of which were found in the leaves of commercial *T. diversifolia* and the same plant from Nigeria, as observed with tithonin above. While in the fungal

amylase assay, 5-*O*-feruloylquinic acid was discriminated as important, 4-*O*-feruloyl 5-*O*-caffeoylquinic acid was indicated as important in the glucose retardation and PPA assays.

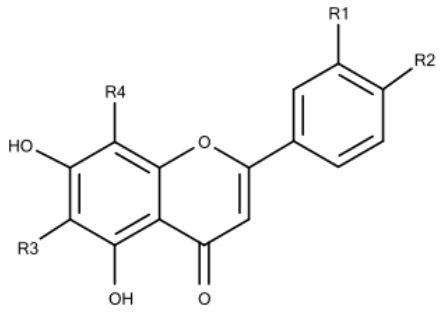

	R1	R2	R3	R4
apigenin 6-*C*-arabinoside-8-*C*-glucoside	H	OH	ara	glu
acacetin	H	OMe	H	H

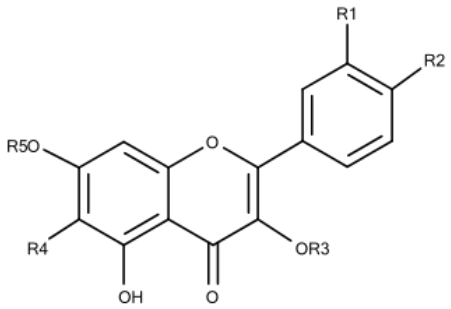

	R1	R2	R3	R4	R5
quercetin	OH	OH	H	H	H
3,4',6-trimethoxy quercetagetin	OH	OMe	Me	OMe	H
6-methoxyquercetin-7-*O*-glucoside	OH	OH	H	OMe	glu
6-methoxykaempferol-3-*O*-glucoside	H	OH	glu	OMe	H

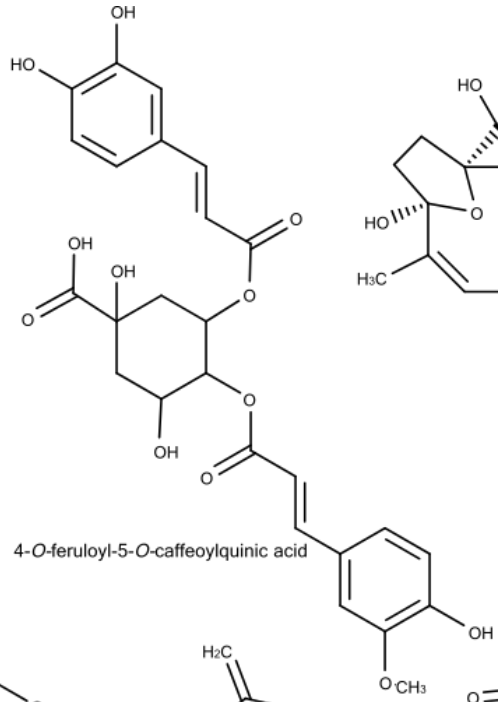

4-*O*-feruloyl-5-*O*-caffeoylquinic acid

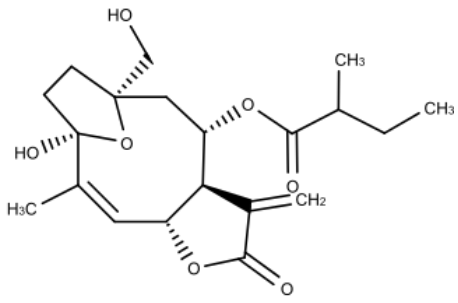

tithonin

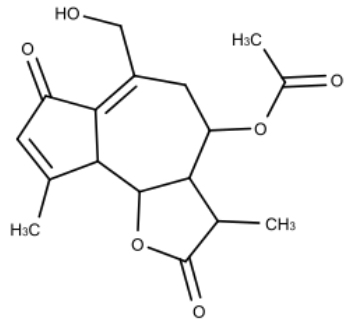

azuleno[4,5-b]furan-2,7-dione, 4-(acetyloxy)-3,3a,4,5,9a,9b-hexahydro-6-(hydroxymethyl)-3,9-dimethyl-

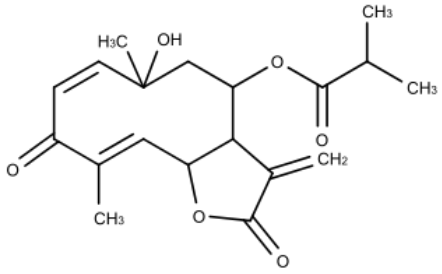

tagitinin C

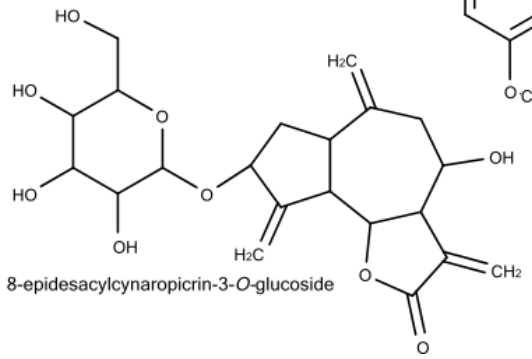

8-epidesacylcynaropicrin-3-*O*-glucoside

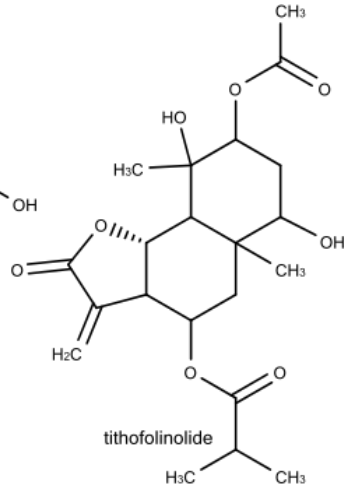

tithofolinolide

Figure 25: Structures of discriminant metabolites for porcine pancreatic α-amylase inhibitory assay

4.2.3.4. Glucose uptake assay PLS-DA model

The metabolic fingerprints of the investigated plants and the results obtained from the glucose uptake assay wre also subjected to multivariate statistical analysis in order to correlate the observed activity with the metabolic features. Therefore, a PLS-DA model was developed. Two classes were also defined respectively as active and inactive with the 36 extracts that elicited significant activity (16.6%; 10.0 µg/mL) in the insulin-mediated assay compared with negative control (Figures 9) supervised into one class, while the remaining inactive 32 plants were supervised into the second class (Figure 26). The statistical measures for the PLS-DA model developed were R^2X(cum), 0.907; R^2Y(cum), 0.818 and Q^2(cum), 0.439.

From the VIP (Figure 27) and coefficient (Figure 28) plots, the first few variables respectively with positive coefficients and VIP scores > 1 were selected as the significant features responsible for the observed glucose uptake activity in the active plants. The selected variables were subjected to dereplication techniques in order to annotate them (as stated in section 3.12; Table 6).

It was observed from the dereplication results that flavonoids and their glycosides were similarly predominant in the discrimination of the class of the plants observed with glucose uptake enhancing activity. Other significant annotated metabolites include some sesquiterpene lactones and feruloylquinic acid derivative (Table 6; Figure 29). The metabolites annotated in this study occurred variably in all the plants with the activity. It was not possible to dereplicate the first two discriminant variables with the highest coefficients. There may therefore be a need for further purification procedures on the features with *m/z* 809.433 $[M-H]^-$ and 319.227 $[M+H]^+$ at retention time 15.12 and 14.90 min, respectively, dedicated for the purpose of characterizing them. It was observed that the feature at *m/z* 367 $[M+NH_4]^+$ suggested to correspond to the ammonium adduct of tagitinin C was detected with the highest relative abundance in the control leaves of cultivated *T. diversifolia* and leaves of *T. diversifolia* from Nigeria both eliciting about 17.0% insulin-mediated glucose uptake activity and leaves of commercial *T. diversifolia* eliciting 31.0 ± 3.3% activity (Figure 9). The feature with *m/z* 493.099 $[M-H]^-$ and retention time 11.99 min suggested to correspond to a possible isomer of 6-methoxyquercetin-7-

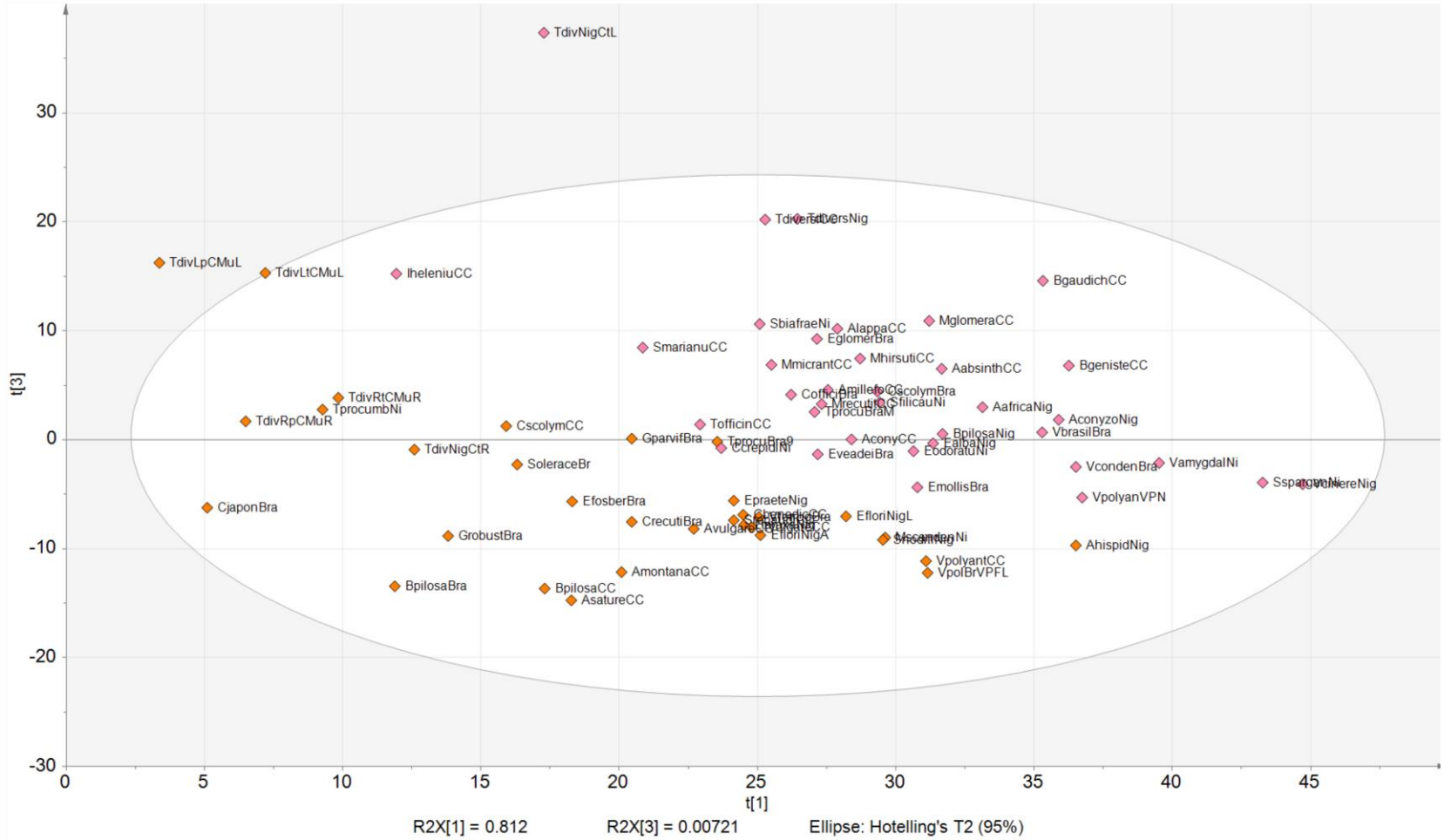

Figure 26: Partial Least Square Discriminant Analysis score plot of the first versus the third principal component in insulin-stimulating glucose uptake assay

Key: Active class (pink) and inactive class (orange) -1, inactive class, +1, active class; A, number of components, 4; $R^2X(cum)$, 0.907; $R^2Y(cum)$, 0.818 and $Q^2(cum)$, 0.439; the first component explains 81.2% of the variation and the third component 0.7%; the codes represent the names of the investigated plants (see LIST OF ABBREVIATIONS AND CODES)

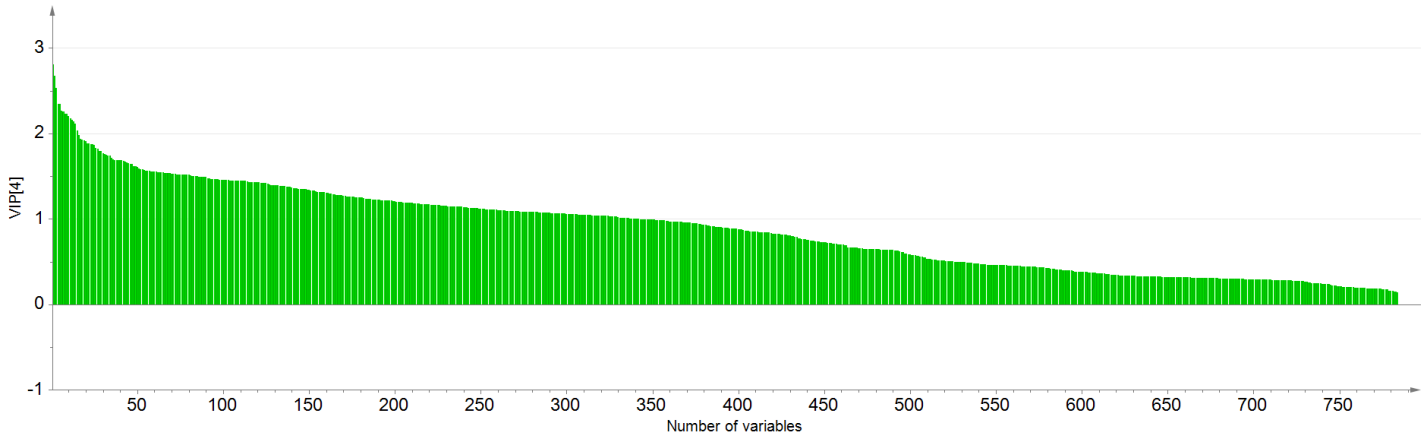

Figure 27: Variable importance in projection (VIP) plot obtained from partial least squares discriminant analysis (PLS-DA), supervised according to active and inactive plants in insulin-stimulating glucose uptake assay

Key: VIP, Variable importance in projection; Key: the higher the VIP score (>1), the more the importance of the variable on the model, irrespective of activity class

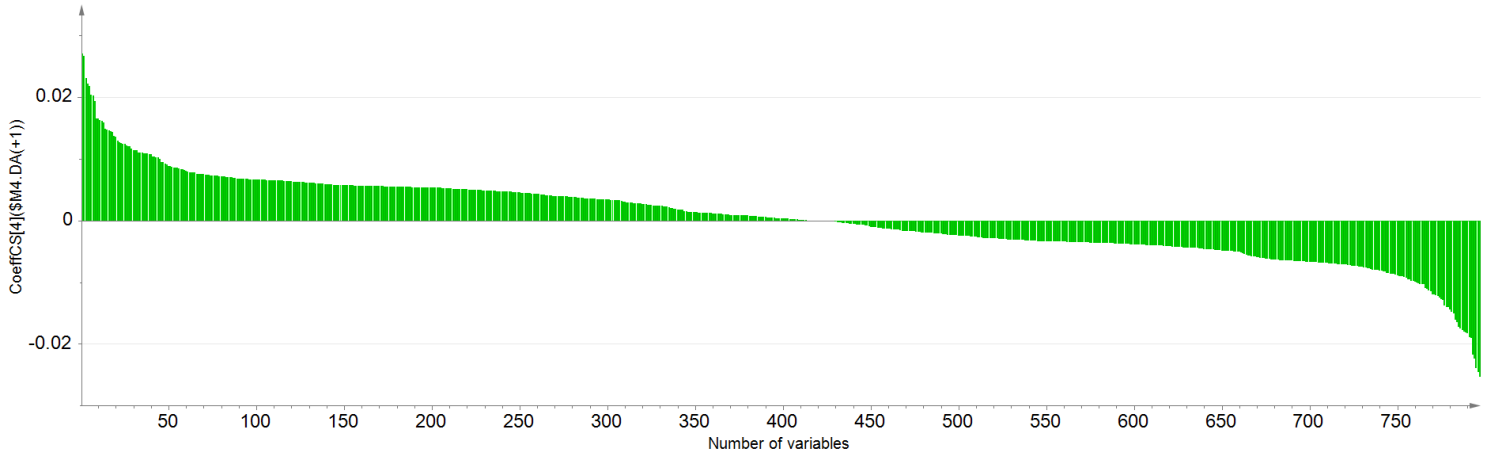

Figure 28: Coefficient plot obtained from partial least squares discriminant analysis (PLS-DA), supervised according to the active and inactive plants in insulin-stimulating glucose uptake assay

Key: The variables, grouped to the right, with positive coefficients are important in the classification of the active group; while the variables, grouped to the left of the plot, with negative coefficients are important in the classification of the inactive group

Table 6: Annotated discriminant metabolites for glucose uptake assay

RT (min)	Compound name	$[M+H]^+$ (m/z)	AIF $[M+H]^+$	$[M-H]^-$ (m/z)	AIF $[M-H]^-$	UV_{max} (nm)
5.86	umbelliferone 7-*O*-glucopyranoside	325.0917 VIP, 1.2	325 > 163, 162			
8.8	rutin	611.1602bp, 633 $[M+Na]^+$	611 > 593, 465, 453, 331, 303, 273, 245, 217	609.1458bp VIP, 1.1	609 > 591, 300, 271, 255, 151	255, 355
9.25	kaemferol	287.0544 VIP, 1.7	287 > 269, 259, 258, 245, 165, 153, 133, 127, 121	285.1715	285 > 268, 257, 255, 245, 239, 229, 227, 187, 171, 159, 145, 143, 135	266, 365
9.94	kaempferol-6-methoxy-3-*O*-glucoside			477.1039 VIP, 1.1	477 > 315, 299, 271	253sh, 352
11.74	4-*O*-feruloyl 5-*O*-caffeoylquinic acid	530.1291	531 > 517, 369, 355, 337, 193, 175	529.1353 VIP, 1.0	529 > 515, 367, 353, 335, 191, 173	245, 328
11.99	6-methoxyquercetin-7-*O*-glucoside			493.099 VIP, 1.5	493 > 331, 316	253sh, 336, 352
12.23	quercetin	303.0498 VIP, 1.0	303 > 287, 259, 153, 149			257, 284sh, 317, 335, 343, 354
13.26	tagitinin C	367.1749	367 $[M+NH_4]^+$, 349, 333, 243, 279, 261	365.1606 VIP, 2.8	365, 331, 259, 241	248
14.43	tagitinin C	367.1749 VIP, 1.2	367 $[M+NH_4]^+$, 349, 333, 243, 279, 261	365.1605 VIP, 2.2	365, 331, 259, 241	248

14.59	tagitinin C	$[M+H+FA]^+$, 395.6413	349. 261,	393.1558 $[M-H+FA]^-$ VIP, 1.4	393 > 365, 331	248
15.50	3,4'-dimethoxyquercetin			329.0668 VIP, 1.3	329 > 316, 301, 286, 180, 151, 135	253, 266sh, 296sh, 352
15.84	azuleno[4,5-b]furan-2,7-dione, 3,3a,4,5,9a,9b-hexahydro-4-hydroxy-6-(hydroxymethyl)-3,9-dimethyl-	279.1227 VIP, 1.5	279 > 249, 231, 215			
18.35	3',4'-dimethoxyluteolin			313.0719 VIP, 1.3	313 > 298, 284, 269. 255, 163	266, 296sh, 346
18.44	4-(acetyloxy)-3,3a,4,5,9a,9b-hexahydro-6-(hydroxymethyl)-3,9-dimethyl-azuleno[4,5-b]furan-2,7-dione	321.1328 VIP, 1.1	321 > 291, 249, 235			

Key: ID – Compound identity; RT – retention time (min); FA – formic acid; AIF, All Ion Fragmentation; UVmax, wavelength of maximum absorption in the ultraviolet spectral region; sh, shoulder

O-glucoside was detected in the investigated plants with abundance that correlates positively with the insulin-mediated glucose uptake activity exhibited by each of the plants containing it. For example, *B. gaudichaudiana* and *B. genistelloides* exhibited about 27.0% insulin-mediated glucose uptake activity and they expressed the feature with *m/z* 493.099 with high relative abundance. The feature was detected at a high relative abundance in commercial *A. conyzoides* and *C. officinalis*, though lower than in the *Bacharis* samples; and with this successive reduction was observed corresponding reduction in glucose uptake activity to about 20.0%. The relative abundance in commercial *M. glomerata* and *E. odoratum* from Nigeria were comparable but lower than in the *Bacharis* samples and higher than in *A. conyzoides* and *C. officinalis.* A corresponding comparable glucose uptake activity was observed at 25.6 ± 4.3 and 25.8 ± 3.4% for commercial *M. glomerata* and *E. odoratum* from Nigeria respectively. It is suggested that *E. alba* exhibited a lower activity (17.7 ± 3.3%) than the previous plants as a result of the lower relative abundance of *m/z* 493.099, which was annotated as an isomer of 6-methoxyquercetin 7-*O*-glucoside, similarly discriminated in the PPA assay.

The positive correlation was also observed with the feature abundance and insulin-mediated glucose uptake activity of *C. crepidioides* from Nigeria (41.6 ± 2.7%) and *A. conyzoides* from Nigeria (27.7 ± 1.1%). The feature at *m/z* 393.156 and retention time 14.59 min was suspected to be an analogue of tagitinin C based on the observed fragmentation pattern, retention time and presence with significantly the highest amount in *Tithonia* samples, especially the leaves of commercial *T. diversifolia* and same plant from Nigeria. The insulin-mediated glucose uptake activity observed with commercial *E. glomerulatus* (20.4 ± 1.9%), commercial *M. recutita* (32.9 ± 2.1%) and *V. phosphorica* from Brazil (24.2 ± 1.8%) corresponded with the high relative abundance of umbelliferone 7-*O*-glucopyranoside. The control leaves of cultivated *T. diversifolia* from Nigeria, leaves of commercial *T. diversifolia* and leaves of *T. diversifolia* from Nigeria also exhibited a glucose uptake enhancement activity that was positively correlated with their constitution of tagitinin C at *m/z* 367.175 $[M+NH_4]^+$.

It was observed that phenolics were predominantly determined responsible for the observed activity. The presence of phenolic and flavonoid compounds have previously been reported responsible for the antidiabetic activity observed in plants (BAHADORAN et al., 2013; KHAN et al., 2018). Isolates from *Artemisia dracunculus* L. (Asteraceae), 6-demethoxycapillarisin and 2',4'-dihydroxy-4-methoxydihydrochalcone have been reported to activate the PI3K, similar to insulin, and the AMP-activated protein kinase (AMPK) pathways (GOVORKO et al., 2007) respectively. Stevioside, a diterpene glycoside, isolated from *Stevia rebaudiana* leaves, has also been reported responsible for the plant's anti-hyperglycaemic, insulinotropic and glucagonostatic actions (JEPPESEN et al., 2002). The methanolic extract of *Smalanthus sonchifolius* H. Robinson, rich in flavonoids and chlorogenic acids, was reported to have antioxidant and antidiabetic properties (RUSSO et al., 2015) with its leaf extracts exhibiting antihyperglycaemic properties through the reduction of hepatic glucose production via gluconeogenesis and glycogenolysis (VALENTOVA; ULRICHOVA, 2003). It was reported that the potential of yacon to treat hyperglycaemia and its cytoprotective activity of its leaves is mostly related to its oligofructan and phenolic content, respectively. *A. conyzoides* L., which has been reported to be antidiabetic, was found to contain some active principles, including alkaloids, cardenolides, tannins, saponins and flavonoids

(EGUNYOMI et al., 2011). The ethanolic extract of *T. procumbens* exhibited antidiabetic activity against streptozotocin-induced diabetes mellitus in rats and was effective in managing the complications associated with diabetes mellitus (PETCHI et al., 2013). This supports the classes of discriminant metabolites that were annotated in this study.

In addition, tannins, saponins, alkaloids, amino acids, steroids and terpenoids from *Anacyclus pyrethrum* L. (SELLES et al., 2012), the ethanolic root extract of A. lappa L. (CAO et al., 2012), flavonoids, saponins, terpenes and tannins from *Artemisia judaica* L. (NOFAL et al., 2009), aqueous seed extract of *Artemisia sphaerocephala* Krasch (ZHANG et al., 2006), aqueous extract of *Bidens pilosa* L. var. *radiata* (HSU et al., 2009), carotenoids, flavonoids, glycosides, steroids and sterols from *C. officinalis* L. (CHAKRABORTHY et al., 2011), alkaloids, tannins, saponins and cardiac glycosides from *V. amygdalina* Del. (EKEOCHA et al., 2012) and aqueous leaf extract of *Vernonia colorata* (Wilid.) Drake (SY et al., 2004), have all been reported to be the active principles in these antidiabetic Asteraceae plants. This indicates that Asteraceae may be an important source of antidiabetic active compounds.

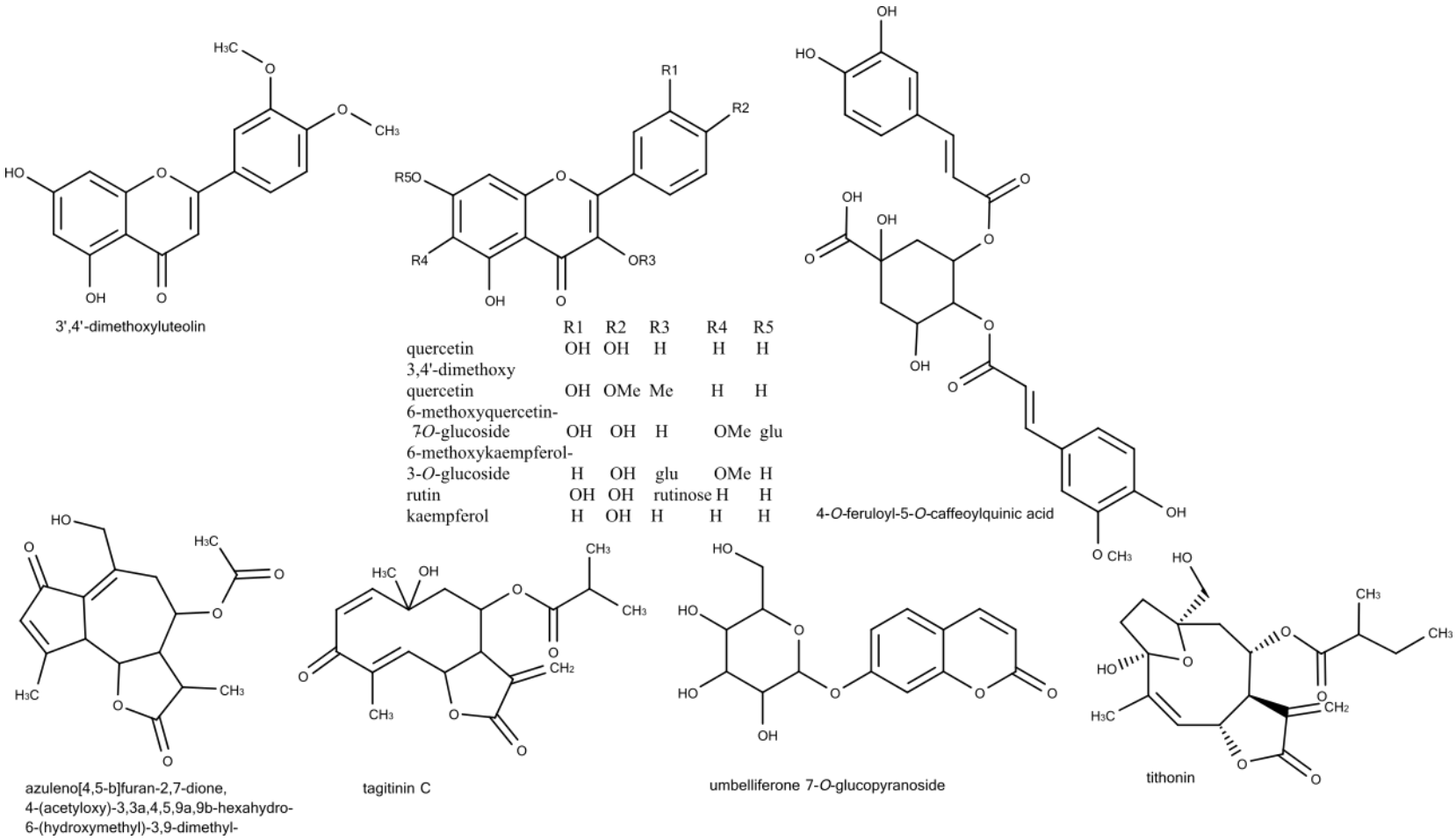

	R1	R2	R3	R4	R5
quercetin	OH	OH	H	H	H
3,4'-dimethoxy quercetin	OH	OMe	Me	H	H
6-methoxyquercetin-7-*O*-glucoside	OH	OH	H	OMe	glu
6-methoxykaempferol-3-*O*-glucoside	H	OH	glu	OMe	H
rutin	OH	OH	rutinose	H	H
kaempferol	H	OH	H	H	H

Figure 29: Structures of discriminant metabolites for glucose uptake assay

4.2.3.5. Antioxidant assay PLS-DA model

To determine the metabolites responsible for the observed antioxidant activity in this study, a PLS-DA model was developed to enable the comparison of the metabolic fingerprints of the studied plants with their observed activity. Two classes were similarly defined respectively as active and inactive with the 6 extracts eliciting significant activity (> 90%) better than the positive control, quercetin (Figures 11) were supervised into one class, while the remaining inactive 62 plants were supervised into the second class (Figure 30). The statistical measures for the PLS-DA model developed were R^2X(cum), 0.923; R^2Y(cum), 0.985 and Q^2(cum), 0.71.

From the VIP (Figure 31) and coefficient (Figure 32) plots, the first few variables respectively with positive coefficients and VIP scores greater than 1 were selected as the significant features responsible for the observed antioxidant activity in the active plants. The selected variables were subjected to dereplication techniques in order to annotate them (as stated in section 3.12; Table 7).

It was observed from the dereplication results that flavonoids and their glycosides were important (Table 7; Figure 33) in the discrimination of the class of the plants observed with antioxidant activity (Table 2). The metabolites annotated in this study also occurred variably in all the plants with the activity. For example, apigenin 6-*C*-arabinoside-8-*C*-glucoside, which was discriminated with a high coefficient in this assay, was similarly discriminated in the glucose retardation and PPA assays, indicating a potential to reduce or prevent gut glucose absorption, inhibit PPA and prevent oxidative stress. It was detected at *m/z* 563.141 $[M-H]^-$ and retention time 8.05 min with high relative abundance in commercial *A. millefolium* and *B. gaudichaudiana*, which in addition to exhibiting antioxidant activity (Table 2) also exhibited glucose retardation, fungal α-amylase inhibitory, PPA inhibitory and glucose uptake enhancement activity while commercial *B. genistelloides*, in addition to its antioxidant activity (EC_{50}, 23.0 µg/mL) similarly exhibited fungal α-amylase inhibitory (51.1 ± 0.03%) and insulin-mediated glucose uptake enhancement activity (26.6 ± 2.6%) (Figure 9). Similarly, the feature with *m/z* 477.104 $[M-H]^-$ and retention time 9.94 min, annotated as kaempferol-6-methoxy-3-*O*-glucoside was discriminated in antioxidant assay as well as in the PPA and glucose uptake assays;

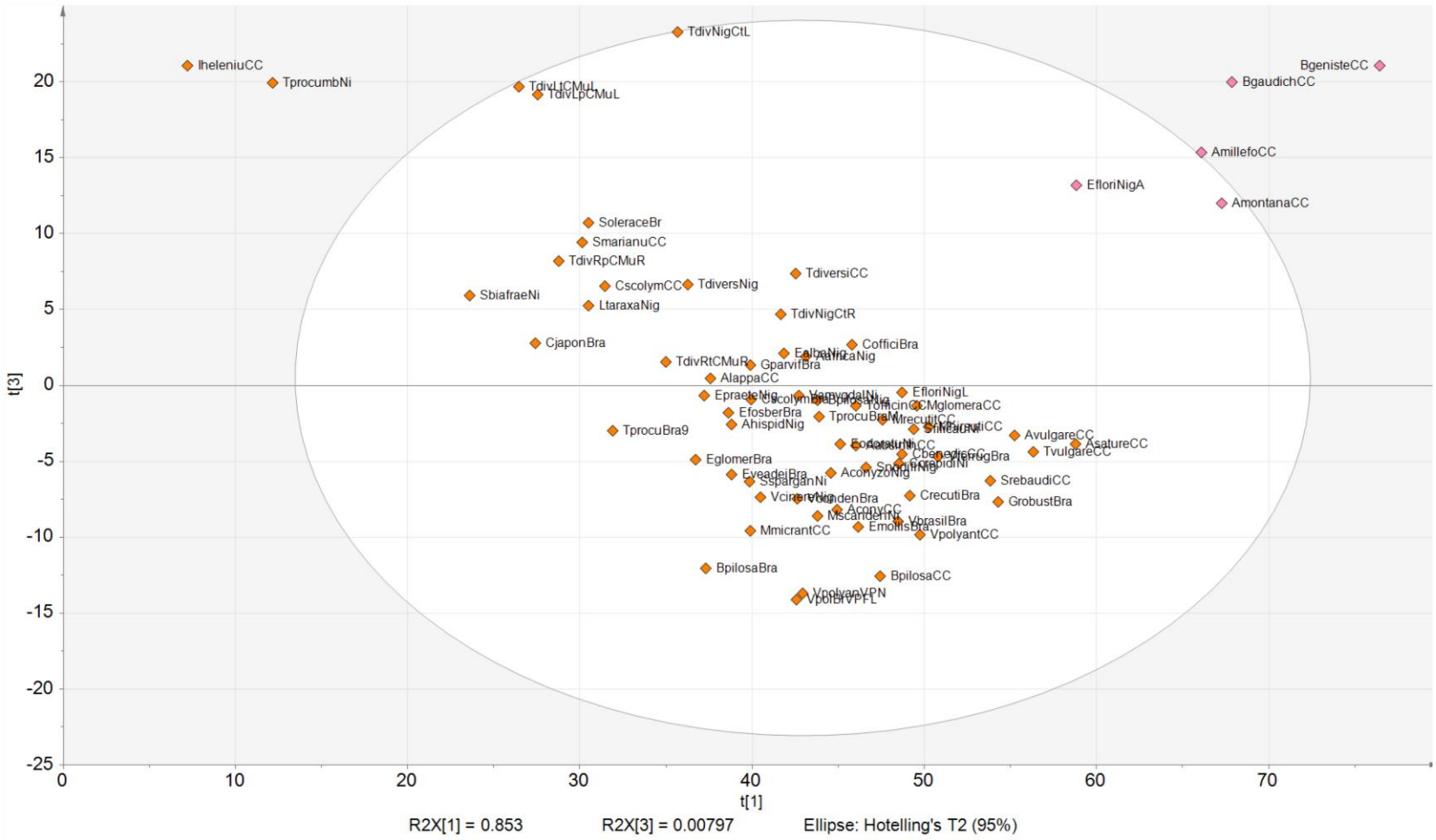

Figure 30: Partial Least Square Discriminant Analysis score plot of the first versus the third principal component in antioxidant assay
Key: Active class (pink) and inactive class (orange) -1, inactive class, +1, active class; A, number of components, 7; R2X(cum), 0.923; R2Y(cum), 0.985 and Q2(cum), 0.71; the first component explains 85.3% of the variation and the third component 0.8%; the codes represent the names of the investigated plants (see LIST OF ABBREVIATIONS AND CODES)

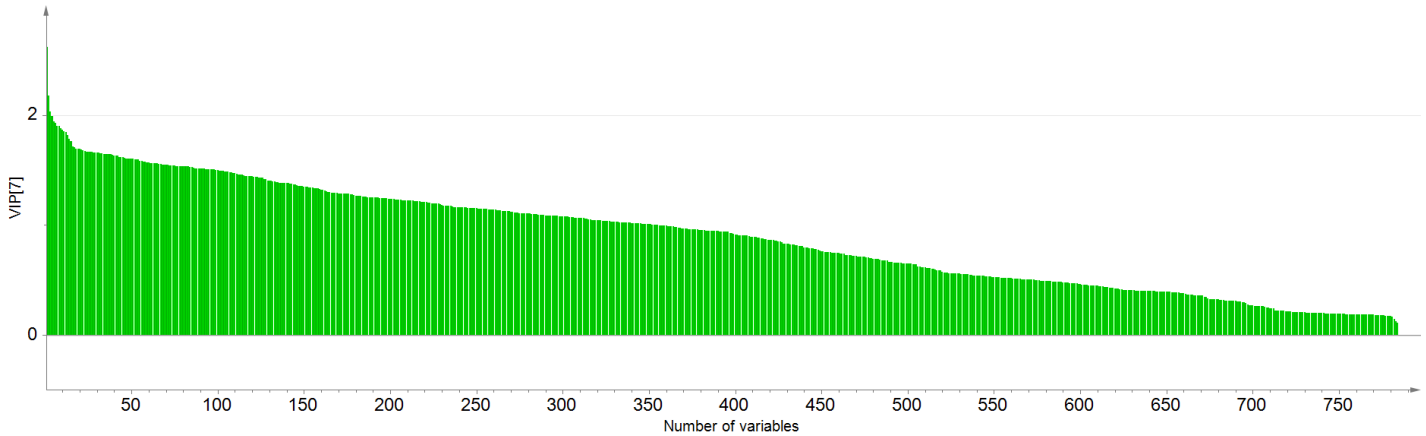

Figure 31: Variable importance in projection (VIP) plot obtained from partial least squares discriminant analysis (PLS-DA), supervised according to active and inactive plants in antioxidant assay

Key: VIP, Variable importance in projection; Key: the higher the VIP score (>1), the more the importance of the variable on the model, irrespective of activity class

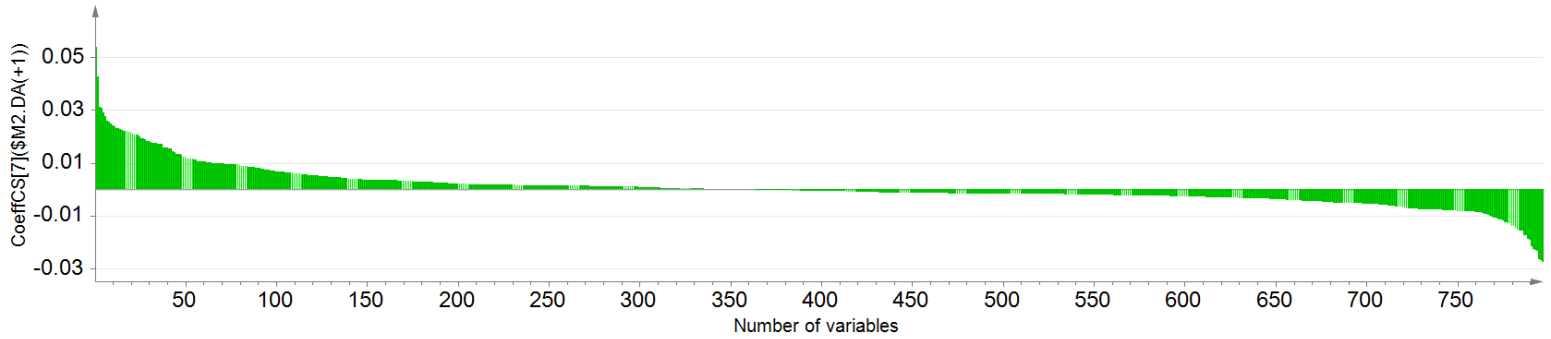

Figure 32: Coefficient plot obtained from partial least squares discriminant analysis (PLS-DA), supervised according to the active and inactive plants in antioxidant assay

Key: the variables, grouped to the right, with positive coefficients are important in the classification of the active group; while the variables, grouped to the left of the plot, with negative coefficients are important in the classification of the inactive group

Table 7: Annotated discriminant metabolites for antioxidant assay

RT (min)	Compound name	$[M+H]^+$ (m/z)	AIF $[M+H]^+$	$[M-H]^-$ (m/z)	AIF $[M-H]^-$	UV_{max} (nm)
5.07	5,6,7,4'-tetramethoxyflavone			341.1243 VIP, 1.0	341 > 327, 313, 295, 285, 240, 209, 195, 167, 132	268, 326, 352
8.05	apigenin 6-*C*-arabinoside-8-*C*-glucoside	565.1551bp-VIP, 2.0		563.1407bp VIP, 2.6	563 > 503, 473, 443, 383, 353	270, 333
9.09	kaempferol-6-methoxy-3-*O*-glucoside			477.0675 VIP, 1.4	477 > 315, 299, 271	253sh, 352
10.04	7,4'-dimethoxyapigenin			297.0040 VIP, 1.3	297 > 284, 252, 165, 135, 132	268, 333
15.39	3,4',6-trimethoxyquercetagetin			359.0773 VIP, 1.8	359 > 344, 329, 314, 301, 286, 258	268, 337, 345, 362, 372
17.81	acacetin	285.0613 VIP, 1.1	285 > 161	283.0405 VIP, 1.4	283 > 268	267, 336, 345
18.93	5-hydroxy-3,6,7,4'-tetramethoxyflavone	359.1122 VIP, 1.2	359 > 344, 330, 328, 318,			273, 290, 339

Key: ID – Compound identity; RT – retention time (min); AIF, All Ion Fragmentation; UVmax, wavelength of maximum absorption in the ultraviolet spectral region; sh, shoulder

being detected with highest relative abundance in commercial *A. satureioides*, which showed significant activity against fungal (Figure 7) and PPA (Figure 8) α-amylases as well as antioxidant potential (79.0 ± 2.4%) with 8.9 ± 1.1% and 12.3 ± 2.9% insulin-mediated and insulin-like glucose uptake enhancement activity respectively; *E. glomerulatus* from Brazil, which showed significant activity against fungal α-amylase (Figure 7), insulin-mediated (Figure 9) and insulin-like glucose (Figure 10) uptake enhancement activity, as well as antioxidant activity (77.3 ± 1.9%); commercial *M. recutita*, which showed significant activity against fungal α-amylase, 32.9 ± 2.1% (Figure 7) and 14.9 ± 2.0% insulin-mediated and insulin-like glucose uptake enhancement activity respectively with a low PPA inhibitory activity (7.1 ± 0.3%) as well as antioxidant activity (67.6 ± 2.6%). Additionally, it was detected with high relative abundance in *V. phosphorica* from Brazil which inhibited PPA (Figure 8) also showed 23.9 ± 0.5% fungal

α-amylase inhibitory activity, insulin-mediated and insulin-like glucose uptake enhancement activity as well as antioxidant activity (73.7 ± 2.6%). Other investigated plants that exhibited significant antioxidant activity, also eliciting activity in one or more of the other *in vitro* antidiabetic assay procedures in this study and which have a relatively high relative abundance include commercial *A. millefolium*, which exhibited significant glucose retardation (Figure 6), fungal α-amylase inhibitory (22.5 ± 0.4%), PPA inhibitory (Figure 8), insulin-mediated and insulin-like glucose uptake (Figures 9 and 10) and antioxidant (EC_{50}, 82.89 µg/mL) (Table 2) activity; commercial *A. vulgare*, which exhibited 13.3 ± 1.6% insulin-mediated glucose uptake enhancement activity with significantly low insulin-like activity (2.8 ± 0.1%); fungal α-amylase inhibition (25.3 ± 1.0%), and antioxidant activity (88.2 ± 3.4%); *B. pilosa* from Brazil, which exhibited glucose retardation (30 min, 10.1 ± 0.4%; 60 min, 11.1 ± 0.6%; 120 min, 4.1 ± 0.2% and 180 min, 3.8 ± 0.1%); PPA inhibitory (4.1 ± 0.4%); fungal α-amylase inhibitory (32.1 ± 0.6%); insulin-like glucose uptake (26.2 ± 1.2%); insulin-mediated glucose uptake (15.5 ± 1.8%) and antioxidant (65.8 ± 1.2%) activity; commercial *C. officinalis*, which exhibited fungal α-amylase inhibitory (20.3 ± 1.0%); insulin-like glucose uptake (19.5 ± 3.2%); insulin-mediated glucose uptake (20.7 ± 2.3%) and antioxidant (36.7 ± 1.1%) activity; commercial *C. recutita*, which exhibited PPA inhibitory (11.7 ± 0.2%); fungal α-amylase inhibitory (Figure 7); insulin-like glucose uptake (7.4 ± 0.9%); insulin-mediated glucose uptake (7.9 ± 0.7%) and antioxidant (67.6 ± 2.6%) activity; *T. procumbens* from Brazil, which exhibited insulin-like glucose uptake (21.8 ± 2.4%); insulin-mediated glucose uptake (27.6 ± 1.6%); fungal α-amylase inhibitory (Figure 7); PPA inhibitory (7.8 ± 0.05%) and antioxidant (48.7 ± 1.3%) activity; commercial *T. vulgare* , which exhibited insulin-like glucose uptake (12.7 ± 1.5%); insulin-mediated glucose uptake (11.2 ± 1.5%); fungal α-amylase inhibitory (23.4 ± 0.6%) and antioxidant (73.5 ± 2.6%) activity; *V. brasiliana* from Brazil, which exhibited glucose retardation (Figure 6); fungal α-amylase inhibitory (Figure 7); insulin-like glucose uptake (15.6 ± 1.4%); insulin-mediated glucose uptake (16.3 ± 1.8%) and antioxidant (88.3 ± 2.9%) activity; *V. condensata* from Brazil, which exhibited insulin-like glucose uptake (Figure 10); insulin-mediated glucose uptake (Figure 9); fungal α-amylase inhibitory (Figure 7); glucose retardation (Figure 6) and antioxidant (64.6 ± 2.1%) activity.

The features at *m/z* 359.112 $[M+H]^+$ and *m/z* 341.124 $[M-H]^-$ and retention times 18.93 and 5.07 min, representing 5-hydroxy-3,6,7,4'-tetramethoxyflavone and 5,6,7,4'-tetramethoxyflavone respectively were detected with high relative abundance in commercial *A. millefolium*, shown to exhibit significant activity in all the assays (Figures 6, 8, 9, 10 and 11), with 22.5 ± 0.4% fungal α-amylase inhibition, not reported because it is lower than 30.0 %. The feature at *m/z* 297.004 $[M-H]^-$ and retention time 10.04 min representing 7,4'-dimethoxyapigenin was detected with high relative abundance in *E. alba* from Nigeria, which was shown to exhibit glucose uptake enhancement activity (Figures 9 and 10), fungal α-amylase inhibition (27.9 ± 0.9%) and a low antioxidant (6.6 ± 0.5%) activity. The observed low antioxidant activity of this feature indicated its lower significance, which may be due to the presence of antagonism or the effect of methoxylation, which may reduce the antioxidative effect. However, higher significance was observed with other polymethoxylated flavonoids. This may indicate that the metabolites are acting synergistically. The feature at *m/z* 359.077 $[M-H]^-$ and retention time 15.39 min representing 3,4',6-trimethoxyquercetagetin was detected with the highest relative abundance in commercial *S. rebaudiana* and *T. vulgare*. While the former exhibited significant glucose retardation (30 min, 10.4 ± 0.7%; 60 min, 4.8 ± 0.2%; 120 min, 19.2 ± 0.5% and 180 min, 16.0 ± 0.4%), fungal α-amylase inhibitory (53.6 ± 0.2%) (Figure 7), PPA inhibitory (4.6 ± 0.4%), insulin-like (11.2 ± 1.1%) and insulin-mediated glucose uptake enhancement (8.2 ± 1.0%) activity and antioxidant (56.0 ± 1.5%) activity; the latter exhibited fungal α-amylase inhibitory (23.4 ± 0.6%), insulin-like (12.7 ± 1.5%) and insulin-mediated glucose uptake enhancement (11.2 ± 1.5%) activity and antioxidant (73.5 ± 2.5%) activity. Other plants with high relative abundance of this feature includes commercial *A. montana*, with PPA inhibitory (6.4 ± 0.5%), fungal α-amylase inhibitory (17.2 ± 0.9%), insulin-like (12.3 ± 1.1%) and insulin-mediated glucose uptake enhancement (13.3 ± 1.2%) and antioxidant (EC_{50}, 14.16 µg/mL); commercial *C. recutita* with low glucose retardation activity, significant fungal (51.5 ± 0.8%) and PPA (11.7 ± 0.2%) α-amylase inhibitory, insulin-like (7.4 ± 0.9%) and insulin-mediated glucose uptake enhancement (7.9 ± 0.7%) and antioxidant (67.6 ± 2.6%) activity. Finally, the feature at *m/z* 283.05 $[M-H]^-$ and retention time 17.81 min, annotated as acacetin and discriminated in antioxidant assay as well as in the enzymes and glucose uptake assays; being detected

with the highest relative abundance in commercial *A. satureioides*, which showed significant activity against fungal (Figure 7) and PPA (Figure 8) α-amylases as well as antioxidant potential (79.0 ± 2.2%) with 8.9 ± 1.1% and 12.3 ± 2.9% insulin-mediated and insulin-like glucose uptake enhancement activity respectively; commercial *B. genistelloides* with significant activity in the glucose uptake assays (Figures 9 and 10), fungal α-amylase inhibitory (Figure 7), glucose retardation (30 min, 13.7 ± 0.6%; 60 min, 5.94 ± 0.2%; 120 min, 4.61 ± 0.1%; 180 min, 0.6 ± 0.02%) and antioxidant (EC_{50}, 22.98 µg/mL) activity; commercial *V. brasiliana*; *V. phosphorica*; *S. sparganophora* and *V. cinerea*; *V. amygdalina* from Nigeria, which was observed to enhance the PPA exhibited significant insulin-mediated and insulin-like glucose uptake enhancement activity (Figures 9 and 10), fungal α-amylase inhibitory (Figure 7) and glucose retardation (30 min, 12.8 ± 1.2%; 60 min, 9.6 ± 0.3%; 120 min, 13.9 ± 0.6%; 180 min, 2.3 ± 0.1%) activity; *A. hispidum* from Nigeria, with fungal α-amylase inhibitory (Figure 7) and 11.3 ± 1.2% insulin-mediated glucose uptake enhancement activity; and *M. scandens* from Nigeria, with insulin-mediated (13.7 ± 1.5%) and insulin-like (19.3 ± 1.7%) glucose uptake enhancement activity, fungal α-amylase inhibitory (21.5 ± 0.2%). Put together, this indicates the significance of these flavonoids and their glycosides, with antidiabetic as well as antioxidant properties, in preventing postprandial hyperglycaemia with potential to prevent diabetes development.

Such plants with the potential to reduce or prevent postprandial hyperglycaemia through various mechanisms of action are important in the consideration of diet and/or their metabolites individually or synergistically for the purpose of reducing postprandial hyperglycaemia. In preventing the development of T2DM, subjects who are prone to its development need to adopt strategies that are life-long, and therefore need to be safe over a protracted period to encourage compliance (AL-DABBAS et al., 2006). Such strategies may include lifestyle modifications, exercise and diet and/or nutritional supplements (ADEMILUYI; OBOH, 2013), which may be considered safe for human ingestion. Therefore, the plants which exhibited significant antioxidant activity in this study, and by virture of their discriminant antioxidant metabolites, observed to elicit additional activity in other antidiabetic assays, may be suggested to be important for the reduction or prevention of postprandial hyperglycaemia. Further studies are required to

investigate the *in vivo* properties of these discriminant metabolites to delay the progression of prediabetes to diabetes or prevent the development of diabetes. The metabolites discriminated and annotated in this study also requires further extensive investigation to establish their usefulness for the purposes highlighted.

Liu et al. (2014) reported that flavonoids may be responsible for beneficial effects of *Agrimonia pilosa* on T2D, by targeting oxidative stress and postprandial hyperglycaemia (LIU et al., 2014).

The prevention of progressive impairment of pancreatic β-cell function as a result of oxidative stress has also been ascribed to flavonoids, thereby reducing T2D development (SONG et al., 2005).

Flavonoids and chlorogenic acids have also been reported responsible for the significant α-amylase and α-glucosidase inhibition of plants, with both anti-oxidant and antidiabetic properties (RUSSO et al., 2015).

In order to further verify the structures annotated with dereplication techniques, and identify them, the MS, MS/MS and UV spectra of some of the metabolites were compared along with their retention time profile, against those of their purified standards, including chrysoeriol, tiliroside and rutin, using an ion trap MS detector to obtain the LC-MS/MS data. This analysis showed that the spectra of the three standard compounds are superimposable on those of the selected metabolites, and were as such identified; the spectra of tiliroside and rutin compared with their pure standards are presented in Appendix I.

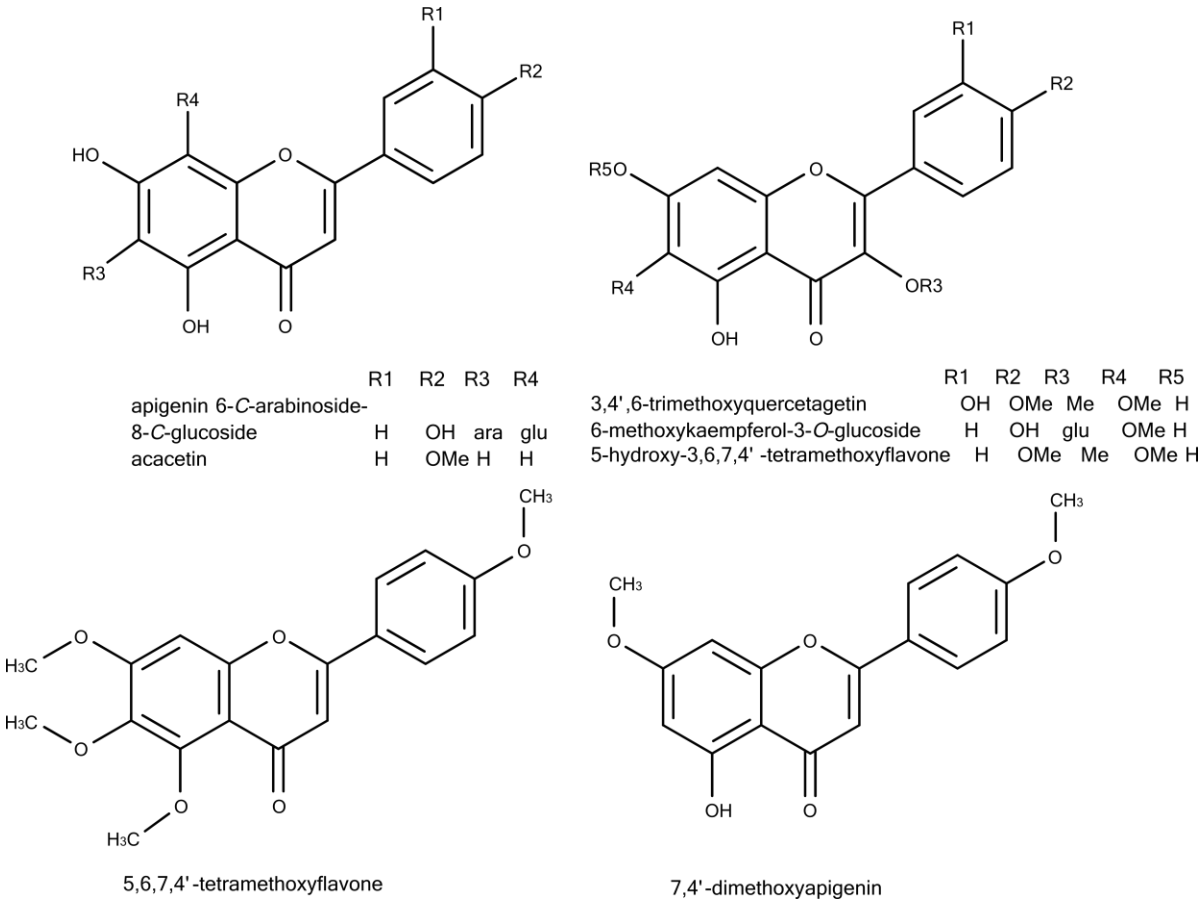

Figure 33: Structures of discriminant metabolites for antioxidant assay

4.2.5. Isolation and characterization of some discriminant features

The detected features *m/z* 349.164 $[M+H]^+$, RT, 14.60 min, dereplicated as tagitinin C; *m/z* 367.175 $[M+NH_4+H]^+$, RT, 14.43 min and *m/z* 365.161 $[M+NH_4-H]^-$, RT, 14.43 min, which were discriminated in the glucose retardation and porcine pancreatic α-amylase inhibitory assays and *m/z* 393.156, RT 14.59 min discriminated in the glucose uptake assay were billed for isolation and characterization based on the similarity in their MS spectra and retention time. It was suspected that the features may all be from a common structural backbone. Also, wedelolactone, *m/z* 313.035 $[M-H]^-$, RT 12.91 min which was discriminated in the glucose retardation assay but which has been previously reported with amylase inhibition (93.8%, unreported concentration) (Kumar *et al*., 2018) was similarly isolated and characterized.

4.2.5.1. Isolation of tagitinin C and related features

Tagitinin C, being a sesquiterpene lactone, has been reported to occur in the glandular trichomes of the leaves and flowers of *T. diversifolia*, with reports of cytotoxic and anti-inflammatory activities (AMBRÓSIO et al., 2008). The leaves of *T. diversifolia* (235 g) were air-dried and individually rinsed for a few seconds with acetone to extract the contents in the glandular trichomes (CHAGAS-PAULA et al., 2011; ROCHA et al., 2012), yielding 1.3 g of the acetone leaf-rinse extract (LRE). The extract solution was filtered and the filterate was subjected to evaporation under reduced pressure. The dry residue was kept at - 20 ^{o}C until use. The extraction procedure involving rinsing whole leaves with suitable solvents has been shown to enhance the selective extraction of sesquiterpene lactones present in the glandular trichomes on leaf surfaces (PASSONI et al., 2013). The leaf rinse extract was therefore expected to be STL-rich (CHAGAS-PAULA et al., 2011). Using an ion trap MS detector to obtain the LC-MS/MS data of the LRE, the features discriminated at *m/z* 367.175 $[M+H]^+$, RT, 14.43 min and *m/z* 365.161 $[M-H]^-$, RT, 14.43 min were detected in the MS spectra from ion trap at *m/z* 367.13 $[M+H]^+$ and retention time, 14.9 min. The fragmentation patterns were characteristic for tagitinin C (Appendix II), with ions at *m/z* 367 $[M+NH_4]^+$, 349, 331, 279, 261 (base peak), 243, 215, 173 (SUT et al., 2018).

In the negative mode, the feature discriminated at *m/z* 393.156, RT 14.59 min was detected in the LRE at *m/z* 393.10, RT, 14.9 min similarly giving fragment ions at *m/z* 349, 261 (Appendix III) characteristic of tagitinin C.

The residue of the LRE (1.3 g) was resuspended in CH_2Cl_2, triturated to homogeneity and dryness using mortar and pestle. The dry homogenous mixture of the LRE and silica gel was gently transferred to the top of a prepared silica gel-based open column and subjected to flash chromatography, using as eluent 100.0 mL + 1.0% formic acid (FA) of a gradient of solvents comprising 100:0 - 0:100 of hexane in ethylacetate successively reducing the hexane and increasing the ethylacetate volume by 10% each. For each gradient, 100.0 mL eluates were collected and dried under reduced pressure using rotary evaporator and their yields were obtained: (hexane:ethylacetate fractions),

100:0 (4.6 mg), 90:10 (13.6 mg), 80:20 (20.0 mg), 70:30 (94.3 mg), 60:40 (531.4 mg), 50:50 (452.2 mg), 40:60 (210.0 mg), 30:70 (73.5 mg), 20:80 (39.5 mg), 10:90 (20.2 mg) and 0:100 (10.4 mg). Eleven fractions were thus obtained and their total ion chromatograms are as presented in positive (Appendix IV and VI) as well as negative modes (Appendices V and VII). It was observed that the features of interest with retention time range of 14.4 – 14.6 min (see **4.2.5.** above) appeared more prominently in the negative than the positive mode. In the negative mode, they appeared in fractions 0:100 – 70:30 and in the positive mode, only in fraction 60:40. It was also observed that the feature in fraction 60:40 had the highest relative abundance as detected in both modes (Appendices V and VII). Thin layer chromatography (silica gel based TLC plates, Sigma-Aldrich) showed a clear separation of the constituents of the fractions using an optimized solvent system consisting of hexane:EtOAc (2.5:1.5) + 1.0% FA.

Therefore, the fraction, 60:40 (531.4 mg) based on its high yield and significant amount of the feature of interest at the required retention time, was submitted to semi-preparative HPLC on a C_{18} ONYX monolithic column (5.0 µm, 30 X 100 mm) using a linear gradient of H_2O:MeCN (80:20 - 0:100, in 55 min, 0.5 mL/min), both with 0.1% FA, as mobile phase.

Ion trap mass spectrometry was used to monitor the purity of the fractions. The MS, MS/MS and UV spectra of the first four fractions (Fr1, 3.3 mg; Fr2, 34.9 mg; Fr3, 15.3 mg; Fr4, 14.1 mg) from this step were similar, revealing the presence of a base peak in the negative mode, *m/z* 393 at retention time, 14.0 min. Appendices VIII and IX displays the spectra of fractions Fr3 and Fr4, respectively. The *m/z* 349 was detected in the spectra as a fragment ion, suggesting that the feature at *m/z* 393 is tagitinin C at *m/z* 349 coupled with formic acid. To further determine the purity of the fractions Fr1-Fr4, their NMR spectra were measured on a Bruker DRX500 (operating at 500 MHz for ^1H; 25 ^oC) NMR spectrometer. The samples, Fr1 (3.0 mg), Fr2 (20.0 mg), Fr3 (14.0 mg) and Fr4 (12.0 mg) were dissolved in 700.0 µL of $CDCl_3$. It was observed that the ^1H NMR spectra of the fractions (Fr1-Fr4) were similar. Fr3, which has a high yield, appeared the purest and its spectrum was chosen for further interpretation of the signals recorded (Figure 34). The spectra of Fractions Fr1, Fr2 and Fr4 are presented in Appendices X, XI and XII, respectively.

The signals observed in the NMR spectrum of Fr3 are characteristic of tagitinin C as previously reported (Figure 34; Table 8), establishing its structure (WAHYUNINGSIH et al., 2015). The feature corresponding to *m/z* 349 $[M+H]^+$ is therefore identified as tagitinin C (Figures 17, 21, 25 and 29), while those at *m/z* 365 and 367 are suggested to be ammonium adducts of tagitinic C and *m/z* 393 as deprotonated formic acid artefact of tagitinin C.

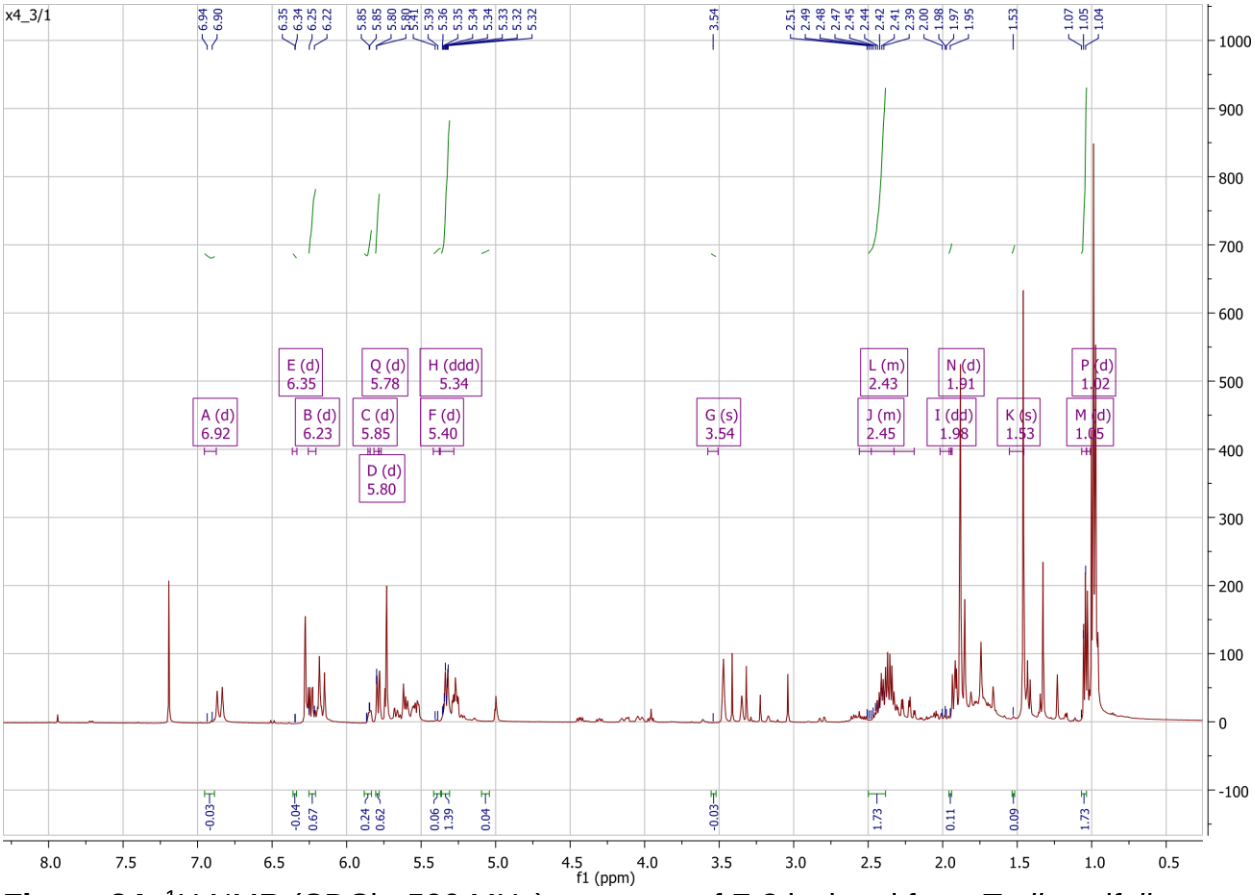

Figure 34: ^{1}H NMR ($CDCl_3$, 500 MHz) spectrum of Fr3 isolated from *T. diversifolia*

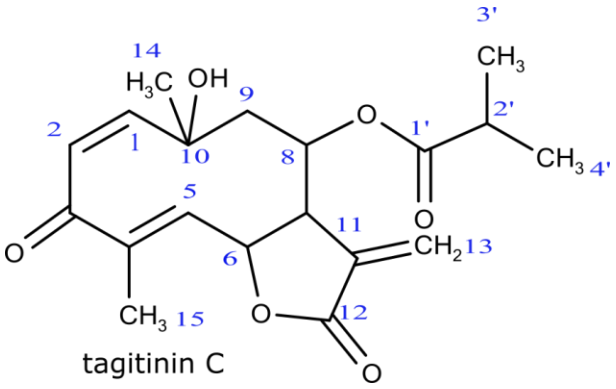

Table 8: ^{1}H NMR chemical shifts for tagitinin C

C–H number	**1H-NMR (δ, ppm), J (Hz)** (experimental data)	**1H-NMR (δ, ppm), J (Hz)** (data from literature)
1	6.92 (d. 17.1)	6.93 (d. 16.8)
2	6.23 (d. 17.2)	6.23 (d.16.8)
3		-
4		-
5	5.85 (d. 9.1)	5.84 (d. 9.3)
6	5.40 (d. 8.9)	5.39 (d.8.4)
7	3.54 (br. s)	3.54 (br. s)
8	5.34 (ddd. 3.2, 6.2, 9.7)	5.34 (m)
9	1.98 (dd. 11.2, 15.4); 2.4 (m)	1.98 (dd 10.14); 2.46(m)
10	-	-
11	-	-
12	-	-
13	5.78 (d. 1.3); 6.35 (d. 1.3)	5.80 (d 1.6); 6.36 (d 1.6)
14	1.53 (s)	1.53 (s)
15	1.91 (d. 1.7)	1.95 (d 1.2)
1’	-	-
2’	2.45 (m. 7.0, 7.0, 13.9, 28.2)	2.44 (m 6.9)
3’	1.02 (d. 6.7)	1.04 (d 6,9)
4’	1.05 (d. 7.2)	1.05 (d 6,9)
10-OH	-	2.45 (br. s)

Key: C-H number, position of hydrogen on the compound; 1H-NMR, proton nuclear magnetic resonance; δ, proton chemical shift in ppm (parts per million); J, coupling constant in Hz; second column presents experimental data; third column presents literature data (WAHYUNINGSIH et al., 2015)

4.2.5.2. Isolation of wedelolactone

The air-dried leaves of *E. alba* (300.0 g) was extracted with 4.0 L of MeOH:H_2O (9:1) on a sonicator for 10 min. The extract solution was filtered and the solvent removed under reduced pressure. The extract was resuspended with MeOH:H_2O (9:1) and

analysed with ion trap MS detector to obtain the LC-MS/MS data. The feature discriminated at *m/z* 313.035 $[M-H]^-$, RT, 12.91 min was detected in the MSspectra obtained with ion trap at *m/z* 312.98 $[M-H]^-$, retention time 13.5 min, with a precursor ion at *m/z* 626.77 $[2M-H]^-$ representing a dimer. Other characteristic fragment of wedelolactone was observed at *m/z* 297.94 representing the loss of a methyl substituent (Appendix XIII).

To isolate this feature, the dry extract (26.7 g) was resuspended in MeOH:H_2O (9:1) and partitioned with hexane, CH_2Cl_2 and EtOAc respectively to obtain their hexane (3.5 g), CH_2Cl_2 (1.9 g) and EtOAc (8.1 g) fractions. Solvent systems, consisting hexane:EtOAc (3:1 – 0:4) did not show good separation of the constituents of these fractions.

About 8 g of the dry ethylacetate fraction was resuspended in minimum amount of MeOH and subjected to column chromatography using Sephadex LH-20 column (5 X 60 cm) eluting with isocratic MeOH. An Advatec® SF-2120 Super Fraction collector was set to automatically collect 3.2 mL of the eluate every 10 min. Thin layer chromatography (EtOAc:formic acid:glacial acetic acid:water, 100:11:11:26) was used to monitor and combine similar fractions. Towards the end of the run, the solvent system was changed to *n*-butanol:water:glacial acetic acid (65:25:15) to compensate for the highly polar compounds. Forteen fractions were thus obtained and were analysed using HRESIMS. Their chromatograms revealed that fractions 5 (302.9 mg), 6 (756.0 mg) and 6+ (187.4 mg) possess the feature of interest with high relative abundance, at retention times 12.66, 12.67 and 12.71 min in the negative mode (Appendices XIV and XV) and 12.65, 12.66 and 12.70 min in the positive mode (Appendices XVI and XVII), respectively.

Therefore, Frcs 5, 6 and 6+ were combined, resuspended in MeOH:H_2O (9:1) and the supernatant (Fr_{sn}) submitted to Shimadzu semi-preparative HPLC on a C_{18} ONYX monolithic column (5.0 µm, 30 X 100 mm) using a linear gradient of H_2O:MeCN (85:15 - 0:100, in 43 min, 0.5 mL/min), both with 0.1% FA, as mobile phase. Also, upon resuspension, there was observed precipitation, which was dissolved in minimum DMSO and recrystallized in ethanol. The crystallization product (Fr_{cp}) was also submitted to semi-preparative HPLC as described above. The MS, MS/MS and UV spectra of Fr_{sn} (Appendix XVIII) and Fr_{cp} (Appendix XIX) are presented.

The MS spectra (Appendices XVIII and XIX) revealed similar peaks, *m/z* 313 $[M-H]^-$ and 627 $[2M-H]^-$ at retention time 12.6 min in the negative mode suggesting their similarity. There were no interefering peaks suggesting the purity of the isolated compounds through the two approaches. This feature was identified as wedelolactone by UV spectrum, MS spectra and ^{1}H-NMR. For the preparation of samples for ^{1}H-NMR, 4.0 mg and 6.0 mg of the Fr_{sn} and Fr_{cp} were dissolved in 700.0 µL of DMSO-D_6 respectively. The ^{1}H-NMR spectra of Fr_{sn} (Figure 35) and Fr_{cp} (Appendix XX) are presented.

The signals observed in the NMR spectrum (Figure 35) are characteristic of wedelolactone as previously reported (Table 9), establishing its structure ((Liu et al., 2012; Kumar et al., 2018)). Similarly, the absence of interfering signals in the NMR spectrum of wedelolactone (Figure 35) suggests high purity. The signals at 2.50 and 3.31 represent DMSO and residual MeOH, respectively.

The feature corresponding to *m/z* 313 $[M-H]^-$ is therefore identified as wedelolactone (Figure 17).

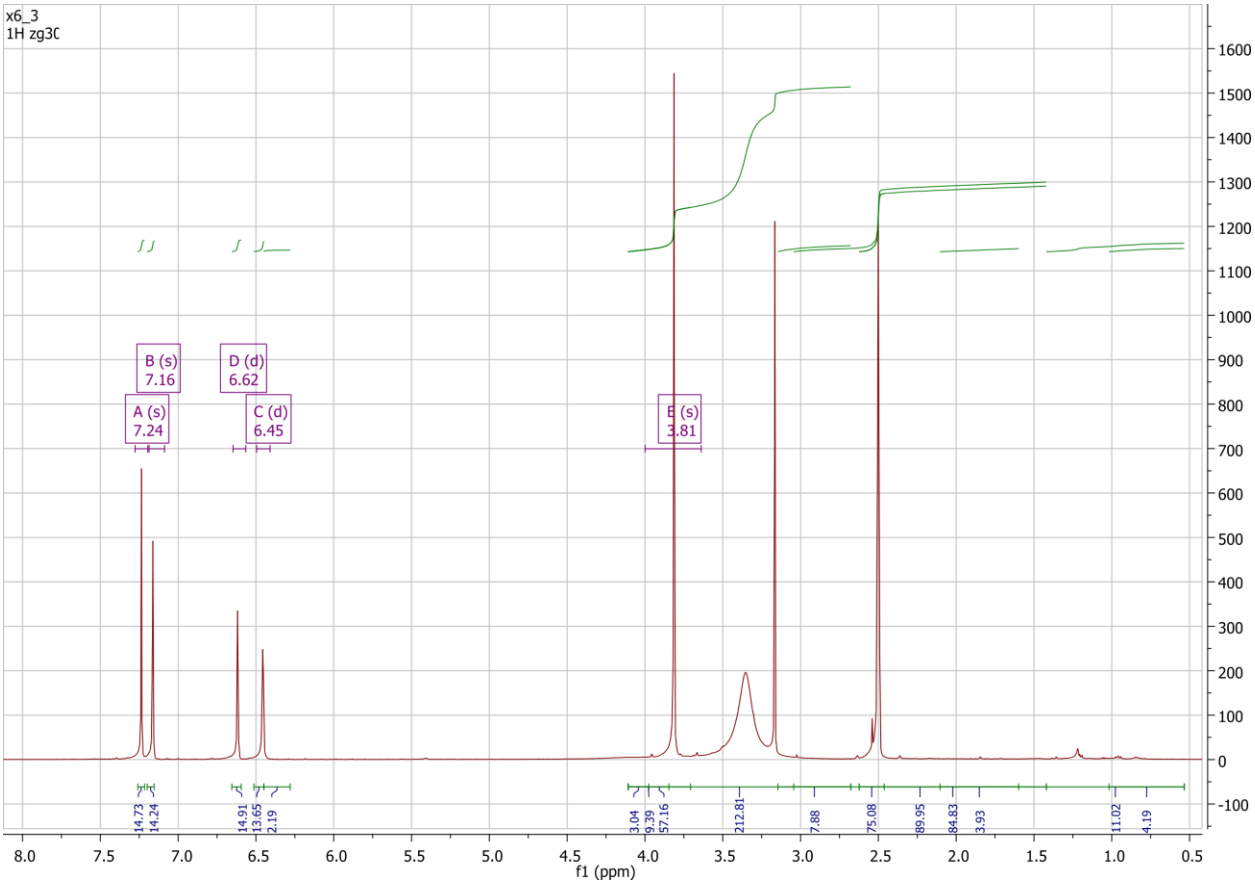

Figure 35: ^{1}H NMR (DMSO-D6, 500 MHz) spectrum of Wedelolactone obtained from Fr_{sn}

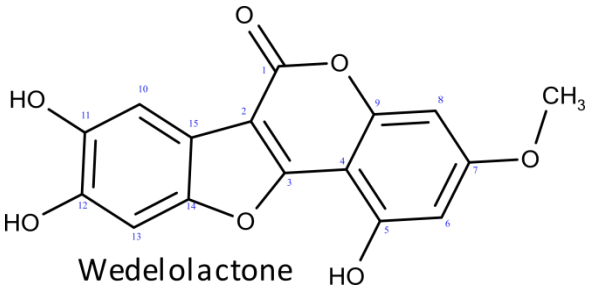

Wedelolactone

Table 9: ^{1}H NMR chemical shifts for wedelolactone

C–H number	**1H-NMR (δ, ppm), J (Hz) Experimental data**	**1H-NMR (δ, ppm), J (Hz) (LIU et al., 2012; KUMAR et al., 2018)**
1	-	-
2	-	-
3	-	-
4	-	-
5	-	-
6	6.45 (d, 1.7)	6.46 (d, 2.0)
7	3.81 (s)	3.82 (s)
8	6.62 (d, 2.0)	6.62 (d, 2.0)
9	-	-
10	7.24 (s)	7.27 (s)
11	-	-
12	-	9.41 (s)
13	7.16 (s)	7.19 (s)
14	-	-
15-	-	-

Key: C-H number, position of hydrogen on the compound; 1H-NMR, proton nuclear magnetic resonance; δ, proton chemical shift in ppm (parts per million); J, coupling constant in Hz; second column presents experimental data; third column presents literature data (LIU et al., 2012; KUMAR et al., 2018)

5. OVERVIEW OF STRUCTURAL FEATURES FOR PORCINE PANCREATIC α-AMYLASE INHIBITION

To determine the structural features required for the inhibition of porcine pancreatic α-amylase, being a mammalian enzyme closest to the human amylase, structure activity relationship determination was carried out. Some of the discriminant metabolites determined in this study and dereplicated accordingly and their analogues were additionally evaluated for their ability to inhibit porcine pancreatic α-amylase *in vitro* at 200.0 µg/mL (Figure 36).

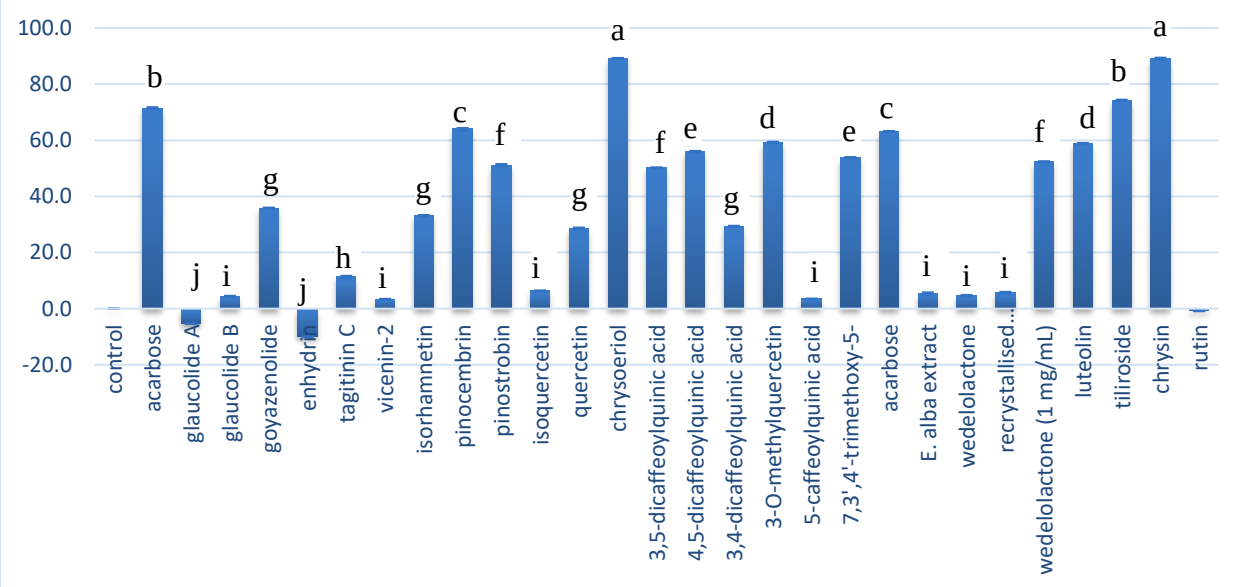

Figure 36: Percentage porcine pancreatic α-amylase inhibitory activity of compounds
Key: Alphabets indicate statistical comparison of the activity of each sample compared with negative control. For each timepoint, "a" indicates statistically the highest activity; followed by subsequent alphabets, indicating decreasing activity.

It was observed that flavonoids and their glycosides elicited significantly the highest inhibitory activity in this study, except the glycosides, rutin, isoquercetin and vicenin-2 (Figure 36), in support of report establishing that monoglycosides of flavonoids inhibit metabolic enzymes better than their polyglycoside forms (KIM et al., 2000). This may be responsible for the higher activity observed with the aglycone, quercetin (28.6%), being better than its glycoside, isoquercetin (6.3%). The inactivity of rutin and vicenin-2 may be as a result of the bulky diglycoside group interfering with the affinity of the metaboilite to the amylase active site. However, glycosylation at C3 has been shown to improve inhibition (LIAO et al., 2018). They were not evaluated further.

Tiliroside, which was discriminated in the glucose retardation assay showed inhibitory activity better than acarbose, 74.2% at 200.0 µg/mL (Figure 36). Its IC_{50} was determined to be 83.8 µg/mL; lower than a reported data with an IC_{50} of 166.5 µg/mL. It has been reported that glycosylation at C3 improves the inhibitory activity in addition to the unsaturation at C2-3, presence of -OH at C4', 5 and 7 (LIAO et al., 2018). *E. veadeiroensis* inhibited porcine pancreatic amylase by 25.3% expressing the metabolite with a high relative abundance.

At 200.0 µg/mL, chrysoeriol, which was discriminated in the glucose retardation assay and its dehydroxy- and demethoxy derivative, chrysin (Figure 36) both elicited comparable inhibition of about 89.0%, significantly better than acarbose. This comparable result may indicate the significance of C5 and 7-OH and an unsaturation at C2-3 in the inhibition of amylase. The presence of C3'-OCH_3 may be suggested unimportant but it has been reported that a -OCH_3 beside an -OH on the B ring is favourable for activity, explaining the activty for chrysoeriol. The IC_{50} of chrysoeriol and chrysin were determined to be 41.1 µg/mL and 48.0 µg/mL, which are significantly lower than the reported value of 381.3 µg/mL for chrysoeriol (Nickavar and Abolhasani, 2013) and 450.0 µg/mL for chrysin (LI et al., 2017) but exhibiting similar pattern with chrysoeriol having slightly higher activity. However, isorhamnetin (Figure 36), which is similar to chrysoeriol but with an additional -OH group at position 3 on ring C elicited a significantly lower inhibition, 33.1% at 200 µg/mL. This reduced activity may be due to the C3-OH, which has been shown to be unfavourable for amylase inhibition. However, glycosylation at C3 has been shown to improve activity as reported for isorhamnetin-3-O-β-D-glucopyranoside (METIBEMU et al., 2016) as similarly supported by tiliroside (LIAO et al., 2018). This was also supported by the results of Tundis et al. (2007), which showed that isorhamnetin-3-*O*-rutinoside exhibited inhibition with IC_{50} of 80.57 µg/mL (TUNDIS et al., 2007).

Pinocembrin and pinostrobin also elicited significant activity of 64% and 51.1% respectively (Figure 36). Their IC_{50} were respectively determined as 117.6 and 123.6 µg/mL. Despite the presence of a C7-OH group on the A ring of pinocembrin, it elicited a significantly lower inhibition, compared to chrysin. This reduced activity may be due to the structural difference between pinocembrin and chrysin, which is the absence of unsaturation at the C2-3 of pinocembrin. Pinostrobin inhibition was further reduced as a

result of the replacement of the C7-OH group in pinocembrin with a methoxy group in pinostrobin, further establishing the importance of C7-OH.

Luteolin, discriminated in the fungal α-amylase inhibitory assay showed a significant inhibitory activity comparable with acarbose. Its analogue, 3',4'-dimethoxyluteolin, was also discriminated active in the fungal α-amylase inhibitory and glucose uptake assays. The observed high activity of luteolin (200.0 µg/mL, 58.7%) (Figure 36) was suggested to be due to 5,7,4'-OH groups, unsaturation at C2-3 and absence of –OH at C3. Its IC_{50} was determined to be 168.6 µg/mL agreeing with the IC_{50} reported in literature, 103.0 µg/mL (TADERA et al., 2006).

Wedelolactone elicited a low activity (4.6%) compared with control at 200.0 µg/mL and the activity improved at a higher concentration (1.0 mg/mL) > 50.0% (Figure 36). *A. satureioides* (12.0%) and *B. gaudichaudiana* (21.5%), with a high relative abundance of the feature annotated as wedelolactone were observed to be active against the enzyme. The low inhibitory activity of the extract of *E. alba*, which has a high relative abundance of the feature may be as a result of the presence of reducing agents (BENES et al., 2012) in its matrix. Wedelolactone was evaluated for its activity because it had previously been shown to elicit significant amylase inhibition (93.8%) at an unreported concentration (KUMAR et al., 2018). In addition, *E. alba* was reported to have *in vivo* hypoglycaemic activity (at 20.0 mg/kg) (FRED-JAIYESIMI et al., 2009). Wedelolactone occurs in Wedelia calendulacea (KUMAR et al., 2018) and *E. alba* (SAVITA; PRAKASHCHANDRA, 2011; MENDES et al., 2014; CHERUVU et al., 2018). Furthermore, based on its activity > 50%, the IC_{50} was subsequently determined (640.5 µg/mL).

For the caffeoyl quinic acid derivatives, it was observed that the mono-substituted 5-caffeoylQA (3.5%) had significantly low inhibition of PPA compared with the di-caffeoyl quinic acids. The inhibitory activity at 200.0 µg/mL of 3,5-dicaffeoylQA, 4,5-dicaffeoylQA and 3,4-dicaffeoylQA were 50.2, 55.9 and 29.4% respectively (Figure 36). A similar pattern of activity has been previously reported with IC_{50} values of 26.5, 21.9 and 34.7 µg/mL for 3,5-dicaffeoylQA, 4,5-dicaffeoylQA and 3,4-dicaffeoylQA respectively (OLENNIKOV et al., 2018). 4,5-di-*O*-CQA and 3,5-di-*O*-CQA were also reported with significant amylase inhibition (RUSSO et al., 2015). This may justify the discrimination of

the quinic acid derivatives in the fungal and porcine pancreatic α-amylase inhibitory assays, as well as in the glucose retardation and uptake assays.

A stronger activity was observed with 3-*O*-methylquercetin (200.0 µg/mL, 59.3%; IC_{50}, 82.0%) better than quercetin and its glycoside (Figure 36). It was suggested that the methylation of the C3-OH improves the inhibitory activity. The presence of -OCH_3 at C3 may contribute to the electron density of the ring system thereby increasing the acidity of its phenyl –OH group.

A PPA inhibitory activity of 53.8% was observed with 7,3',4'-trimethoxy-5-hydroxyflavone. This high observed activity is contrary to reported data that showed that the inhibition of α-amylase by flavonols was associated with the number of hydroxyl groups in their structures (AL-DABBAS et al., 2006). The compound, 7,3',4'-trimethoxy-5-hydroxyflavone has only one hydroxyl group but elicited a significant activity (Figure 36). This may be as a result of the contribution of methoxyl substituents which are electron-donating. A study concluded that 3-methoxyflavones may have potential to prevent diabetes and obesity (AL-DABBAS et al., 2006).

Tagitinin C, which was discriminated active in the PPA, glucose retardation and glucose uptake assays, and other sesquiterpene lactones (200.0 ug/mL) were also evaluated for their inhibitory potential against PPA, and they all have significantly low activity (Figure 36). All except goyanzenolide (35.8%) and tagitinin C (11.3%) have < 5.0% activity indicating that STLs may not be good inhibitors of α-amylase. However, the low activity of the STLs may suggest that the metabolites act synergistically or exert their antidiabetic properties through mechanisms that need to be further evaluated, for example through mechanisms involved in enhancing insulin sensitivity. However, this lower amylase inhibition may be an added advantage considering possibly lower side effects; although, sesquiterpene lactones are generally regarded to be toxic.

The flavonoids and their analogues, discriminated in this study as active against amylase, such as acacetin, show general structural features that are favourable for the inhibition of amylase. In addition, they may exhibit their antidiabetic potential through other mechanisms of action. Such may include acacetin and kaempferol-6-methoxy-3-*O*-glucoside, which were observed as discriminants for PPA and antioxidant assays as well as the latter for glucose retardation and the former for glucose uptake assays.

In this study, the metabolites that were discriminated in each of the assays with as metabolomics analysis may have antidiabetic potential, aiming to prevent the development of diabetes by reducing or preventing postprandial hyperglycaemia through various mechanisms. In the glucose retardation assay, wedelolactone, chrysoeriol, apigenin 6-*C*-arabinoside-8-*C*-glucoside, rutin, 4-(acetyloxy)-3,3a,4,5,9a,9b-hexahydro-6-(hydroxymethyl)-3,9-dimethyl-azuleno[4,5-*b*]furan-2,7-dione, 4-*O*-feruloyl 5-*O*-caffeoylquinic acid, tiliroside, umbelliferone 7-*O*-glucopyranoside, quercetin, benzenemethanol, α-[1-[2,6-dimethoxy-4-(2-propenyl)phenoxy]ethyl]-3,4,5-trimethoxy-, tithonin, tagitinin C, 8-epidesacylcynaropicrin-3-*O*-glucoside, acacetin, apigenin and flavanokanin were pointed as responsible for the observed activity; while in the fungal α-amylase inhibitory assay, luteolin, apigenin, cynarascoloside C, isorhamnetin, tithonin, 5,7,4’-trihydroxy-8-methoxyflavone, 3',4'-dimethoxyluteolin, molephantinin, 5-*O*-feruloylquinic acid, 3,4'-dimethoxyquercetin, flavanokanin, quercetin-3-*O*-glucuronide and tagitinin C were the metabolites pointed as responsible for the activity. Furthermore, 8-epidesacylcynaropicrin-3-*O*-glucoside, apigenin 6-*C*-arabinoside-8-*C*-glucoside, tithonin, tagitinin C, acacetin, 4-(acetyloxy)-3,3a,4,5,9a,9b-hexahydro-6-(hydroxymethyl)-3,9-dimethyl-azuleno[4,5-*b*]furan-2,7-dione, 3,4',6-trimethoxyquercetagetin, 4-*O*-feruloyl 5-*O*-caffeoylquinic acid, 6-methoxyquercetin-7-*O*-glucoside, quercetin, kaempferol-6-methoxy-3-*O*-glucoside and tithofolinolide were pointed as responsible for the observed porcine pancreatic α-amylase inhibitory activity in this study. In the insulin-mediated glucose uptake assay, tagitinin C, 6-methoxyquercetin-7-*O*-glucoside, 3',4'-dimethoxyluteolin, rutin, azuleno[4,5-b]furan-2,7-dione, 3,3a,4,5,9a,9b-hexahydro-4-hydroxy-6-(hydroxymethyl)-3,9-dimethyl-, kaempferol, umbelliferone 7-*O*-glucopyranoside, quercetin, 4-*O*-feruloyl 5-*O*-caffeoylquinic acid, kaempferol-6-methoxy-3-*O*-glucoside and 3,4'-dimethoxyquercetin were indicated as responsible for the observed activity. Finally, apigenin 6-*C*-arabinoside-8-*C*-glucoside, kaempferol-6-methoxy-3-O-glucoside, 5-hydroxy-3,6,7,4'-tetramethoxyflavone, 5,6,7,4'-tetramethoxyflavone, 7,4'-dimethoxyapigenin, 3,4',6-trimethoxyquercetagetin and acacetin were pointed as active in the antioxidant assay.

It was observed that some of the metabolites were pointed out as responsible for the activity observed in more than one of the assays in this study, including apigenin 6-

C-arabinoside-8-*C*-glucoside and acacetin pointed as active in the glucose retardation, porcine pancreatic α-amylase inhibitory and antioxidant assays; rutin, 8-epidesacylcynaropicrin-3-*O*-glucoside and umbelliferone 7-*O*-glucopyranoside, in the glucose retardation and insulin-mediated glucose uptake enhancement assays; 4-(acetyloxy)-3,3a,4,5,9a,9b-hexahydro-6-(hydroxymethyl)-3,9-dimethyl-azuleno[4,5-*b*]furan-2,7-dione, quercetin and 4-*O*-feruloyl 5-*O*-caffeoylquinic acid, in the glucose retardation, porcine pancreatic α-amylase inhibitory and insulin-mediated glucose uptake assays; tithonin, in the glucose retardation, fungal α-amylase inhibitory and porcine pancreatic α-amylase inhibitory assays; tagitinin C, in the glucose retardation, fungal and porcine pancreatic α-amylases inhibitory and insulin-mediated glucose uptake assays; apigenin and flavanokanin, in the glucose retardation and fungal α-amylase inhibitory assays; 3',4'-dimethoxyluteolin and 3,4'-dimethoxyquercetin in the fungal α-amylase inhibitory and insulin-mediated glucose uptake assays; 3,4',6-trimethoxyquercetagetin, in the porcine pancreatic α-amylase inhibitory and antioxidant assays; 6-methoxyquercetin-7-*O*-glucoside, in the porcine pancreatic α-amylase inhibitory and insulin-mediated glucose uptake assays; and kaempferol-6-methoxy-3-*O*-glucoside, in the porcine pancreatic α-amylase inhibitory, insulin-mediated glucose uptake and antioxidant assays.

6. CONCLUSIONS

The comparison of metabolic fingerprints of the investigated plants afforded classifications based on geographical source of the plants. The plants were grouped into two main groups, based on their chemical similarity or differences.

The metabolomics analysis revealed important metabolites, especially phenolics, from the selected Asteraceae plants that were discriminated as active in each of the assays. Such includes a coumestan, flavonoids and their glycosides, sesquiterpene lactones and caffeoylquinic acid derivatives. Specifically, metabolomics approaches afforded the determination of flavonoids and their glycosides as the important variables responsible for the antioxidant activity, as well as for the activity observed in the other *in vitro* antidiabetic assays in this study, indicating additional potential for the prevention of diabetes. The discrimination of flavonoids, with established antioxidant property, in the other *in vitro* antidiabetic assays in this study suggest the potential of the plants with such metabolites to reduce or prevent postprandial hyperglycaemia and protect the pancreatic β-cells from oxidative stress-induced damage thereby indicating their potential to prevent diabetes development. Such includes apigenin 6-*C*-arabinoside-8-*C*-glucoside occurring with high relative abundance in commercial *A. millefolium*, *B. gaudichaudiana* and *B. genistelloides*; kaempferol-6-methoxy-3-*O*-glucoside detected with high relative abundance in the commercial samples including *A. satureioides*, *A. millefolium*, *C. officinalis*, *C. recutita*, *M. recutita, A. vulgare* and *T. vulgare*; samples from Brazil including *V. brasiliana*, *V. condensata*, *V. ferruginea*, *V. phosphorica, B. pilosa*, *E. glomerulatus* and *T. procumbens*; samples from Nigeria including *V. cinerea*, *S. sparganophora*, *E. odoratum*, *C. crepidioides* and *S. filicaulis*; 5-hydroxy-3,6,7,4'-tetramethoxyflavone and 5,6,7,4'-tetramethoxyflavone both found with high relative abundance in commercial *A. millefolium*; 7,4'-dimethoxyapigenin detected with high relative abundance in *E. alba* from Nigeria; 3,4',6-trimethoxyquercetagetin detected with the high relative abundance in commercial samples including *S. rebaudiana*, *T. vulgare*, *A. montana*, *C. recutita*; and acacetin detected with the high relative abundance in commercial samples including *A. satureioides*, *B. genistelloides* and *V. brasiliana*; samples from Nigeria including *S. sparganophora* and *V. cinerea, V. amygdalina*, *A. hispidum* and *M. scandens*. Purified flavonoids elicited significantly the highest inhibitory activity against porcine pancreatic α-

amylase. Glycosides of flavonoids, rutin, isoquercetin and vicenin-2 elicited significantly low inhibition. This was suggested to be a result of the steric hindrance to affinity of the flavonoids to the catalytic sites of the enzyme. Structural features including glycosylation at C3, unsaturation at C2-3, polyhydroxylations especially the presence of -OH at C4', 5 and 7, -OCH_3 beside an -OH on the B ring and absence of –OH group at position C3 on ring C were observed to be required for the inhibition of porcine pancreatic α-amylase. Finally, the evaluation of different Asteraceae species from different tribes, countries and geographical sources afforded a rigorous, strong and unbias correlation using multivariate statistical methods. Metabolomics successfully indicated some metabolites that have previously been reported with antidiabetic properties, though not specifically for the possibility of preventing diabetes through reduction or prevention of postprandial hyperglycaemia. This study therefore establishes a proof-of-principle for the use of untargeted metabolomics for the determination of plant specialized metabolites with antidiabetic potentials.

7. REFERENCES

ADEMILUYI, A. O.; OBOH, G. Aqueous extracts of Roselle (Hibiscus sabdariffa Linn.) varieties inhibit α-amylase and α-glucosidase activities in vitro. **Journal of medicinal food,** v.16, n.1, p. 88-93, 2013.

ADISAKWATTANA, S.; CHANATHONG, B. Alpha-glucosidase inhibitory activity and lipid-lowering mechanisms of Moringa oleifera leaf extract**. Eur Rev Med Pharmacol Sci,** v.15, n.7, p. 803-808, 2011.

AL-DABBAS, M. M.; KITAHARA, K.; SUGANUMA, T.; HASHIMOTO, F.; TADERA, K. **Antioxidant and -Amylase Inhibitory Compounds from Aerial Parts of Varthemia iphionoides Boiss**. v.70, n.9, p. 2178–2184, 2006.

ALI, H.; HOUGHTON, P. J.; SOUMYANATH, A. α-Amylase inhibitory activity of some Malaysian plants used to treat diabetes; with particular reference to Phyllanthus amarus. **Journal of Ethnopharmacology**, v. 107, n. 3, p. 449–455, 2006.

AMBRÓSIO, S. R.; OKI, Y.; HELENO, V. C. G.; CHAVES, J. S.; NASCIMENTO, P. G. B. D.; LICHSTON, J. E.; ... & DA COSTA, F. B. Constituents of glandular trichomes of Tithonia diversifolia : Relationships to herbivory and antifeedant activity. **Phytochemistry**, v. 69, p. 2052–2060, 2008.

BAHADORAN, Z.; MIRMIRAN, P.; AZIZI, F. Dietary polyphenols as potential nutraceuticals in management of diabetes: a review. *J Diabetes Metab Disord,* v. 12, n. 5, p. 43–51, 2013.

BALLABIO, D.; CONSONNI, V. Classification tools in chemistry. Part 1: linear models. PLS-DA. **Analytical Methods**, v. 5, n. 16, p. 3790-3798, 2013.

BAPTISTA, R.; FAZAKERLEY, D. M.; BECKMANN, M.; BAILLIE, L.; MUR, L. A. Untargeted metabolomics reveals a new mode of action of pretomanid (PA-824). **Scientific reports**, p. 1–7, 2018.

BASHA, S. K.; KUMARI, V. S. In vitro antidiabetic activity of psidium guajava leaves extracts. **Asian Pacific Journal of Tropical Diseases**, p. 98–100,2012.

Baynes, J. W., Thorpe, S. R. (1999). Role of oxidative stress in diabetic complications: a new perspective on an old paradigm. Diabetes, ***48***: 1-9.

BENES, P.; ALEXOVA, P.; KNOPFOVA, L.; SPANOVA, A; SMARDA, J. Redox state alters anti-cancer effects of wedelolactone**. Environmental and molecular mutagenesis,** v.*53, n.*7, p. 515-524, 2012.

BLACKWELL, L. R. **Great Basin: A Guide to Common Wildflowers of the High Deserts of Nevada, Utah, and Oregon.** Globe Pequot. 2006.

BRUNNER, Y.; SCHVARTZ, D.; PRIEGO-CAPOTE, F.; COUTÉ, Y.; SANCHEZ, J. C. Glucotoxicity and pancreatic proteomics. **J Proteomics**, v.71, p.576-591,2009.

CAO, J.; LI, C.; ZHANG, P.; CAO, X.; HUANG, T.; BAI, Y.; ET AL. Antidiabetic effect of burdock (*Arctium lappa* L.) root ethanolic extract on streptozotocin-induced diabetic rats. **African Journalof Biotechnology**, v.11, n.37, p. 9079-9085, 2012.

CHAGAS-PAULA, D. A.; DE OLIVEIRA, R. B.; DA SILVA, V. C.; GOBBO-NETO, L.; GASPAROTO, T. H.; CAMPANELLI, A. P.; DA COSTA, F. B. Chlorogenic acids from Tithonia diversifolia demonstrate better anti-inflammatory effect than indomethacin and its sesquiterpene lactones. **Journal of Ethnopharmacology**, v.136, n. 2, p.355-362, 2011.

CHAKRABORTHY, G. S.; ARORA, R.; MAJEE, C. Antidiabetic and antihyperlipidaemic effect of hydro-alcoholic extrct of Calendula officinalis. ***International Research Journal of Pharmacy***, v.2, n.1, p. 61-65.2011.

CHETAN, J.; KUMAR, P. M.; PRAKASH, H. S. Antidiabetic and Antihypertensive Potent ial of Selected Asteraceae Plant Species**.** ***American Journal of Advanced Drug Delivery*****,** v.2***,*** n.3, p.355-363, 2014.

CHIAIA-HERNANDEZ, A. C.; SCHYMANSKI, E. L.; KUMAR, P; SINGER, H. P.; HOLLENDER, J. Suspect and nontarget screening approaches to identify organic contaminant records in lake sediments. **Anal. Bioanal. Chem**., v.***406***, n. 28 p. 7323–7335.2014.

CHOI, Y. H. The cytoprotective effect of isorhamnetin against oxidative stress is mediated by the upregulation of the Nrf2-dependent HO-1 expression in C2C12 myoblasts through scavenging reactive oxygen species and ERK inactivation. **General physiology and biophysics,** v.35 ,n.2,p.145-154,2016.

CLEMENT, S.; BRAITHWAITE, S. S.; MAGEE, M.F.; AHMANN, A.; SMITH, E. P.; SCHAFER, R. G.; HIRSCH, I. B. Management of diabetes and hyperglycemia in hospitals. **Diabetes Care**, v.*27,* p.553-591,2004.

DAVIDSON, M. B.; BOUCH, C.; VENKATESAN, N.; AND KARJALA, R. G. Impaired glucose transport in skeletal muscle but normal GLUT-4 tissue distribution in glucose-infused rats. **Am J Physiol Endocrinol Metab**, v.*267*, p.808–813,1994.

DE MELO, E. B.; DA SILVEIRA GOMES, A.; CARVALHO, I. α-and β-Glucosidase inhibitors: chemical structure and biological activity. **Tetrahedron**, v. 62, n. 44, p.10277-10302, 2006.

DEUTSCHLÄNDER, M. S.; VAN DE VENTER, M.; ROUX, S.; LOUW, J.; LALL, N. Hypoglycaemic activity of four plant extracts traditionally used in South Africa for diabetes. **Journal of ethnopharmacology**, v. 124, n. 3, p. 619-624, 2009.

DI GUIDA, R.; ENGEL, J.; ALLWOOD, J. W.; WEBER, R. J.; JONES, M. R.; SOMMER, U.; MARK R. VIANT; DUNN, W. B. Non-targeted UHPLC-MS metabolomic data processing methods: a comparative investigation of normalisation, missing value imputation, transformation and scaling. **Metabolomics**, v. 12, n. 5, p. 93, 2016.

DUBOIS, M.; VACHER, P.; ROGER, B.; HUYGHE, D.; VANDEWALLE, B.; KERR-CONTE, J.; PATTOU, F.; MOUSTAÏD-MOUSSA, N.; LANG, J. Glucotoxicity inhibits late steps of insulin exocytosis. **Endocrinology**, v. 148, p. 1605-1614, 2007.

EDWARDS, C. A.; BLACKBURN, N. A.; CRAIGNE, L.; DAVISON, P.; TOMLIN, J.; SUGDEN, K.; JOHNSON, I. T.; READ, N. W. Viscosity of food gums determined in vitro related to their hypoglycaemic actions. **Am J Clin Nutr**; v. 46, p. 72–77, 1987.

EGUNYOMI, A.; GBADAMOSI, I. T.; ANIMASHAHUN, M. O. Hypoglycaemic activity of the ethanol extract of *Ageratum conyzoides* Linn. shoots on alloxan-induced diabetic rats. **Journal of Medicinal Plant Research**, v. 5, n. 22, p. 5346-5350, 2011.

EKEOCHA, P. C.; FASOLA, T. R.; EKEOCHA, A. H. The effect of *Vernonia amygdalina* on alloxan induced diabetic albino rats. **African Journal of Food Science and Technology***,* v. 3, n. 3, p. 73-77, 2012.

ERASTO, P.; VAN DE VENTER, M.; ROUX, S.; GRIERSON, D. S.; AFOLAYAN, A. J. Effect of leaf extracts of Vernonia amygdalina on glucose utilization in chang-liver, C2C12 muscle and 3T3-L1 cells. **Pharmaceutical biology**, v. 47, n. 2, p. 175-181, 2009.

ERIKSSON, J. G.; LEHTOVIRTA, M.; EHRNSTRÖM, B.; SALMELA, S.; GROOP, L. Long-term beneficial effects of glipizide treatment on glucose tolerance in subjects with impaired glucose tolerance. **Journal of internal medicine**, v. 256, n. 6, p. 553-560, 2006.

ERIKSSON, J. W. Metabolic stress in insulin's target cells leads to ROS accumulation - a hypothetical common pathway causing insulin resistance. **FEBS Lett**, v. 581, p. 3734-3742, 2007.

ERIKSSON, J.; FRANSSILA-KALLUNKI, A.; EKSTRAND, A.; SALORANTA, C.; WIDÉN, E.; SCHALIN, C.; GROOP, L. Early metabolic defects in persons at increased risk for non-insulin-dependent diabetes mellitus. **New Engl J Med***,* v. 321, p. 337-343, 1989.

FADINI, G. P.; PUCCI, L.; VANACORE, R.; BAESSO, I.; PENNO, G.; BALBARINI, A.; DI STEFANO, R.; MICCOLI, R.; DE KREUTZENBERG, S.; CORACINA, A.; TIENGO, A. Glucose tolerance is negatively associated with circulating progenitor cell levels. **Diabetologia**, v. 50, n. 10, p. 2156-2163, 2007.

FRED-JAIYESIMI, A.; KIO, A.; RICHARD, W. α-Amylase inhibitory effect of 3β-olean-12-en-3-yl (9Z)-hexadec-9-enoate isolated from Spondias mombin leaf. **Food Chemistry**, v. 116, n. 1, p. 285-288, 2009.

FUJIMURA, Y.; KURIHARA, K.; IDA, M.; KOSAKA, R.; MIURA, D.; WARIISHI, H.; MAEDA-YAMAMOTO, M.; NESUMI, A.; SAITO, T.; KANDA, T.; YAMADA, K. Metabolomics-driven nutraceutical evaluation of diverse green tea cultivars. **PloS one**, v. 6, n. 8, p. 1-16, 2011.

GALLAGHER, A. M.; FLATT, P. R.; DUFFY, G.; ABDEL-WAHAB, Y. H. A. The effects of traditional antidiabetic plants on in vitro glucose diffusion. **Nutrition research**, v. 23, n. 3, p. 413-424, 2003.

GALLON, M. E.; MONGE, M.; CASOTI, R.; DA COSTA, F. B.; SEMIR, J.; GOBBO-NETO, L. Metabolomic analysis applied to chemosystematics and evolution of megadiverse Brazilian Vernonieae (Asteraceae). **Phytochemistry**, v. 150, p. 93-105, 2018.

GHAVAMI, A.; JOHNSTON, B. D.; JENSEN, M. T.; SVENSSON, B.; PINTO, B. M. Synthesis of nitrogen analogues of salacinol and their evaluation as glycosidase inhibitors. **J Am Chem Soc**, v. 123, p. 6268-6271, 2001.

GIRI, B.; DEY, S.; DAS, T.; SARKAR, M.; BANERJEE, J; DASH, S. K. Chronic hyperglycemia mediated physiological alteration and metabolic distortion leads to organ dysfunction, infection, cancer progression and other pathophysiological consequences: an update on glucose toxicity. **Biomedicine & Pharmacotherapy**, v. 107, p. 306-328, 2018.

GOBBO-NETO, L.; GATES, P. J; LOPES, N. P. Negative Ion ‘Chip-Based’ Nanospray Tandem Mass Spectrometry for the Analysis of Flavonoids in Glandular Trichomes of Lychnophora ericoides Mart. (Asteraceae). **Rapid Communications in Mass Spectrometry**, v. 22, p. 3802-3808, 2008.

GOVORKO, D.; LOGENDRA, S.; WANG, Y.; ESPOSITO, D.; KOMARNYTSKY, S.; RIBNICKY, D.; POULEV, A.; WANG, Z.; CEFALU, W. T.; RASKIN, I. Polyphenolic compounds from Artemisia dracunculus L. inhibit PEPCK gene expression and gluconeogenesis in an H4IIE hepatoma cell line. **Am. J. Physiol.: Endocrinol. Metab.**, v. 293, p. 1503–1510, 2007.

GROBBEE, D. E. (2003). How to ADVANCE prevention of cardiovascular complications in type 2 diabetes. **Metabolism**, v. 52, p. 24-28, 2003.

GROOP, P. H.; ARO, A.; STENMAN, S.; GROOP, L. Long-term effects of guar gum in subjects with non-insulindependent diabetes mellitus. **Am J Clin Nutr**, v. 58, p. 513-518, 1993.

HADRICH, F.; GARCIA, M.; MAALEJ, A.; MOLDES, M.; ISODA, H.; FEVE, B.; SAYADI, S. Oleuropein activated AMPK and induced insulin sensitivity in C2C12 muscle cells. **Life sciences**, v. 151, p. 167-173, 2016.

HALLEN-ADAMS, H. E.; SUHR, M. J. Fungi in the healthy human gastrointestinal tract. **Virulence**, v. 8, n. 3, p. 352-358, 2017.

HARMON, J. S.; GLEASON, C. E.; TANAKA, Y.; OSEID, E. A.; HUNTER-BERGER, K. K.; ROBERTSON, R. P. In vivo prevention of hyperglycemia also prevents glucotoxic effects on PDX-1 and insulin gene expression. **Diabetes**, v. 48, n. 10, p. 1995-2000, 1999.

HOLLENDER, J.; SCHYMANSKI, E. L.; SINGER, H. P.; LEE FERGUSON, P. Nontarget Screening with High Resolution Mass Spectrometry in the Environment: Ready to Go? **Environ. Sci. Technol.**, v. 51, p. 11505-11512, 2017.

HOLMAN, R. R. Long-term efficacy of sulfonylureas: a United Kingdom Prospective Diabetes Study perspective. **Metab. Clin.**, v. 55, n. 1, p. 2-5, 2006.

HOSTETTMANN, K.; WOLFENDER, J. L.; TERREAUX, C. Modern Screening Techniques for Plant Extracts. **Pharmaceutical Biology**, v. 39, p. 18-32, 2001.

HSU, Y.; LEE, T.; CHANG, C. L.; HUANG, Y.; YANG, W. Anti-hyperglycaemic effects and mechanism of Bidens pilosa water extract. **Journal of Ethanopharmacology**, v. 122, p. 379-383, 2009

INTERNATIONAL DIABETES FEDERATION. **Diabetes atlas**. Available at: <http://www.idf.org/diabetesatlas>. Accessed on May 3, 2019.

JEFFREY, C. (2007). Compositae: Introduction with key to tribes. **Families and Genera of Vascular Plants**, v. 8, p. 61-87, 2007

JENKINS, D. J.; LEEDS, A. R.; GASSULL, M. A.; COCHET, B.; ALBERTI, K. G. G. M. Decrease in postprandial insulin and glucose concentrations by guar and pectin. **Ann Intern Med**, v. 86, p. 20-23, 1976

JEPPESEN, P. B.; GREGERSEN, S.; ALSTRUP, K. K.; HERMANSEN, K. Stevioside induces antihyperglycaemic, insulinotropic and glucagonostatic effects in vivo: studies in the diabetic Goto-Kakizaki (GK) rats. **Phytomedicine**. v. 9, p. 9-14, 2002

JORDAN, K. W.; NORDENSTAM, J.; LAUWERS, G. Y.; ROTHENBERGER, D. A.; ALAVI, K.; GARWOOD, M.; CHENG, L. L. Metabolomic Characterization of Human Rectal Adenocarcinoma with Intact Tissue Magnetic Resonance Spectroscopy. **Diseases of the Colon and Rectum**, v. 52, p. 520-525, 2009

JOSHI, S. R.; KARNE, R. Pre-Diabetes, Dysglycaemia and Early Glucose Intolerance and Vascular Health. **JAPI**, v. 55, p. 829-831, 2007

KAISER, N.; CORCOS, A. P.; SAREL, I.; CERASI, E. Monolayer culture of adult rat pancreatic islets on extracellular matrix: modulation of B-cell function by chronic exposure to high glucose. **Endocrinology**, v. 129, p. 2067-2076, 1991.

KATAJAMAA, M.; ORESIC, M. Data Processing for Mass Spectrometry-Based Metabolomics. **Journal of Chromatography**, v. 1158, p. 318-328, 2007.

KAWAHITO, S.; KITAHATA, H.; OSHITA, S. Problems associated with glucose toxicity: Role of hyperglycemia-induced oxidative stress. **World J Gastroenterol**, v. 15, n. 33, p. 4137-4142, 2009.

KHAN, M. F.; RAWAT, A. K.; KHATOON, S.; HUSSAIN, M. K.; MISHRA, A.; NEGI, D. S. In vitro and in vivo Antidiabetic Effect of Extracts of Melia azedarach, Zanthoxylum alatum, and Tanacetum nubigenum. **Integrative medicine research**, v. 7, n. 2, p. 176-183, 2018.

KIM, J. S.; KWON, C. S.; SON, K. H. Inhibition of alpha-glucosidase and amylase by luteolin, a flavonoid. **Bioscience, biotechnology, and biochemistry**, v. 64, n. 11, p. 2458-2461, 2000.

KIM, S. H.; SUNG, M. J.; PARK, J. H.; YANG, H. J.; HWANG, J. T. Boehmeria nivea stimulates glucose uptake by activating peroxisome proliferator-activated receptor gamma in C2C12 cells and improves glucose intolerance in mice fed a high-fat diet. **Evidence-Based Complementary and Alternative Medicine**, p. 1-9, 2013.

KIM, Y.; WANG, M.; RHEE, Y. A novel a-glucosidase inhibitor from pine bark. **Carbohydrate Research**, v. 339, p. 715-717, 2004.

KOISTINEN, H. A.; ZIERATH, J. R. Regulation of glucose transport in human skeletal muscle. **Ann Med**, v. 34, p. 410-418, 2002.

KRAUSS, M.; SINGER, H.; HOLLENDER, J. LC–high resolution MS in environmental analysis: from target screening to the identification of unknowns. **Anal. Bioanal. Chem.**, v. 397, p. 943-951, 2010.

KUMANAN, R.; MANIMARAN, S.; SALEEMULLA, K.; DHANABAL, S. P.; NANJAN, M. J. Screening of bark of Cinnamomum tamala (Lauraceae) by using α-amylase inhibition assay for anti-diabetic activity. **International Journal of Pharmaceutical and Biomedical Research**, v. 1, n. 2, p. 69-72, 2010.

KUMAR, B. A.; LAKSHMAN, K.; NANDEESH, R.; KUMAR, P. A.; MANOJ, B.; KUMAR, V.; SHEKAR, D. S. In vitro alpha-amylase inhibition and in vivo antioxidant potential of Amaranthus spinosus in alloxan-induced oxidative stress in diabetic rats. **Saudi Journal of biological sciences**, v. 18, n. 1, p. 1-5, 2011.

KUMAR, S.; KARL, P. N.; SAMUEL, J.; SELVAKUMAR, M.; SHALINI, K. Ant i-oxidant , ant i-diabet ic, ant imicrobial and hemolyt ic act ivity of Tridax procumbens. **J Chem Pharm Res**, v. 8, p. 808-812, 2016.

KUMAR, V.; SHARMA, K.; AHMED, B.; AL-ABBASI, F. A.; ANWAR, F.; VERMA, A. Deconvoluting the dual hypoglycemic effect of wedelolactone isolated from Wedelia calendulacea: investigation via experimental validation and molecular docking. **RSC Advances**, v. 8, n.32, p. 18180-18196, 2018.

KWON, Y. I.; SON, H. J.; MOON, K. S.; KIM, J. K.; KIM, J. G.; CHUN, H. S.; AHN, S. K.; HONG, C. I. Novel α-Glucosidase Inhibitors, CKD-711 and CKD-711a Produced by Streptomyces sp. CK-4416. **The Journal of antibiotics**, v. 55, n. 5, p. 462-466, 2002.

LANG, G.; MAYHUDIN, N.A.; MITOVA, M.I.; SUN, L.; VAN DER SAR, S.; BLUNT, J.W.; COLE, A.L.; ELLIS, G.; LAATSCH, H.; MUNRO, M.H. Evolving Trends in the Dereplication of Natural Product Extracts: New Methodology for Rapid, Small Scale Investigation of Natural Product Extracts. **Journal of Natural Products**, v. 71, p. 1595-1599, 2008.

LEROITH, D. Beta-cell dysfunction and insulin resistance in type 2 diabetes: role of metabolic and genetic abnormalities. **Am J Med**, v. 113, n. 6A, p. 3-11, 2002.

LI, S., SULLIVAN, N.L.; ROUPHAEL, N.; YU, T.; BANTON, S.; MADDUR, M.S.; MCCAUSLAND, M.; CHIU, C.; CANNIFF, J.; DUBEY, S.; LIU, K. Metabolic phenotypes of response to vaccination in humans. **Cell**, v. 169, n. 5, p. 862-877, 2017.

LIAN, F.; LI, G.; CHEN, X.; WANG, X.; PIAO, C.; WANG, J.; HONG, Y.; BA, Z.; WU, S.; ZHOU, X.; LANG, J.; LIU, Y.; ZHANG, R.; HAO, J.; ZHU, Z.; LI, H.; LIU, H. F.; CAO, A.; YAN, Z.; AN, Y.; BAI, Y.; WANG, Q.; ZHEN, Z.; YU, C.; WANG, C.; YUAN, C.; TONG, X. Chinese Herbal Medicine Tianqi Reduces Progression From Impaired Glucose Tolerance to Diabetes: A Double-Blind, Randomized, Placebo-Controlled, Multicenter Trial. **The Journal of Clinical Endocrinology & Metabolism**, v. 99, n. 2, p. 648-655, 2014.

LIAO, L.; CHEN, J.; LIU, L.; XIAO, A. Screening and Binding Analysis of Flavonoids with Alpha-Amylase Inhibitory Activity from Lotus Leaf. **J. Braz. Chem. Soc.**, v. 29, n. 3, p. 587-593, 2018.

LILAND, K. H. Multivariate methods in metabolomics–from pre-processing to dimension reduction and statistical analysis. **TrAC Trends in Analytical Chemistry**, v. 30, n. 6, p. 827-841, 2011.

LILLIOJA, S.; MOTT, D.M.; SPRAUL, M.; FERRARO, R.; FOLEY, J.E.; RAVUSSIN, E.; KNOWLER, W.C.; BENNETT, P.H.; BOGARDUS, C. Insulin resistance and insulin secretory dysfunction as precursors of non-insulin-dependent diabetes mellitus. **New Engl J Med**, v. 329, p. 1988-1992, 1992.

LIU, Q. M.; ZHAO, H. Y.; ZHONG, X. K.; JIANG, J. G. Eclipta prostrata L. phytochemicals: isolation, structure elucidation, and their antitumor activity. **Food and Chemical Toxicology**, v. 50, n. 11, p. 4016-4022, 2012.

LIU, W.; WANG, J.; ZHANG, Z.; XU, J.; XIE, Z.; SLAVIN, M.; GAO, X. In vitro and in vivo antioxidant act ivity of a fructan from the roots of Arct ium lappa L. **International journal of biological macromolecules**, v. 65, p. 446-453, 2014.

LO PIPARO, E.; SCHEIB. H.; FREI, N.; WILLIAMSON, G.; GRIGOROV, M.; CHOU, C. J. Flavonoids for controlling starch digest ion: st ructural requirements for inhibit ing human α-amylase. **Journal of medicinal chemistry**, v. 51, n. 12, p. 3555-3561, 2008.

LU, B.; ENNIS, D.; LAI, R.; BOGDANOVIC, E.; NIKOLOV, R.; SALAMON, L.; FANTUS, C.; LE-TIEN, H.; FANTUS, I. G. Enhanced sensitivity of insulin-resistant adipocytes to vanadate is associated with oxidative stress and decreased reduction of vanadate (+5) to vanadyl (+4). **J Biol Chem**, v. 276, p. 35589-35598, 2001.

MAGILI, S. T.; MAINA, H. M.; BARMINAS, J. T.; MAITERA, O. N.; ONEN, A. I. Study of some trace and macroelements in selected antidiabetic medicinal plants used in Adamawa State, Nigeria by neutron activation analysis (NAA). **Peak Journal of Medicinal Plant Research**, v. 2, n. 2, p. 13-22, 2014.

MAHAJAN, R. P.; MAHIRE, R. R.; MORE, D. H. Phytochemical screening of aqueous and ethanol extracts of some medicinal plants and in-vitro study of inhibit ion of α-amylase. **Int J Pharm**, v. 1, p. 501-506, 2014.

METIBEMU, D. S.; SALIU, J. A.; METIBEMU, A. O.; OLUWADAHUNSI, O. J.; OBOH, G.; OMOTUYI, I. O.; AKINLOYE, O. A. Molecular docking studies of isorhamnetin from Corchorusolitorius with target alpha-amylase related to Type 2 diabetes. **Journal of Chemical and Pharmaceutical Research**, v. 8, n. 4, p. 1262-1266, 2016.

MEYER, C.; DOSTOU, J. M.; WELLE, S. L.; GERICH, J. E. Role of human liver, kidney, and skeletal muscle in postprandial glucose homeostasis. **Am J Physiol Endocrinol Metab**, v. 282, p. 419-427, 2002.

NAJAFIAN, M. The effects of curcumin on alpha amylase in diabetics rats. **Zahedan Journal of Research in Medical Sciences**, v. 17, n. 12, p. 1-7, 2016.

NEDACHI, T.; KANZAKI, M. Regulation of glucose transporters by insulin and extracellular glucose in C2C12 myotubes. **American Journal of Physiology-Endocrinology and Metabolism**, v. 291, n. 4, p. 817-828, 2006.

NICHOLSON, J. K.; LINDON, J. C.; HOLMES, E. “Metabonomics”: understanding the metabolic responses of living systems to pathophysiological stimuli via multivariate statistical analysis of biological NMR spectroscopic data. **Xenobiotica**, v. 29, p. 1181-1189, 1999.

NICKAVAR, B.; ABOLHASANI, L. Bioactivity-guided separation of an α-amylase inhibitor flavonoid from Salvia virgata. **Iranian journal of pharmaceutical research: IJPR**, v. 12, n. 1, p. 57, 2013.

NOFAL, S. M.; MAHMOUD, S. S.; RAMADAN, A.; SOLIMAN, G. A.; FAWZY, R. Anti-diabetic effect of Artemisia judaica extracts. **Research Journal of Medicine and Medical Sciences**, v. 4, n. 1, p. 42-48, 2009.

NOTKINS, A. L. Immunologic and genetic factors in type 1 diabetes. **J Biol Chem**, v. 277, n. 46, p. 43545-43548, 2002.

NUUTILA, P.; KNUUTI, M. J.; RAITAKARI, M.; RUOTSALAINEN, U.; TERAS, M.; VOIPIO-PULKKI, L. M.; HAAPARANTA, M.; SOLIN, O.; WEGELIUS, U.; YKI-JARVINEN, H. Effect of antilipolysis on heart and skeletal muscle glucose uptake in overnight fasted humans. **Am J Physiol Endocrinol Metab**, v. 267, p. 941-946, 1994.

OGURTSOVA, K.; DA ROCHA FERNANDES, J.D.; HUANG, Y.; LINNENKAMP, U.; GUARIGUATA, L.; CHO, N.H.; CAVAN, D.; SHAW, J.E.; MAKAROFF, L.E. IDF Diabetes Atlas: Global estimates for the prevalence of diabetes for 2015 and 2040. **Diabetes research and clinical practice**, v. 128, p. 40-50, 2017.

OLENNIKOV, D. N.; CHIRIKOVA, N. K.; KASHCHENKO, N. I.; NIKOLAEV, V. M.; KIM, S. W.; VENNOS, C. Bioactive Phenolics of the Genus Artemisia (Asteraceae): HPLC-DAD-ESI-TQ-MS/MS Profile of the Siberian Species and Their Inhibitory Potential Against α-Amylase and α-Glucosidase. **Frontiers in pharmacology**, v. 9, p. 756, 2017.

OVENDEN, S. P.; PIGOTT, E. J.; ROCHFORT, S.; BOURNE, D. J. Liquid chromatography–mass spectrometry and chemometric analysis of Ricinus communis extracts for cultivar identification. **Phytochemical analysis**, v. 25, n. 5, p. 476-484, 2014.

PASSONI, F. D.; OLIVEIRA, R. B.; CHAGAS-PAULA, D. A.; GOBBO-NETO, L.; DA COSTA, F. B. Repeated-dose toxicological studies of Tithonia diversifolia (Hemsl.) A. gray and identification of the toxic compounds. **Journal of ethnopharmacology**, v. 147, n. 2, p. 389-394, 2013.

PETCHI, R. R.; PARASURAMAN, S.; VIJAYA, C. Antidiabetic and antihyperlipidemic effects of an ethanolic extract of the whole plant of *Tridax procumbens (Linn.)* in streptozotocin-induced diabetic rats. **Journal of Basic and Clinical Pharmacy***,* v. 4, n. 4, p. 88-92, 2013.

PICOT, C. M. N.; SUBRATTY, A. H.; MAHOMOODALLY, M. F. Inhibitory potential of five traditionally used native antidiabetic medicinal plants on α-amylase, α-glucosidase, glucose entrapment, and amylolysis kinetics in vitro. **Advances in Pharmacological Sciences**, p. 1-7, 2014.

RADULOVIC, N. S.; MLADENOVIC, M. Z.; BLAGOJEVIC, P. D. (Un)targeted Metabolomics in Asteraceae: Probing the Applicability of Essential-oil Profiles of Senecio L. (Senecioneae) Taxa in Chemotaxonomy. **Chemistry & Biodiversity**, v. 11, p. 1330-1353, 2014.

RAINS, J. L.; JAIN, S. K. Oxidative stress, insulin signaling, and diabetes. **Free Radic. Biol. Med.**, v. 50, n. 5, p. 567-575, 2010.

REUSCH, J. E. Diabetes, microvascular complications, and cardiovascular complications: what is it about glucose? **J Clin Invest**, v. 112, p. 986-988, 2003.

ROBERTSON, R. P. Oxidative stress and impaired insulin secretion in type 2 diabetes. **Curr Opin Pharmacol**, v. 6, p. 615-619, 2006.

ROBERTSON, R. P.; OLSON, L. K.; ZHANG, H. J. Differentiating glucose toxicity from glucose desensitization: a new message from the insulin gene. **Diabetes**, v. 43, p. 1085-1089, 1994.

ROBINSON, H. Generic and subtribal classification of American Vernonieae. **Smithson. Contrib. to Bot.**, v. 89, n. i-iii, p. 1-116, 1999.

ROCHA, B.A.; PUPO, M.T.; ANTONUCCI, G.A.; SAMPAIO, S.V.; PAIVA, R.D.M.A.; SAID, S.; GOBBO-NETO, L.; DA COSTA, F.B. Microbial transformation of the sesquiterpene lactone tagitinin C by the fungus Aspergillus terreus. **Journal of industrial microbiology & biotechnology**, v. 39, n. 11, p. 1719-1724, 2012.

RUDICH, A.; TIROSH, A.; POTASHNIK, R.; HEMI, R.; KANETY, H.; BASHAN, N. Prolonged oxidative stress impairs insulin-induced GLUT4 translocation in 3T3-L1 adipocytes. **Diabetes**, v. 47, p. 1562-1569, 1998.

RUSSO, D.; VALENTAO, P.; ANDRADE, P. B.; FERNANDEZ, E. C.; MILELLA, L. Evaluation of Antioxidant, Antidiabetic and Anticholinesterase Activities of *Smalanthus sonchifolius* Landraces and Correlation with Their Phytochemical Profiles. **Int. Journal of Mol. Sci.***,* v. 16, n. 8, p. 17696-718, 2015.

RYU, T. Y.; PARK, J.; SCHERER, P. E. Hyperglycemia as a risk factor for cancer progression. **Diabetes & metabolism journal**, v. 38, n. 5, p. 330-336, 2014.

SAOUD, A.; AKOWUAH, G. A.; FATOKUN, O. Determination of acarbose in tablets by attenuated total reflectance Fourier transform infrared spectroscopy. **Arch Ind Biotechnol.**, v. 1, n. 1, p. 20-26, 2017.

SARTOR, G.; SCHERSTÉN, B.; CARLSTRÖM, S.; MELANDER, A.; NORDÉN, Å.; PERSSON, G. Ten-year follow-up of subjects with impaired glucose tolerance. Prevention of diabetes by tolbutamide and diet regulation. **Diabetes**, v. 29, p. 41-49, 1980.

SAS, K. M.; KARNOVSKY, A.; MICHAILIDIS, G.; PENNATHUR, S. Metabolomics and diabetes: analytical and computational approaches. **Diabetes**, v. 64, n. 3, p. 718-732, 2015.

SATHIAVELU, A.; SANGEETHA, S.; ARCHIT, R.; MYTHILI, S. In Vitro anti-diabetic activity of aqueous extract of the medicinal plants Nigella sativa, Eugenia jambolana, Andrographis paniculata and Gymnema sylvestre. **International Journal of Drug Development and Research**, v. 5, n. 2, p. 323-328, 2013.

SATTAR, N. A.; HUSSAIN, F.; IQBAL, T.; SHEIKH, M. A. Determination of in vitro antidiabetic effects of Zingiber officinale Roscoe. **Brazilian Journal of Pharmaceutical Sciences**, v. 48, n. 4, p. 601-607, 2012.

SAWAYA, A. C.; TOMAZELA, D. M.; CUNHA, I. B.; BANKOVA, V. S.; MARCUCCI, M. C.; CUSTODIO, A. R.; EBERLIN, M. N. Electrospray ionization mass spectrometry fingerprinting of propolis. **Analyst**, v. 129, n. 8, p. 739-744, 2004.

Schymanski, E.L.; Singer, H.P.; Slobodnik, J.; Ipolyi, I.M.; Oswald, P.; Krauss, M.; Schulze, T.; Haglund, P.; Letzel, T.; Grosse, S.; Thomaidis, N.S. Non-target screening with high-resolution mass spectrometry: critical review using a collaborative trial on water analysis. **Anal. Bioanal. Chem.**, v. 407, p. 6237-6255, 2015.

SELLES, C.; MEDJDOUB, H.; DIB, M. E. A.; ZERRIOUH, M.; TABTI, B. Antidiabetic activity of aqueous root extract of *Anacyclus pyrethrum* L. in streptozotocin-induceddiabetic rats. **Journal of Medicinal Plants Research**, v. 6, n . 16, p. 3193-3198, 2012.

SHARMA, A.; OLSON, L. K.; ROBERTSON, R. P.; STEIN, R. The reduction of insulin gene transcription in HIT-T15 b cells chronically exposed to high glucose concentration is associated with the loss of RIPE3b1 and STF-1 transcription factor expression. **Mol Endocrinol***,* v. 9, p. 1127-1134, 1995.

SHIM, Y. J.; DOO, H. K.; AHN, S. Y.; KIM, Y. S.; SEONG, J. K.; PARK, I. S.; MIN, B. H. Inhibitory effect of aqueous extract from the gall of Rhuz chinensis on alpha-glucosidase activity and postprandial blood glucose. **J Ethnopharmacol**, v. 85, p. 283-287, 2003.

SOLBRIG, O. T. Subfamilial Nomenclature of Compositae. **Taxon**, v. 12, p. 229-235, 1963.

SONAWANE, A.; SRIVASTAVA, R. S.; SANGHAVI, N.; MALODE, Y.; CHAVAN, B. Anti-diabetic activity of Tridax procumbens. **J. Sci. Innov. Res**, v. 3, n. 2, p. 221-226, 2014.

SONG, Y.; MANSON, J. E.; BURING, J. E.; SESSO, H. D.; LIU, S. Association of dietary flavonoids with risk of type 2 diabetes, and markers of insulin resistance and systemic inflammation in women: a prospective study and cross sectional analysis. **J Am Coll Nutr.**, v. 24, p. 376-384, 2005.

STEGENGA, M.E.; VAN DER CRABBEN, S.N.; BLÜMER, R.M.; LEVI, M.; MEIJERS, J.C.; SERLIE, M.J.; TANCK, M.W.; SAUERWEIN, H.P.; VAN DER POLL, T. Hyperglycemia enhances coagulation and reduces neutrophil degranulation, whereas hyperinsulinemia inhibits fibrinolysis during human endotoxemia. **Blood**, v. 112, n. 1, p. 82-89, 2008.

STEVENS, P. F. Angiosperm Phylogeny Website, v.14, 2001. Available at: <http://www.mobot.org/MOBOT/research/APweb/> Accessed on 28 July, 2019.

SUDHA, P.; ZINJARDE, S. S.; BHARGAVA, S. Y.; KUMAR, A. R. Potent α-amylase inhibitory activity of Indian Ayurvedic medicinal plants. **BMC complementary and alternative medicine**, v. 11, n. 1, p. 5, 2011.

SUMNER, L. W.; MENDES, P.; DIXON, R. A. Plant metabolomics: large-scale phytochemistry in the functional genomics area. **Phytochemistry**, v. 62, p. 817-836, 2003.

SUN, Q.; LI, J.; GAO, F. New insights into insulin: The anti-inflammatory effect and its clinical relevance. **World journal of diabetes**, v. 5, n. 2, p. 89, 2014.

SUT, S.; DALL'ACQUA, S.; BALDAN, V.; KAMTE, S.L.N.; RANJBARIAN, F.; NYA, P.C.B.; VITTORI, S.; BENELLI, G.; MAGGI, F.; CAPPELLACCI, L.; HOFER, A. Identification of tagitinin C from Tithonia diversifolia as antitrypanosomal compound using bioactivity-guided fractionation. **Fitoterapia**, v. 124, p. 145-151, 2018.

SY, G. Y.; NONGONIERMA, R. B.; SARR, M.; CISSE, A.; FAYE, B. Antidiabetic activity of the leaves of *Vernonia colorata* (Wilid.) Drake (Composees) in alloxan-induced diabetic rats. **Dakar Medical**, v. 49, n. 1, p. 36-39, 2004.

TABÁK, A. G.; HERDER C.; RATHMANN, W.; BRUNNER, E. J.; KIVIMÄKI, M. Prediabetes: a high-risk state for diabetes development . **The Lancet**, v. 379, n. 9833, p. 2279-2290, 2012.

TADERA, K.; MINAMI, Y.; TAKAMATSU, K.; MATSUOKA, T. Inhibition of α-glucosidase and α-amylase by flavonoids. **Journal of nutritional science and vitaminology**, v. 52, n. 2, p. 149-153, 2006.

TEDONG, L.; MADIRAJU, P.; MARTINEAU, L.C.; VALLERAND, D.; ARNASON, J.T.; DESIRE, D.D.; LAVOIE, L.; KAMTCHOUING, P.; HADDAD, P.S. Hydro-ethanolic extract of cashew tree (Anacardium occidentale) nut and its principal compound, anacardic acid, stimulate glucose uptake in C2C12 muscle cells. **Molecular nutrition & food research**, v. 54, n. 12, p. 1753-1762, 2010.

THE DIABETES PREVENTION PROGRAM RESEARCH GROUP. The Diabetes Prevention Program. Design and methods for a clinical trial in the prevention of type 2 diabetes. **Diabetes Care**, v. 22, p. 623-634, 1999.

THOMPSON, C. S. Animal models of diabetes mellitus: relevance to vascular complications. **Curr Pharm Des**, v. 14 p. 309-324, 2008.

TIEDGE, M.; LORTZ, S.; DRINKGERN, J.; LENZEN, S. Relation between antioxidant enzyme gene expression and antioxidative defense status of insulin-producing cells. **Diabetes***,* v. 46 p. 1733-1742, 1997.

TIWARI, B. K.; PANDEY, K. B.; ABIDI, A. B.; RIZVI, S. I. Markers of oxidative stress during diabetes mellitus. **J. Biomark.**, p. 1-8, 2013.

TRIVEDI, D. K.; ILES, R.K. The application of SIMCA P+ in shotgun metabolomics analysis of ZIC®HILIC-MS spectra of human urine – experience with the Shimadzu IT-TOF and profiling solutions data extraction software. **Journal of Chromatography Separation Techniques,** v. 3, p. 1-5, 2012.

TUNDIS, R.; LOIZZO, M. R.; STATTI, G. A.; MENICHINI, F. Inhibitory effects on the digestive enzyme α-amylase of three Salsola species (Chenopodiaceae) in vitro. **Die Pharmazie-An International Journal of Pharmaceutical Sciences**, v. 62, n. 6, p. 473-475, 2007.

TURNER, R. C.; MCCARTHY, S. T.; HOLMAN, R. R.; HARRIS, E. Beta-cell function improved by supplementing basal insulin secretion in mild diabetes. **Br Med J**, v. 1, p. 1252-1254, 1976.

U.K. PROSPECTIVE DIABETES STUDY GROUP. U.K. prospective diabetes study 16. Overview of 6 years' therapy of type II diabetes: a progressive disease. U.K. Prospective Diabetes Study Group. **Diabetes**, v. 44, p. 1249-1258, 1995.

UK PROSPECTIVE DIABETES STUDY GROUP. Effect of intensive blood-glucose control with metformin on complications in overweight patients with type 2 diabetes (UKPDS 34). **Lancet**, v. 352, p. 854-865, 1998.

UNWIN, N.; SHAW, J.; ZIMMET, P.; ALBERTI, K. G. Impaired glucose tolerance and impaired fasting glycaemia: the current status on definition and intervention. **Diabet Med.***,* v. 19, p. 708-723, 2002.

VAAG, A.; LUND, S. S. Non-obese patients with type 2 diabetes and prediabetic subjects: distinct phenotypes requiring special diabetes treatment and (or) prevention? **Appl. Physiol. Nutr. Metab.***,* v. 32, p. 912–920, 2007.

VAAG, A. On the pathophysiology of late onset non-insulin dependent diabetes mellitus: current controversies and new insights. **Dan. Med. Bull**, v. 46, p. 197-234, 1999.

VAGUE, P.; MOULIN, J. P. The defective glucose sensitivity of the β-cell in non-insulin-dependent diabetes: improvement after twenty hours normo-glycaemia. **Metabolism**, v. 31, p. 139-142, 1982.

VALENTOVA, K.; ULRICHOVA, J. *Smalanthus sonchifolius* and *Lepidium meyenii* – prospective Andean crops for the prevention of chronic diseases. **Biomed. Papers***,* v. 147, n. 2, p. 119-130, 2003.

VAN DE VENTER, M.; ROUX, S.; BUNGU, L.C.; LOUW, J.; CROUCH, N.R.; GRACE, O.M.; MAHARAJ, V.; PILLAY, P.; SEWNARIAN, P.; BHAGWANDIN, N.; FOLB, P. *Antidiabetic screening and scoring of 11 plants traditionally used in South Africa.* **Journal of ethnopharmacology***,* v. 119, n. 1, p. 81-86, 2008.

VAN DEN BERG, R. A.; HOEFSLOOT, H. C.; WESTERHUIS, J. A.; SMILDE, A. K.; VAN DER WERF, M. J. Centering, scaling, and transformations: improving the biological information content of metabolomics data. **BMC genomics**, v. 7, n. 1, p. 142, 2006.

VAN HUYSSTEEN, M.; MILNE, P. J.; CAMPBELL, E. E.; VAN DE VENTER, M. Antidiabetic and cytotoxicity screening of five medicinal plants used by traditional African health practitioners in the Nelson Mandela Metropole, South Africa. **African Journal of Traditional, Complementary and Alternative Medicines**, v. 8, n. 2, p. 150-158, 2011.

VILLAS-BOAS, S. G.; MAS, S.; AKESSON, M.; SMEDSGAARD, J.; NIELSEN, J. Mass Spectrometry in Metabolome Analysis. **Mass Spectrometry Reviews**, v. 24 p. 613-646, 2005.

WAHYUNINGSIH, M. S. H.; WIJAYANTI, M. A.; BUDIYANTO, A. R. I. E. F.;HANAFI, M. U. H. A. M. M. A. D. Isolation and Identification of Potential Cytotoxic Compound from Kembang bulan [Tithonia diversifolia (Hemsley) A. Gray] Leaves. **Int J Pharm Pharm Sci**, v. 7, n. 6, p. 298-301, 2015.

WAINSTEIN, J.; GANZ, T.; BOAZ, M.; BAR DAYAN, Y.; DOLEV, E.; KEREM. Z. Olive leaf extract as a hypoglycemic agent in both human diabetic subjects and in rats. **J. Med. Food**, v. 15, p. 605-610, 2012.

WARRAM, J.; MARTIN, B.; KROLEWSKI, A.; SOELDNER, J.; KAHN, R. Slow glucose removal rate and hyperinsulinemia precede the development of type II diabetes in offspring of diabetic parents. **Ann Intern Med.**, v. 113 p. 909-915, 1990.

WECKWERTH, W. Metabolomics in Systems Biology. **Annual Review of Plant Biology**, v. 54, p. 669-689, 2003.

WILD, S.; ROGLIC, G.; GREEN, A.; Sicree, R.; King, H. Global prevalence of diabetes: estimates for the year 2000 and projections for 2030. **Diabetes Care**, v. 27 p. 1047-1053, 2004.

WOOD, P. J.; BEER, M. U.; BUTLER, G. Evaluation of role of concentration and molecular weight of oat β-glucan in determining effect of viscosity on plasma glucose and insulin following an oral glucose load. **British Journal of Nutrition**, v. 84, n. 1, p. 19-23, 2000.

YAMAGISHI, S.; IMAIZUMI, T. Diabetic vascular complications: pathophysiology, biochemical basis and potential therapeutic strategy. **Curr Pharm Des**, v. 11 p. 2279-2299, 2005.

YANG, S.; JI, L.; QUE, L.; WANG, K.; YU, S. Metformin activates Nrf2 signaling and induces the expression of antioxidant genes in skeletal muscle and C2C12 myoblasts. **J Chin Pharm Sci**, v. 23, p. 837-843, 2014.

YILMAZER-MUSA, M.; GRIFFITH, A. M.; MICHELS, A. J.; SCHNEIDER, E.; FREI, B. Inhibition of α-amylase and α-glucosidase activity by tea and grape seed extracts and their constituent catechins. **Journal of agricultural and food chemistry**, v. 60, n. 36, p. 8924, 2012.

YOON, S. H.; ROBYT, J. F. Study of the inhibition of four alpha amylases by acarbose and its 4IV-α-maltohexaosyl and 4IV-α-maltododecaosyl analogues. **Carbohydrate research**, v. 338, n. 19, p. 1969-1980, 2003.

YULIANA, N. D.; KHATIB, A.; CHOI, Y. H.; VERPOORTE, R. Metabolomics for Bioactivity Assessment of Natural Products. **Phytotherapy Research**, v. 25, p. 157-169, 2011.

ZHANG, F.; HUANG, Y.; HOU, T.; WANG, Y. Hypoglycaemic effect of *Artemisia sphaerocephala* Krasch seed polysaccharide in alloxan-induced diabetic rats. **Swiss Medical Weekly**, v. 136, p. 529-532, 2006.

APPENDICES

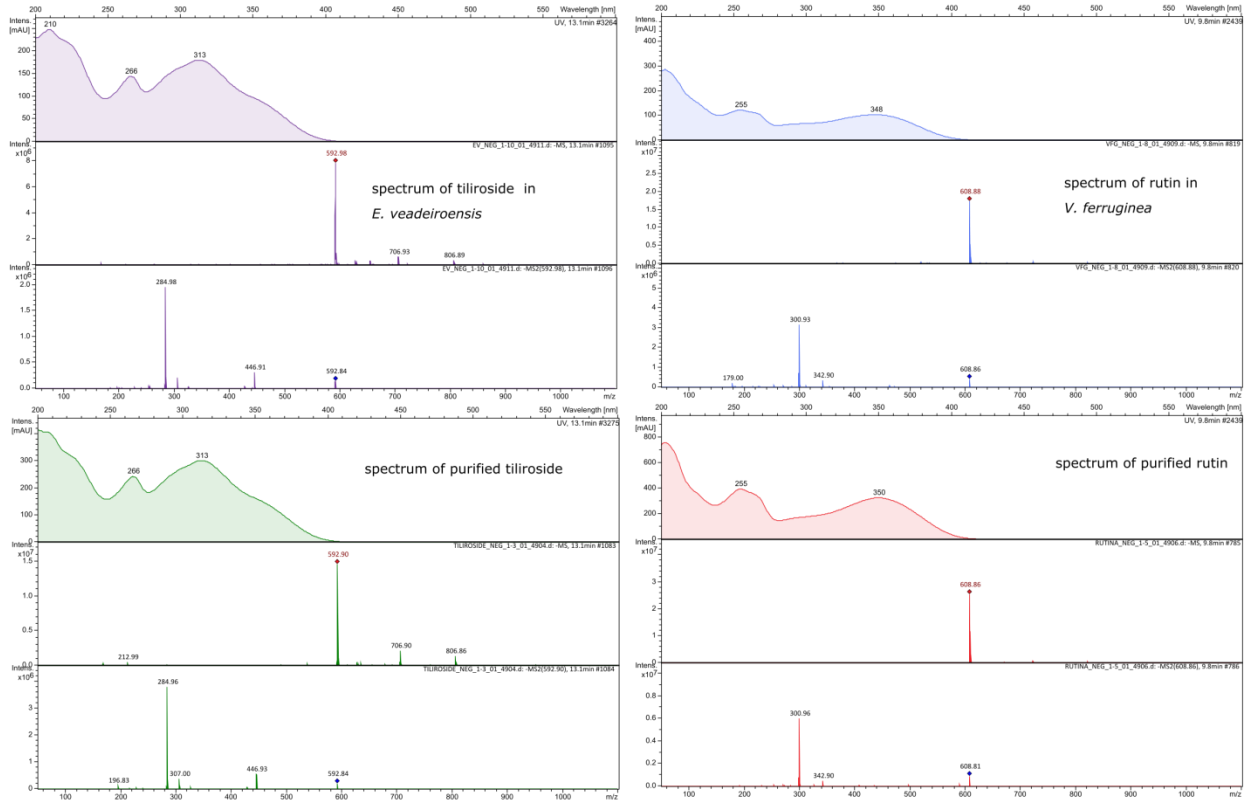

APPENDIX I: Superimposable ion trap spectra (MS, MS/MS and UV) of peaks corresponding to metabolites annotated as tiliroside and rutin, compared with their pure standards

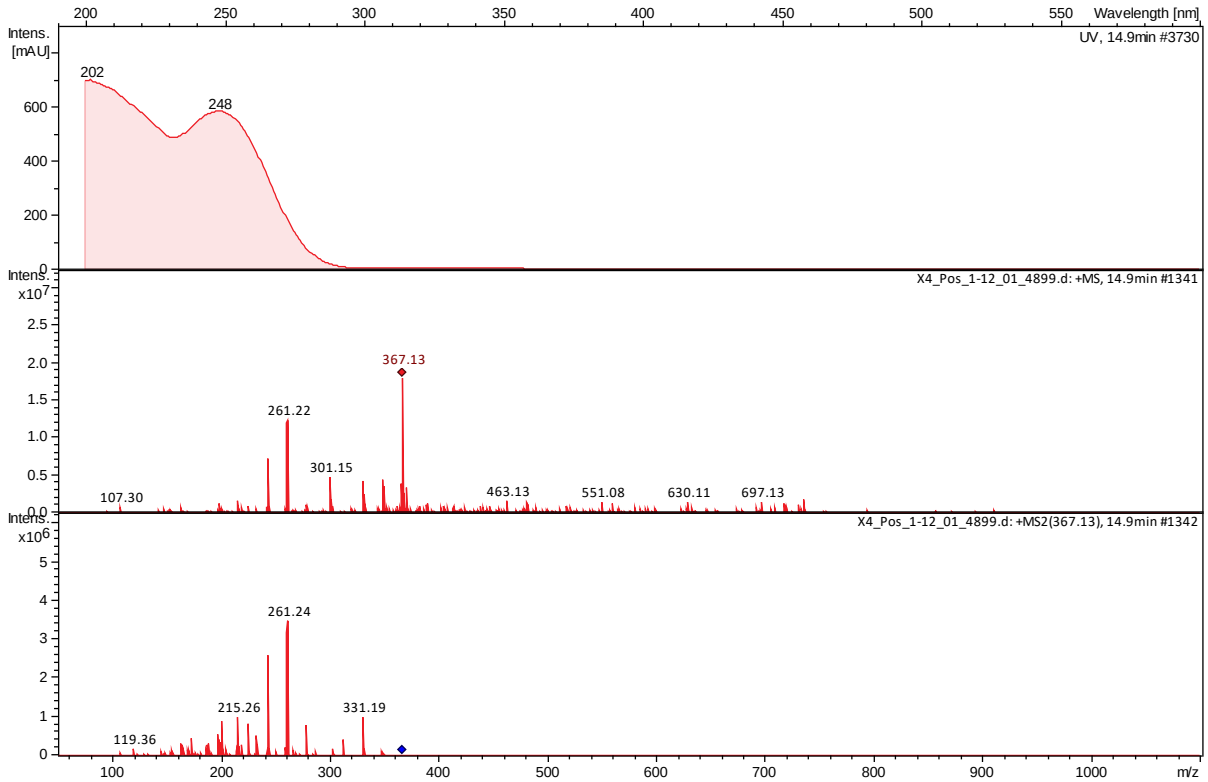

APPENDIX II: Ion trap spectra (MS, MS/MS and UV) of the discriminant metabolite with *m/z* 367.13 $[M+H]^+$ detected in *T. diversifolia* at 14.9 min

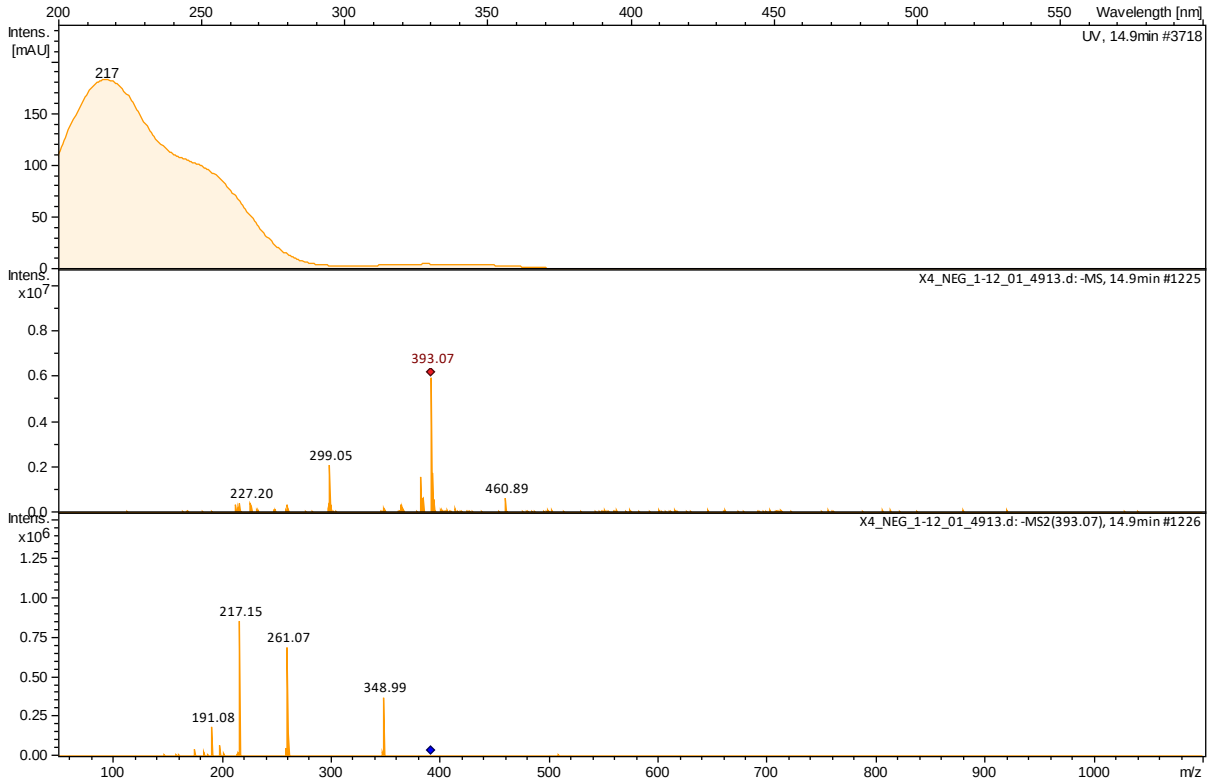

APPENDIX III: Ion trap spectra of the discriminant metabolite with *m/z* 393.10 $[M-H]^-$ detected in *T. diversifolia* at 14.9 min

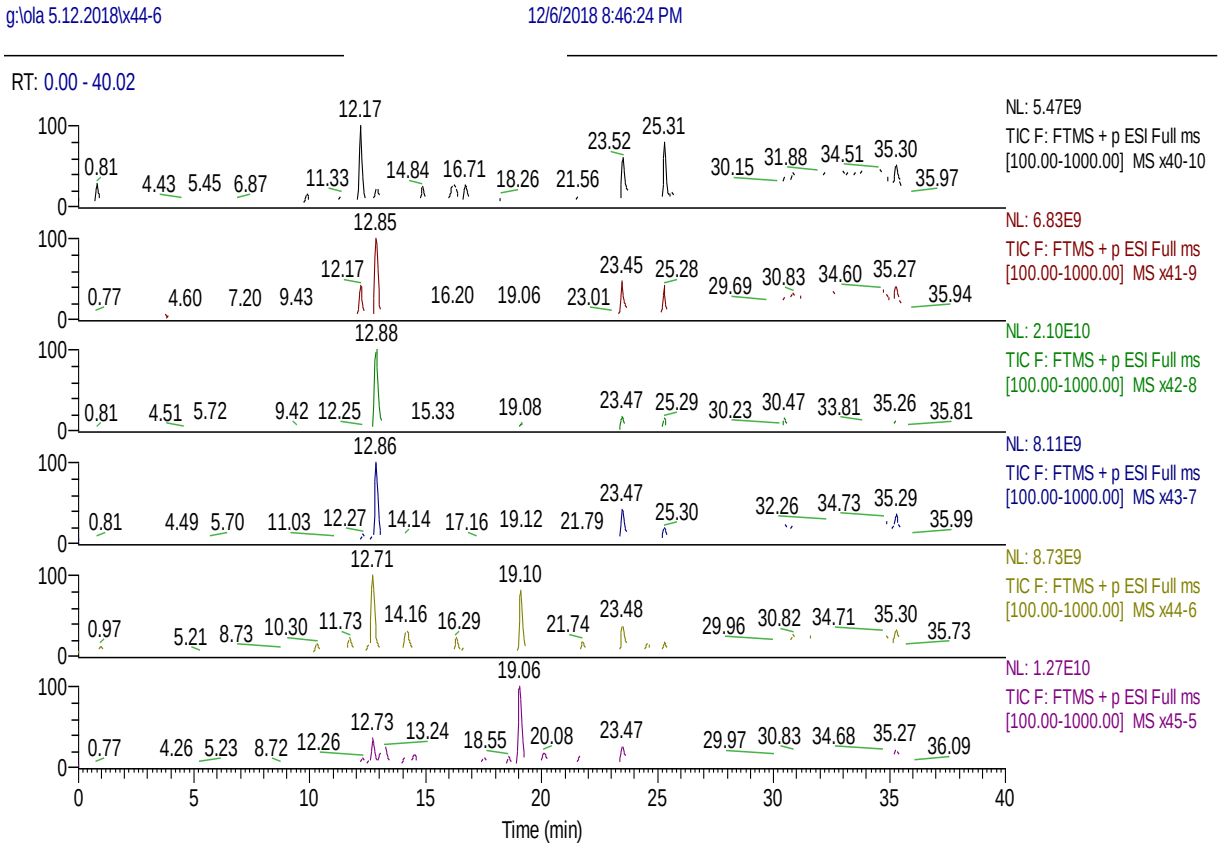

APPENDIX IV: The UHPLC chromatograms of the flash chromatography fractions (hexane:ethylacetate, 0:100 – 50:50%) of the leaf rinse extracts of *T. diversifolia* in the positive mode

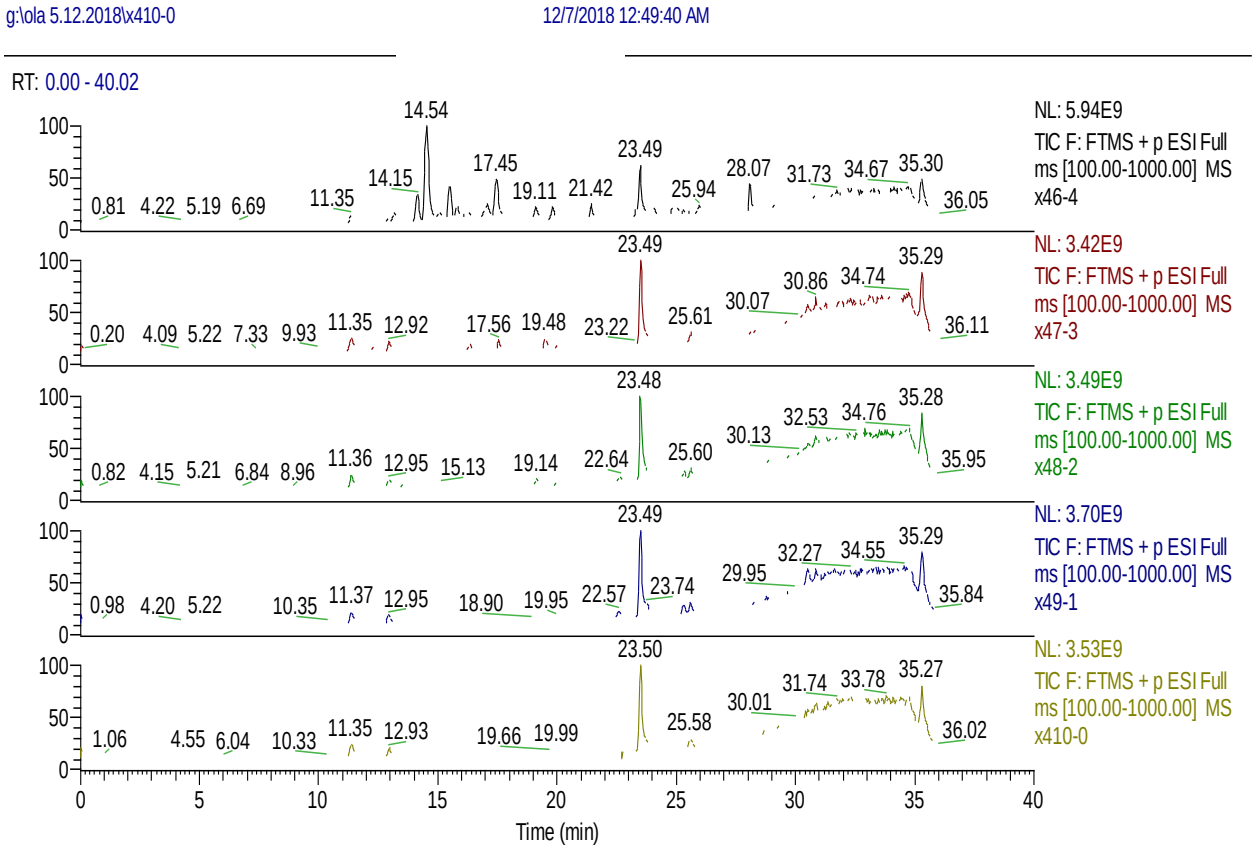

APPENDIX V: The UHPLC chromatograms of the flash chromatography fractions (hexane:ethylacetate, 60:40 – 100:0%) of the leaf rinse extracts of *T. diversifolia* in the positive mode

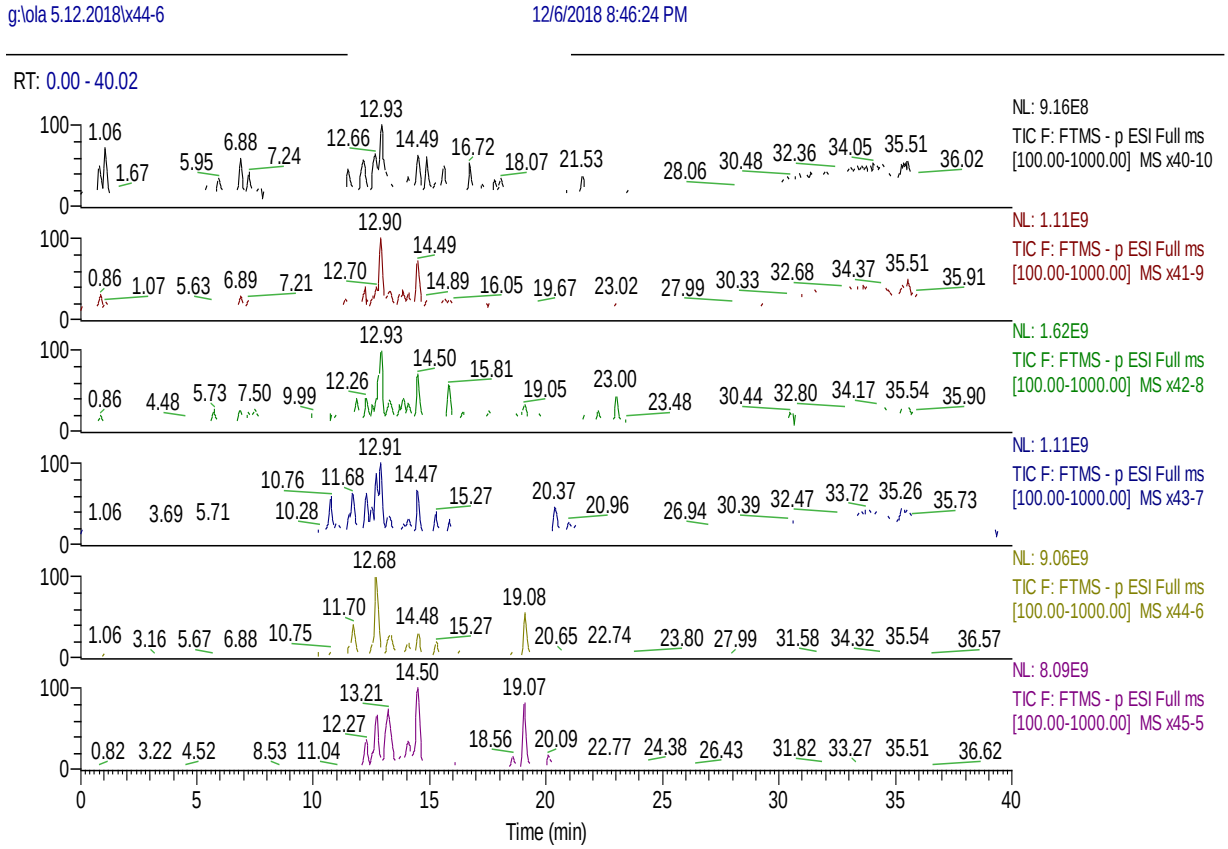

APPENDIX VI: Chromatograms of flash chromatography fractions, 0:100 – 50:50%, of LRE of *T. diversifolia* in the negative mode

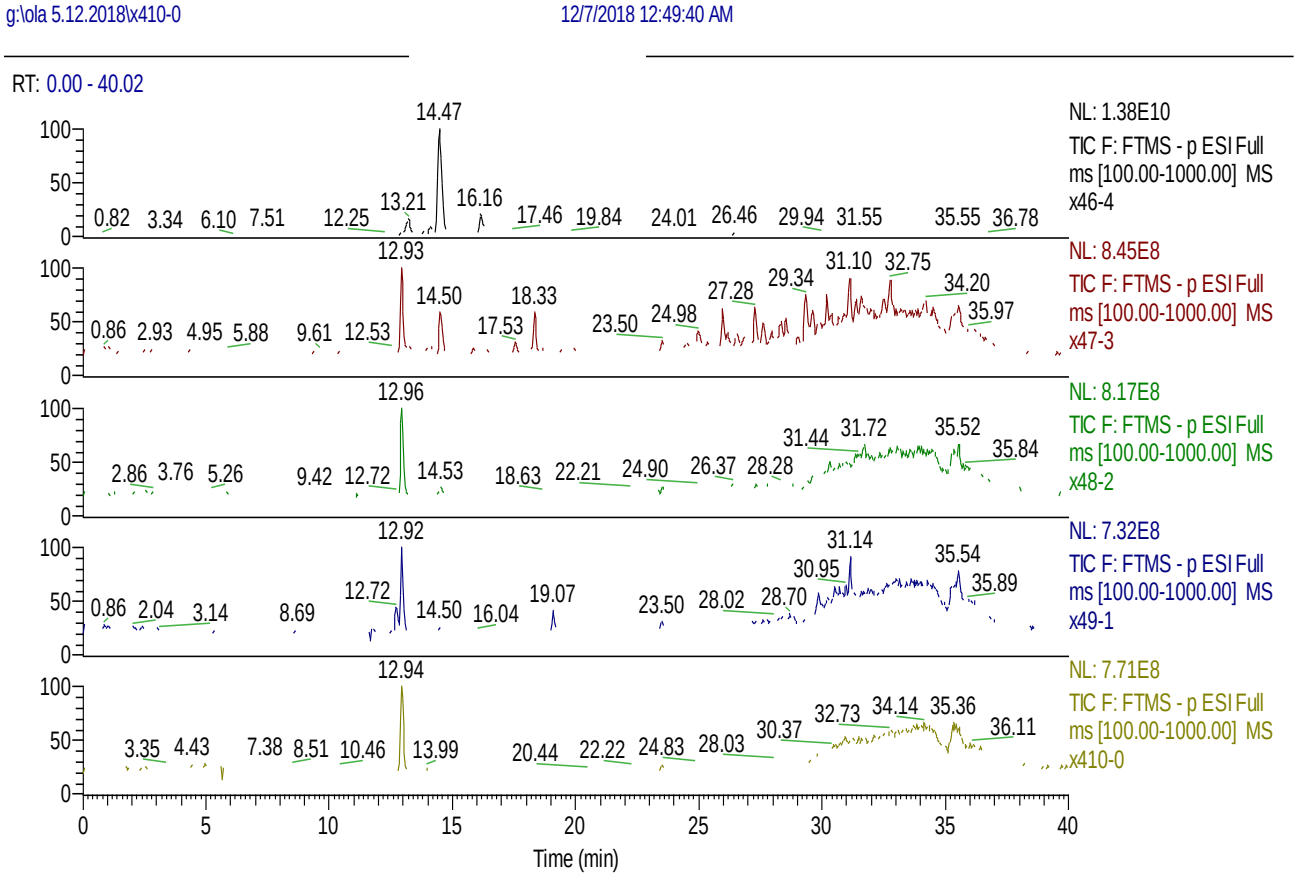

APPENDIX VII: Chromatograms of flash chromatography fractions, 60:40 – 10:100%, of LRE of *T. diversifolia* in the negative mode

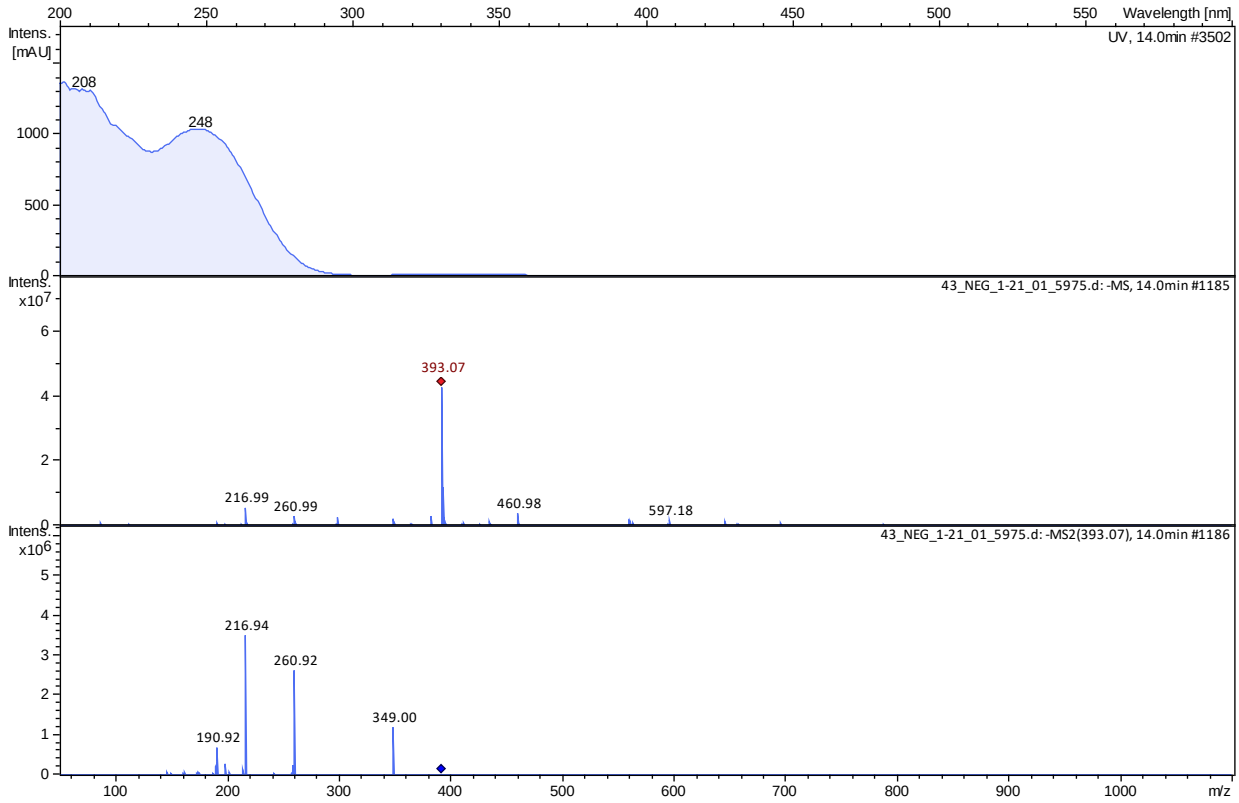

APPENDIX VIII: Ion trap spectra (MS, MS/MS and UV) of the discriminant metabolite with *m/z* 393.16 $[M-H+FA]^-$ detected in fraction Fr3 from *T. diversifolia* at 14.0 min

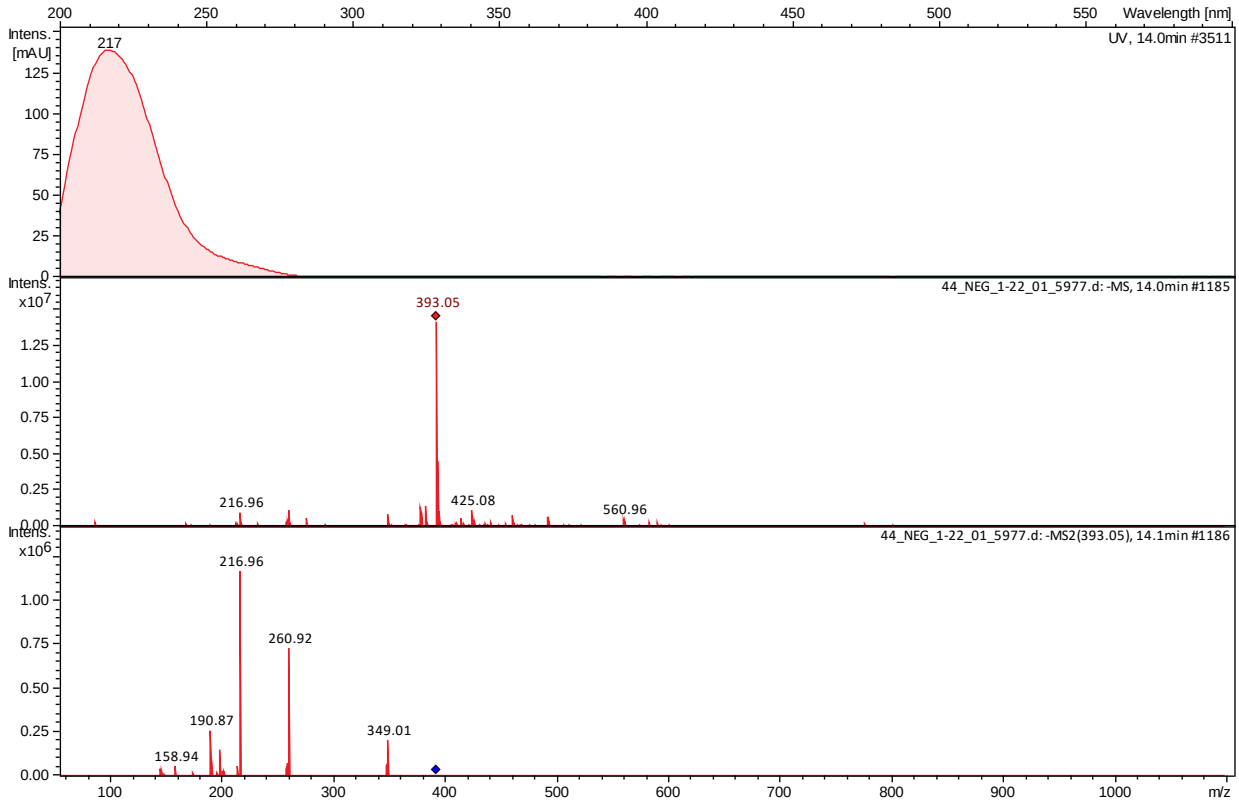

APPENDIX IX: Ion trap spectra (MS, MS/MS and UV) of the discriminant metabolite with *m/z* 393.16 $[M-H+FA]^-$ detected in fraction Fr4 from *T. diversifolia* at 14.0 min

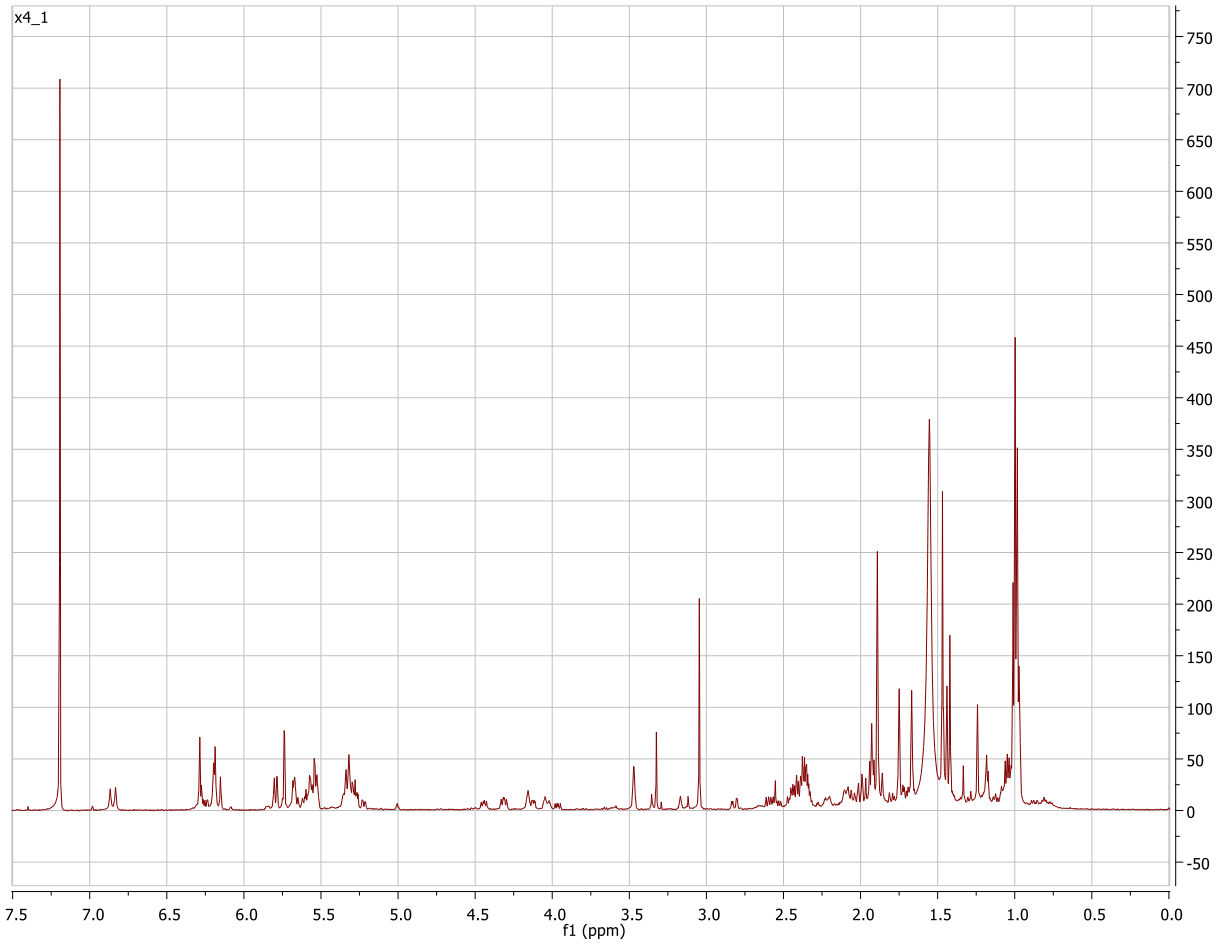

APPENDIX X: ^{1}H NMR ($CDCl_3$, 500 MHz) spectrum of Fr1 isolated from *T. diversifolia*

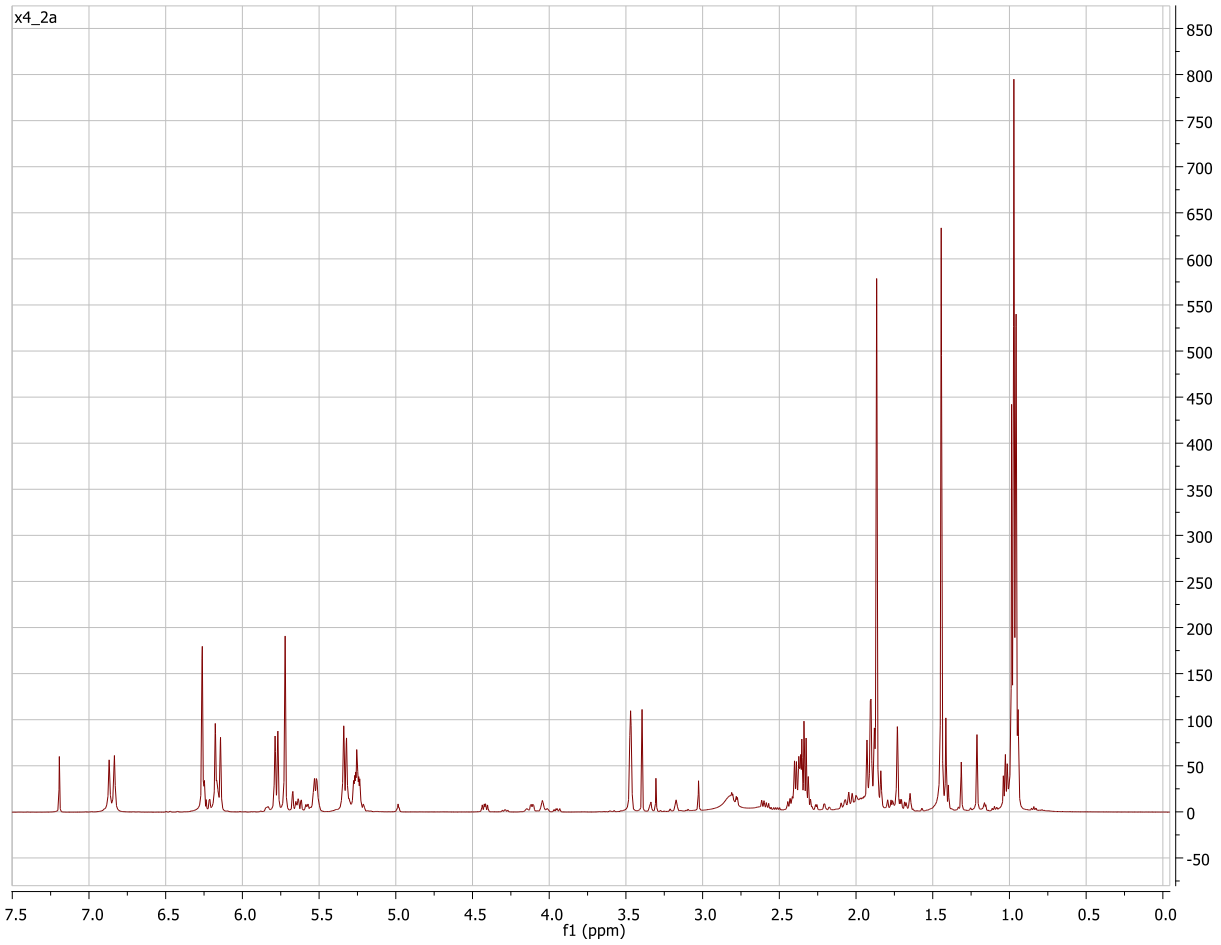

APPENDIX XI: ^{1}H NMR ($CDCl_3$, 500 MHz) spectrum of Fr2 isolated from *T. diversifolia*

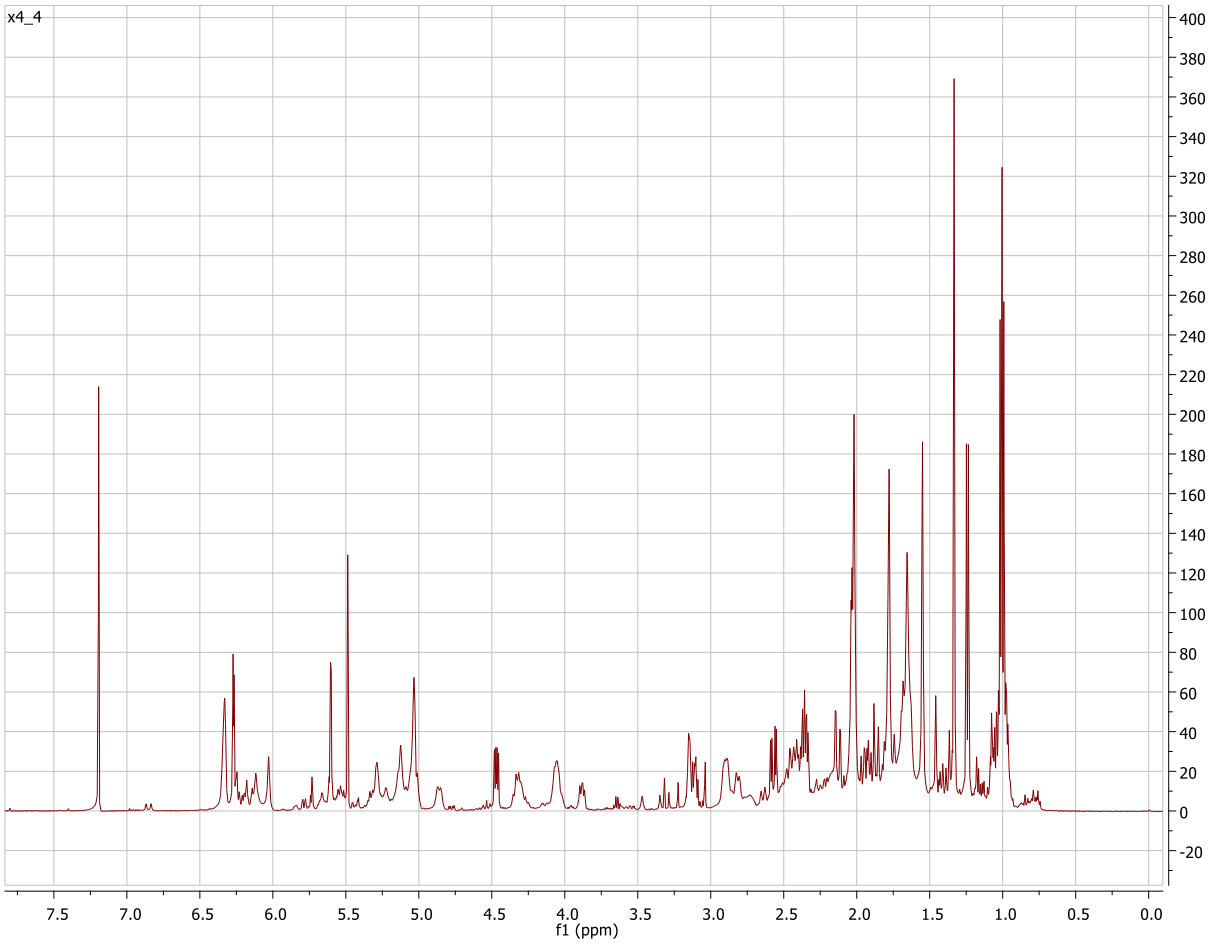

APPENDIX XII: ^{1}H NMR ($CDCl_3$, 500 MHz) spectrum of Fr4 isolated from *T. diversifolia*

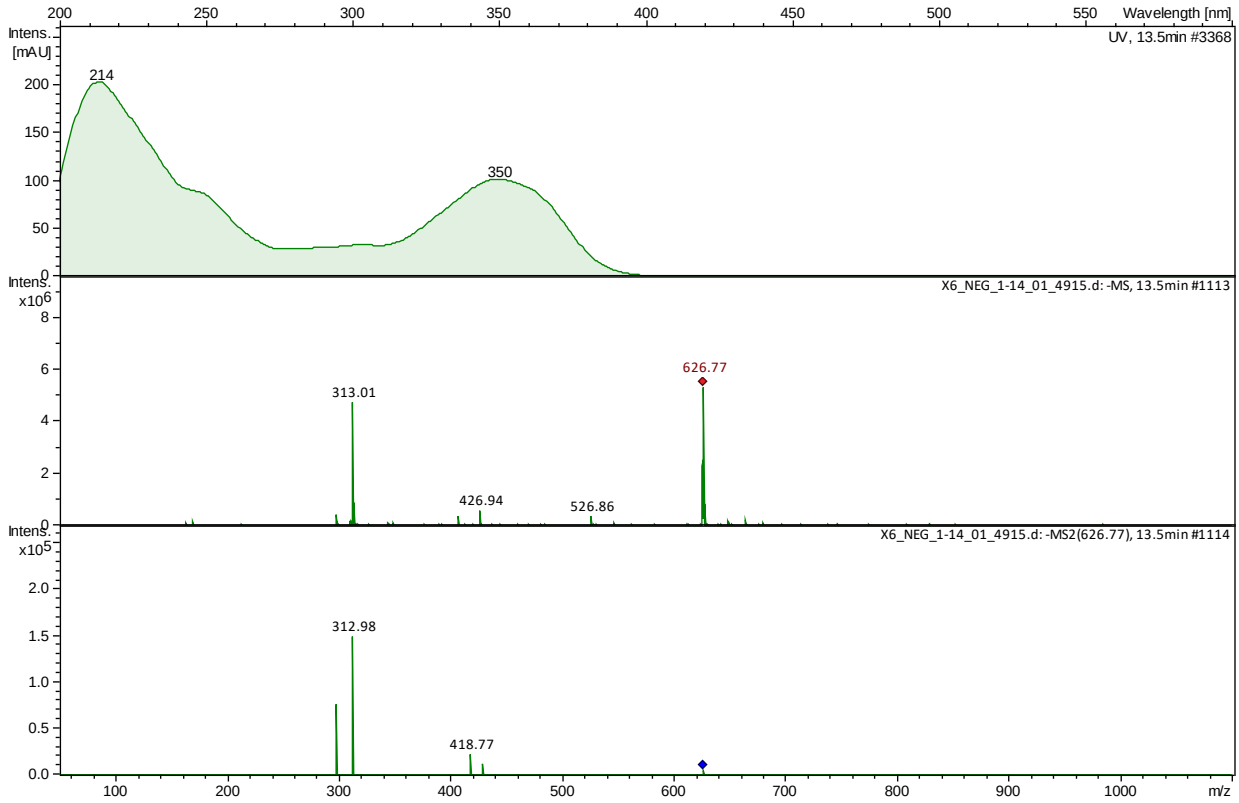

APPENDIX XIII: Ion trap spectra (MS, MS/MS and UV) of *E. alba* presenting the peaks with *m/z* 312.98 $[M-H]^-$ and 626.77 $[2M-H]^-$ at 13.5 min, annotated as wedelolactone

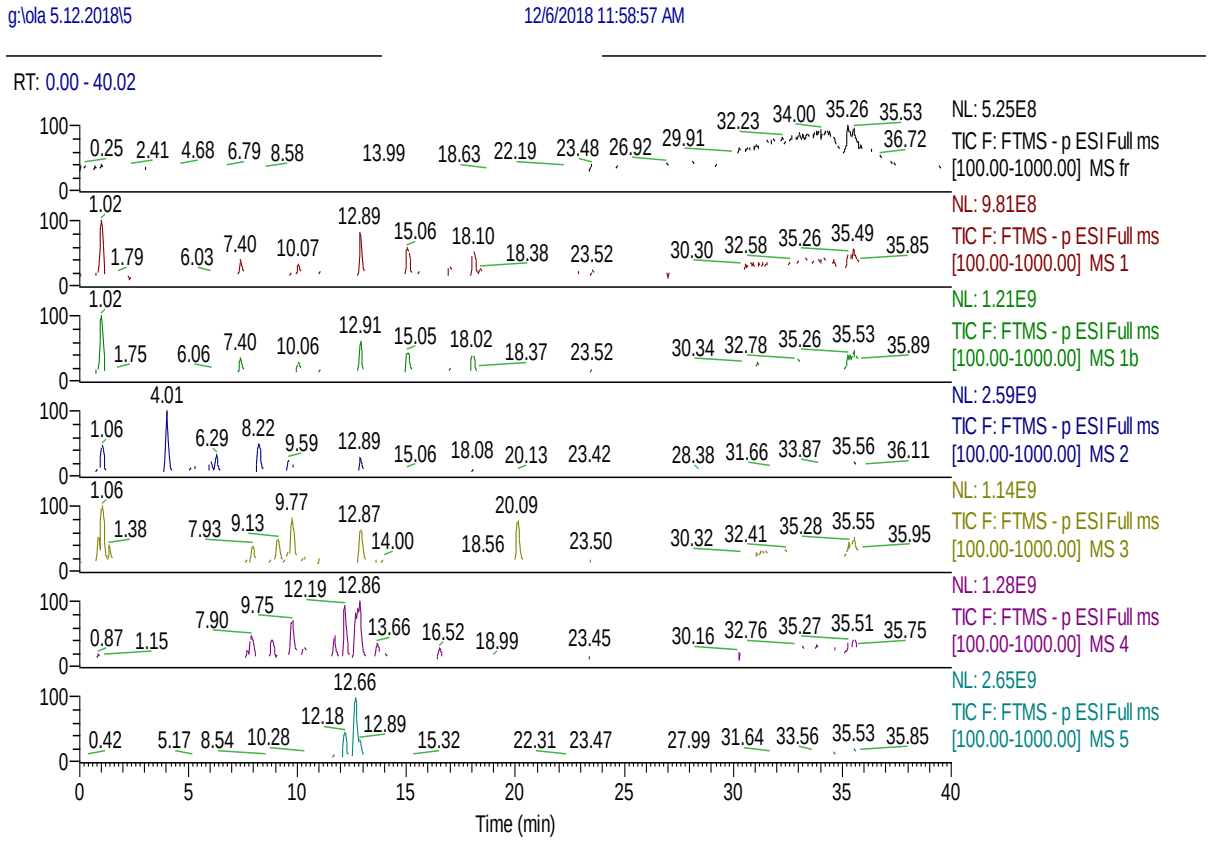

APPENDIX XIV: The UHPLC chromatograms of Sephadex subfractions (isocratic elution with methanol), Frc1-Frc5 of the ethylacetate fraction of *E. alba* in the negative mode

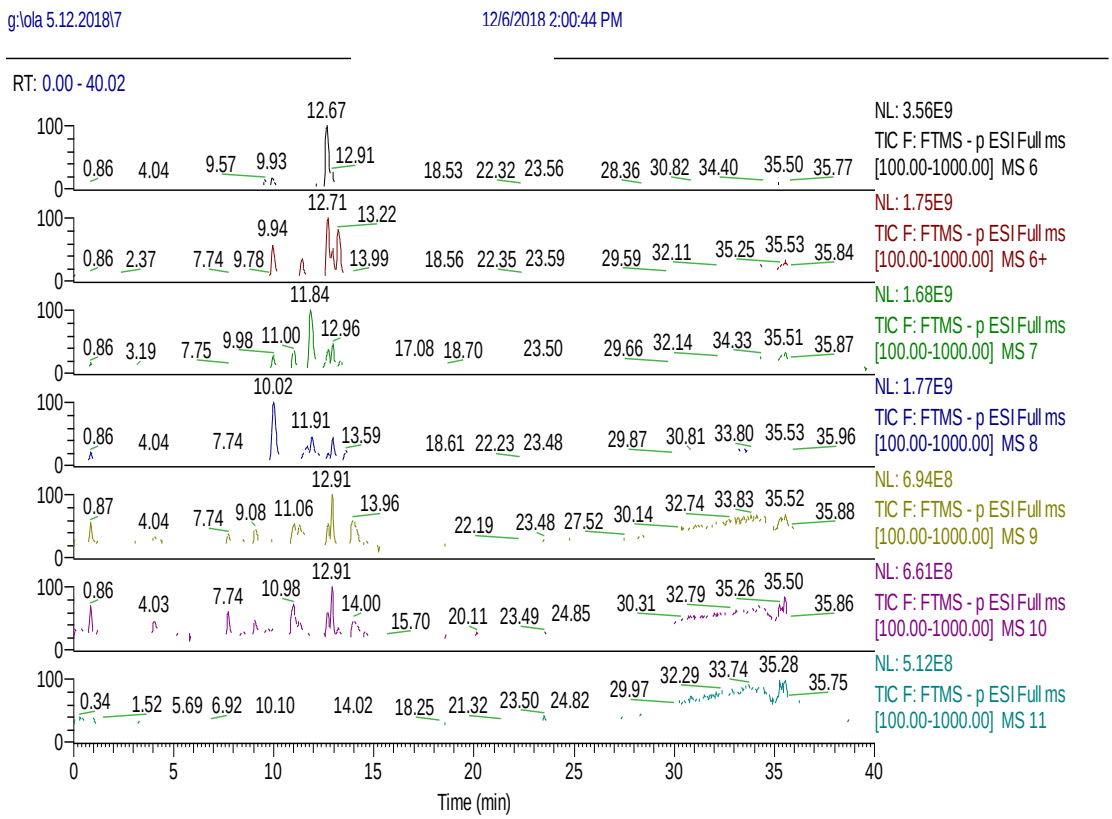

APPENDIX XV: The UHPLC chromatograms of Sephadex subfractions (isocratic elution with methanol), Frc6-Frc11 of the ethylacetate fraction of *E. alba* in the negative mode

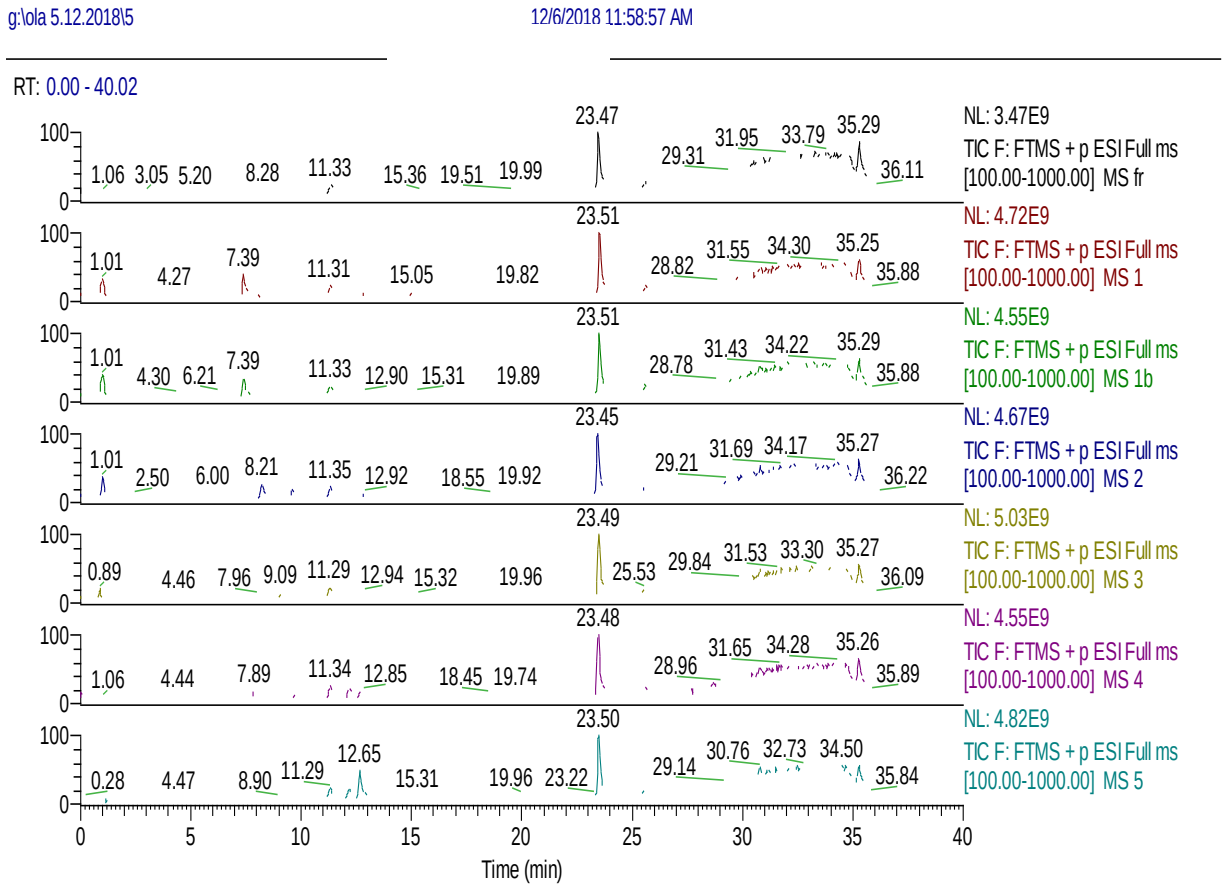

APPENDIX XVI: The UHPLC chromatograms of Sephadex subfractions (isocratic elution with methanol), Frc1-Frc5 of the ethylacetate fraction of *E. alba* in the positive mode

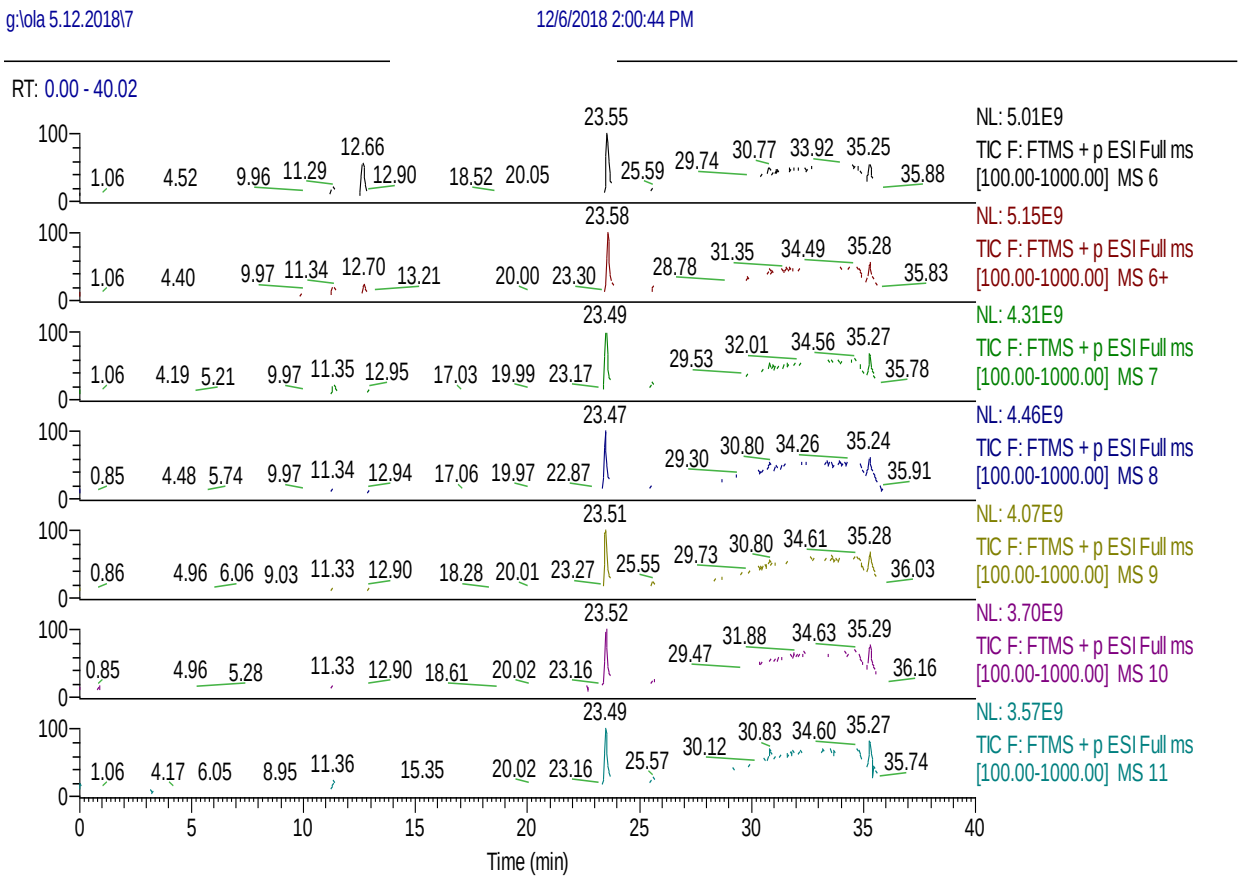

APPENDIX XVII: The UHPLC chromatograms of Sephadex subfractions (isocratic elution with methanol), Frc6-Frc11 of the ethylacetate fraction of *E. alba* in the positive mode

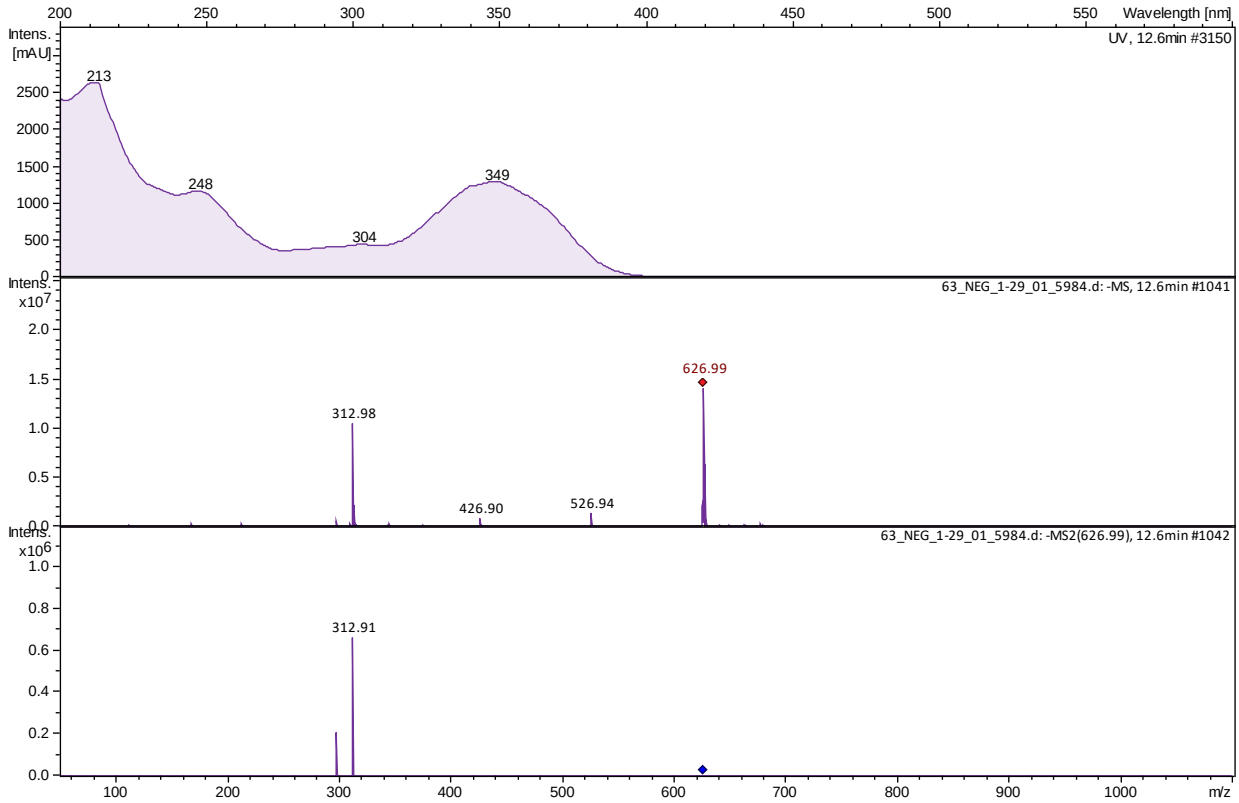

APPENDIX XVIII: Ion trap spectra (MS, MS/MS and UV) of the isolate, wedelolactone (Fr_{sn}) with *m/z* 313 $[M-H]^-$ and 627 $[2M-H]^-$ detected at 12.6 min

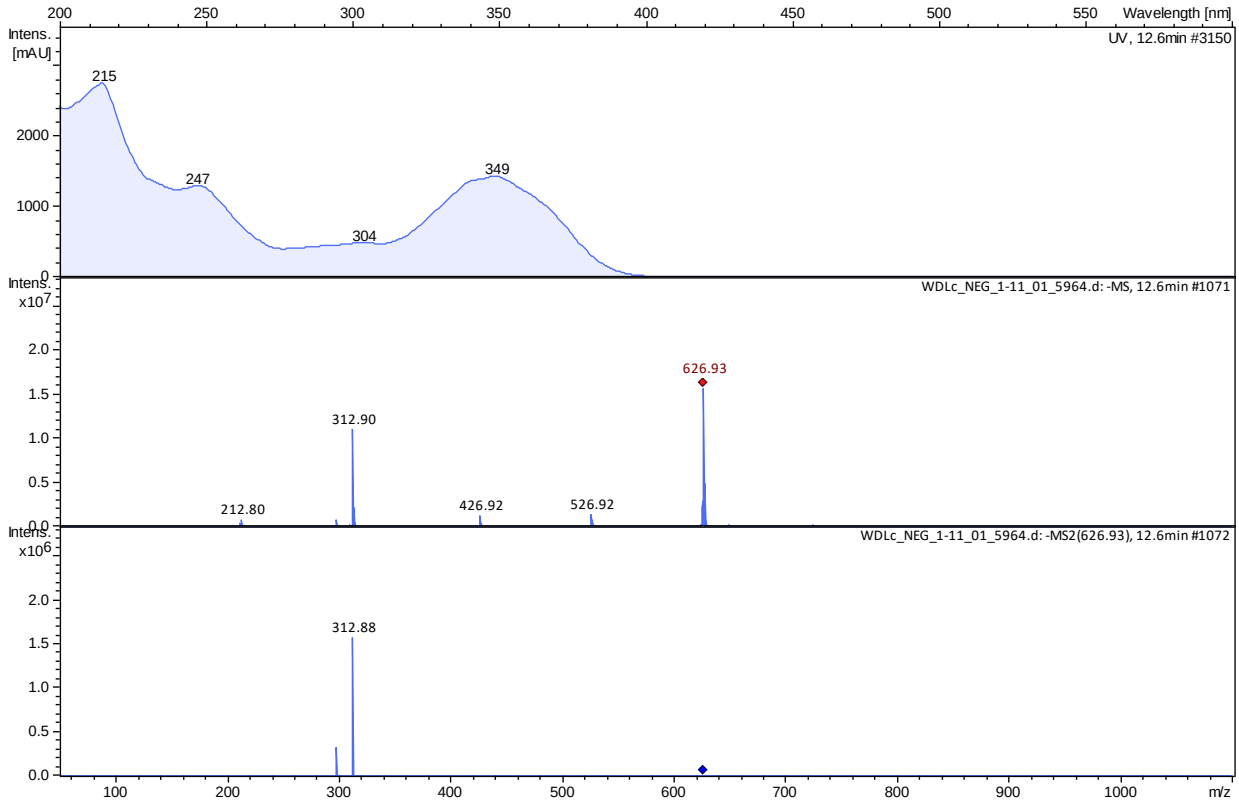

APPENDIX XIX: Ion trap spectra (MS, MS/MS and UV) of the recrystallized wedelolactone (Fr_{cp}) with *m/z* 313 $[M-H]^-$ and 627 $[2M-H]^-$ detected at 12.6 min

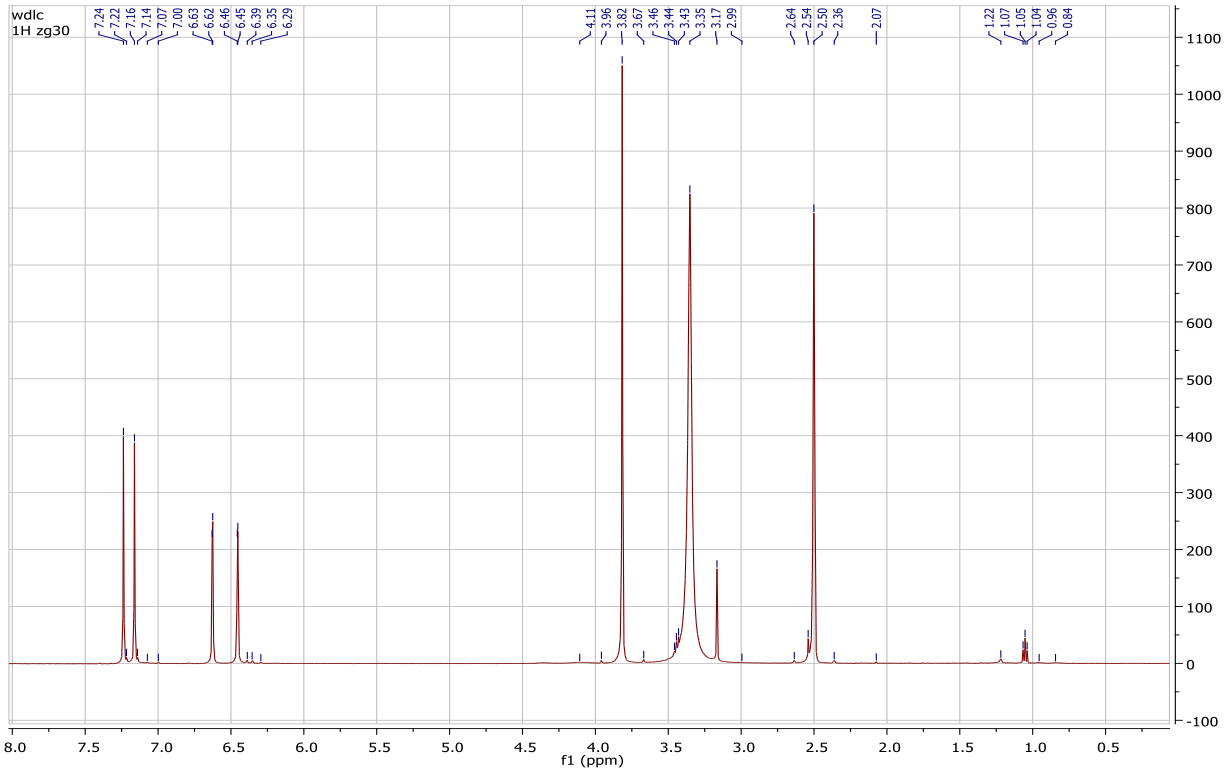

Appendix XX: ^{1}H NMR (DMSO-D_6, 500 MHz) spectrum of wedelolactone (Frcp)